Characterization of fires in multi-suite residential dwellings: final project report: part 2-Analysis of the results of post-flashover room fire tests

Bwalya, Alex; Gibbs, Eric; Lougheed, Gary; Kashef, Ahmed

Research Report (National Research Council of Canada. Construction), 2014-10-24

National Research Council Canada | Conseil national de recherches Canada

NRC · CNRC

Characterization of Fires in Multi-Suite Residential Dwellings

Final Project Report

Part 2 – Analysis of the Results of Post-Flashover Room Fire Tests

Project Title:	**Characterization of Fires in Multi-Suite Residential Dwellings**
Authors:	**Alex Bwalya, Eric Gibbs, Gary Lougheed, Ahmed Kashef**
Date:	24rd October, 2014

Construction Portfolio

Fire Safety

Preface

This report analyzes the results of 14 full-scale post-flashover room fire experiments that were conducted in Phase 2 of the Characterization of Fires in Multi-Suite Residential Dwellings (CFMRD) project. A compilation of the test results from Phase 2 is provided in Part 1 of the final project report.

The CFMRD project was a collaborative undertaking with industry, provincial governments and city authorities that was initiated by NRC-IRC in 2006 to study fires in low-rise multi-suite residential dwellings of light-frame construction. The project was undertaken due to the need to:

a) Address the lack of realistic design fires, which are required to aid the development of methods for achieving performance-based solutions to fire problems, and;
b) Further the understanding of how fires in residential buildings sometimes cause fatalities and substantial property losses, as revealed by fire statistics.

The CFMRD project focused on fires in dwellings, such as apartments, semi-detached houses, duplex houses, townhouses or row houses, secondary suites and residential care facilities as these fires have a potentially greater impact on adjacent suites. To this end, the fully-developed phase of a fire was of particular interest since there is a greater potential for the building assemblies enclosing the room of fire origin to be damaged by high temperatures during this period.

The main objectives of the project were:

1. To conduct fire experiments to characterize fires originating in various living spaces within multi-suite dwellings.
2. To conduct numerical simulations of various fire scenarios in order to interpolate and extend the data beyond that obtained in the experimental studies.
3. To produce a set of realistic design fires for multi-suite dwellings from the test data.
4. To develop an analytical method that can be used to calculate design fires for multi-suite dwellings.

The research approach employed in the project utilized literature reviews, surveys to determine typical configurations and combustibles, computer simulations and fire experiments. In Phase 1 of the project, fire experiments were conducted in a room calorimeter to determine the combustion characteristics of individual typical household furnishings found in living spaces that have a high incidence of fires. In Phase 2, fire experiments were conducted in fully-furnished rooms simulating

residential bedrooms, a living room, a main floor, a secondary suite and a residential care bedroom. Numerical modelling of fire development, using suitable fire models, was conducted in Phase 1 to assist in the design and instrumentation of the full-scale fire experiments as well as to study the effect of various parameters, such as the ventilation conditions and geometry on the development of the fire.

NRC gratefully acknowledges the financial and technical support of the Project Consortium, which consisted of representatives from the following participating organizations:

- Canadian Automatic Sprinkler Association
- Canadian Concrete Masonry Producers Association
- Canadian Furniture Manufacturers Associations
- The Canadian Wood Council
- City of Calgary - Development and Building Approvals
- City of Calgary - Fire Department
- FPInnovations
- Gypsum Association
- Masonry Worx
- Ontario Ministry of Municipal Affairs and Housing
- Ontario Ministry of Community Safety and Correctional Services (Office of the Fire Marshal)
- Régie du Bâtiment du Québec

Abstract

This report presents the analysis of results for 14 full-scale fire experiments that were conducted in a specially constructed full-scale test facility. The facility was instrumented to measure the heat release rate (HRR), heat flux, temperatures, gas velocities, smoke optical density and composition of fire gases at various locations. The test program involved an array of configurations to simulate key areas in a dwelling such as a bedroom, a living room and a main floor (consisting of a kitchen and a living room). Experiments were conducted for different floor areas and under various ventilation conditions. The fuel load consisted of typical residential furnishings. In all of the test scenarios, the first-ignited-item was a primary combustible furnishing, such as a bed assembly or an upholstered seat (sofa). The tests were designed to last for a period of 1 hr in order to capture the key phases of fire development: growth, flashover, fully-developed (post-flashover) and decay phases. In order to achieve one of the main objectives of the research, which was to produce a set of realistic design fires, it was decided that high intensity fires that have the potential to pose a risk to adjacent suites would be the focus of the research.

Flashover typically occurred in less than five minutes. It occurred in as little as 140 seconds in fires started with a strong flame in highly combustible furnishings, such as sofas and beds. The results showed that there were considerable differences in HRR profiles, and peak values varied widely for the resulting post-flashover fires since the HRR is a strong function of ventilation, among other variables such as fuel load composition. For instance, peak HRR values varied from 2,793 kW to 9,230 kW (mean of 5,847 kW and standard deviation of 2,122 kW), whereas the mean maximum temperatures (during the fully-developed phase) only varied from about 1,036°C to 1,203°C (mean of 1,110^{o}C and standard deviation of 54°C). The mean duration of the fully-develop phase was 17 min with a standard deviation of 4 min.

One of the main conclusions was that, in rooms lined primarily with gypsum board, regardless of other variables (such as, ventilation, fuel load, ignition method and room size), the mean maximum temperatures fell within a narrow range of approximately 1,050°C to 1,200°C. However, test variables and particularly ventilation, first-ignited-item and composition of the fuel load had a significant effect on the time of attainment and duration of the fully-developed phase (defined in this work as stage R4), during which the mean maximum temperature occurs. The mean maximum temperature during the fully-developed phase and the duration of stage R4 (over which it is calculated) are considered to be the appropriate measure of fire severity since temperature is the thermodynamic result of the HRR in a given room fire, while the duration defines the exposure time. Another main conclusion was that the primary bedroom scenarios within this research resulted in the most severe fire conditions of the scenarios tested since they had a large floor area and therefore contained the greatest amount of combustible materials.

The one test incorporating a residential sprinkler system had a rapid extinguishment of the fire. The sprinkler activated within 50 seconds and the maximum temperature recorded at a single point in the room was 117°C.

A fire starting in a oil-filled pot on the stove, in a layout simulating a main floor with a kitchen, and living room, developed much more slowly (9 minutes to flashover) than one where the fire originated in a sofa in the same main floor configuration (3 minutes to flashover).

A detailed analysis of the results was carried out to attempt to identify and explain features of the fires that could form the basis of a computation model to calculate the mean maximum temperature and the duration of the fully-developed phase of a room fire. The results of this research provided valuable knowledge about the effect of key parameters such as window size and first-ignited-items on the outcome of the fire. The test results revealed that there was a significant variation in fire severity within a single room due to the complexity of the fire dynamics, which makes it difficult to describe the fires using average values of key fire properties.

Contents

NOMENCLATURE

A	Area	(m^2)
A_f	Surface area of fuel element	(m^2)
A_o	Area of a ventilation opening	(m^2)
A_s	Exposed surface area of the fuel load	(m^2)
A_T	Total internal area of bounding surfaces of an enclosure	(m^2)
b	A parameter in Equation (2.27), = $\sqrt{k\rho c_p}$	($W.s^{0.5}/m^2K$)
b_{ref}	Reference value of b	($W.s^{0.5}/m^2K$)
C_d	Orifice constriction coefficient	(-)
C_p	Specific heat capacity	(kJ/kg.K)
F_o	Opening factor	($m^{1/2}$)
F_{ref}	Reference value of the opening factor	($m^{1/2}$)
F_v	Ventilation factor	($m^{5/2}$)
g	Acceleration due to gravity	(m/s^2)
h	Heat transfer coefficient	($kW/m^2.K$)
H	Height	(m)
H_o	Height of ventilation opening	(m)
$\overline{HRR}_{R4}$	Mean HRR in Stage R4	(kW)
HRR_{pa}	Average peak HRR per m^2 for the fuel load	*(kW/m^2)*
IF_o	Inverse opening factor	($m^{-1/2}$)
k	Thermal conductivity	(kW/m.K)
L	Fuel load	(kg)
M	mass of combustible material	(kg)
M_c	Mass of single combustible item	(kg)
M_f	Total mass of fuel	(kg)
$\dot{m}$	Rate of mass flow	(kg/s)
M_f''	Fuel load per unit area	(kg/m^2)
$\bar{M}_f''$	Mean fuel load	(kg/m^2)
q'', Q''	Bench-scale heat release rate or Heat flux	(kW/m^2)
q''_{mf}	Heat flux at floor level	(kW/m^2)
q''_{mwc}	Maximum heat flux on the walls and ceiling	(kW/m^2)
$\dot{Q}_o$	Reference heat release rate (Equation(2.1))	(kW)
$\dot{Q}$	Heat release rate	(kW)
$\dot{Q}_{FO}$	Heat release rate to cause flashover	(kW)

Q_t	Total fuel load density	(MJ/m^2)
RD	Room depth	(m)
RW	Room width	(m)
T	Temperature	(^{o}C or K)
T_{gm}	Time variable used in Equation (2.19)	(^{o}C)
$T_{g,max}$	Variable used in Equations (2.29)	(^{o}C)
$\bar{T}_{\max}$	Mean maximum hot layer temperature	(^{o}C)
t	Time	(s or min)
t^*	Fictitious time used in Equation (2.26)	(hrs)
t_b	Duration of burning	(s)
t_{HRRv}	Time to reach HRRv	(s)
t_d	Duration of heating phase, given by Equation (2.31)	(hrs)
t_d^*	Modified duration time; given by Equation (2.32)	(hrs)
t_{FD}	Duration of the fully-developed phase, given by Equation (6.3)	(min)
THR	Total heat released	(MJ)
t_m	Time at which maximum temperature occurs	(min)
T_o	Reference temperature	(^{o}C)
t_o	Time to reach a reference heat release rate	(s)
XHT	Value of either temperature or HRR at the start of the decay phase	
X1	Fraction of FL consumed at decay (during the fully-developed phase)	
W_o	Width of ventilation opening	(m)

GREEK LETTERS

β	A constant used in Equations (2.22) and (2.23)	(K s$^{-1/6}$)
ΔT_g	Upper gas temperature rise above ambient (T_g - T_∞)	(K)
Δt_{RX}	Duration of fire development stage RX, where X = 1 to 5	(s)
ρ	Density	(kg/m^3)
ε	Emissivity	
λ	is a correlation coefficient used in Equation (5.1)	(W/s)
Ω	Opening factor parameter in Equation (2.13)	
ψ	Parameter in Equation 2.14 (defined by Equation (2.15))	
δ	Shape constant	(-)
σ	Stefan Boltzmann constant = 5.67 x 10^{-8}	(W m^{-2} K^{-4})
α	thermal diffusivity	(s^{-1})
σX	Standard deviation	
$\sigma X_{HRR_{R4}}$	Standard deviation of HRR at Stage R4	
δ_w	Wall thickness	(m)
ξ	Parameter defined by Equation (2.18)	
τ	Time duration used in Equation (2.16)	

τ_b	Burnt out time, used in Equation (2.25)	(s)
η_{cr}	Variable used in Equation (2.21)	

SUBSCRIPTS

∞	Ambient condition
a	Air
air	Air
avg	Average
f	Fuel
g	Pertains to hot gas
max	Maximum value
n	Number of openings
R	Room condition

ABBREVIATIONS

CFMRD	Characterization of Fires in Multi-Suite Residential Dwellings	
CO	Carbon monoxide	
CO_2	Carbon dioxide	
FL	Fuel load	(MJ)
FLED	Fuel load density	(MJ/m^2)
GWB	Gypsum board	
HC	Heat of combustion (calorific value)	(MJ/kg)
HRR	Heat Release Rate	(kW/m^2)
HRRv	Ventilation controlled HRR	(kW/m^2)
NE	North East	
NW	North West	
NFPA	National Fire Protection Association	
O.C.	On center	
OD/m	Optical density per meter	(m^{-1})
OSB	Oriented strand board	
O_2	Oxygen	
PCF	Primary combustible furnishing	
PRF	Post-flashover Room Fire	
PUF	Polyurethane foam	
RGWB	Regular Gypsum board	
SCF	Secondary combustible furnishing	
SD	Standard deviation	
SE	South East	
SW	South West	
TC	Thermocouple	
TWS	Test Wall Section	

Characterization of Fires in Multi-Suite Residential Dwellings Project

Final Project Report

Part 2 – Analysis of the Results of Post-Flashover Room Fire Tests

by

Alex Bwalya, Eric Gibbs, Gary Lougheed, Ahmed Kashef

1 Introduction

This second part of the project report analyzes the results of a series of 14 full-scale post-flashover room fire experiments that were conducted in Phase 2 of the Characterization of Fires in Multi-Suite Residential Dwellings (CFMRD) project. The CFMRD project was a collaborative undertaking with industry, provincial governments and city authorities that was initiated by NRC-Construction in 2006 to study fires in low-rise multi-suite residential dwellings of light-frame construction. The project was undertaken due to the need to: a) address the lack of realistic design fires, which are required to aid the development of methods for achieving performance-based solutions to fire problems, and b) further the understanding of how fires in residential buildings sometimes cause fatalities and substantial property losses, as revealed by fire statistics.

A description of all the tests, including the raw data, is presented in Part 1 of this report [1]. The CFMRD project focused on fires in dwellings, such as apartments, semi-detached houses, duplex houses, townhouses or row houses, secondary suites and residential care facilities as these fires have the potential to spread to adjacent suites.

In Phase 1 of the project [2], 36 fire experiments were conducted with various individual residential furnishings in a well-instrumented 16 m^2 room (with dimensions 3.8 m wide x 4.2 m long x 2.4 m high) to capture the effect of radiation feedback and other room effects on fire behaviour. The furnishings tested included mattresses, bed clothes, bed assemblies, upholstered seating furniture, clothing arrangements, books, plastic audio/video media and storage cases, toys and a computer workstation setup.

In Phase 2, the fire experiments were conducted in a specially constructed one-storey test facility, which was designed to represent a single storey of a multi-family dwelling, such as a main floor or second storey, having a floor area of approximately 48 m^2. The fire experiments will hereafter be referred to as “tests”, which is typical terminology in the field of fire research. The experimental (or test) facility permitted a flexible array of test configurations to be constructed, such as: single rooms with floor dimensions of 3.8 m x 4.2 m (area: 16 m^2) or 3.2 m x 3.5 m (area: 11.2 m^2), multiple

rooms or a single large room covering the entire 48 m^2 floor area to simulate a main floor in a multi-family dwelling, for example. The fuel load in the tests consisted of real residential furnishings and all of the fires were initiated with a flaming ignition source resulting in rapidly developing fires in all of the 13 tests where the first-ignited item was a primary combustible furnishing (PCF). In order to study a kitchen fire, rather than using direct impingement on a PCF, a more realistic ignition source, a stove-top oil fire, was used. Without direct impingement on a PCF, the growth of the fire was less rapid.

The test variables to develop the complete matrix of 14 tests were derived, in consultation with the project consortium, from six main layouts to explicitly evaluate the effect of ventilation, fuel load density and composition, ignition location, and sprinklers on the room fire. Tenability was studied by conducting a multi-room experiment in which fire effluent from the room of origin was allowed to flow into an adjacent room, where smoke density and the concentration of O_2, CO_2 and CO gases was measured. Two tests were devoted to studying fires in residential care dwellings (bedrooms) and secondary suites, which were considered to have a similar composition of furnishings to those in regular dwellings.

The tests were well-instrumented, with approximately 130 to 150 data measurement points (channels of data) used per test, in order to obtain the following measurements:

a) Heat release rate (HRR);

b) Temperatures;

c) Thermal radiation flux (heat flux)[1];

d) Concentrations of O_2, CO_2 and CO gases at various locations, and;

e) Gas flow velocities in the window openings and the exhaust duct, and;

f) Static pressure.

The HRR and room temperatures (measured using thermocouple trees) were two of the most important measurement quantities given their role in defining the potential of a fire to cause damage to the surrounding building elements by thermal-induced degradation.

[1] The term “heat flux” is used to refer to thermal radiation flux in this report.

2 Literature Review

2.1 Stages of Room Fire Development

The different stages of fire development in a room have been studied intensely for many years and excellent treatises can be found in the widely available literature [3 - 6]. Post-flashover room fires are conventionally understood to undergo four distinct stages of fire development[2], as shown in Figure 1 [7, 8], from ignition to extinction: incipient, growth, ventilation-controlled or fully-developed[3], and decay.

Following ignition, the course of a fire is generally described by [9]:

a) the incipient and growth period (also referred to as the pre-flashover period);
b) whether flashover occurs or not;
c) time to reach a peak HRR;
d) fully-developed or post-flashover period, and;
e) decay period.

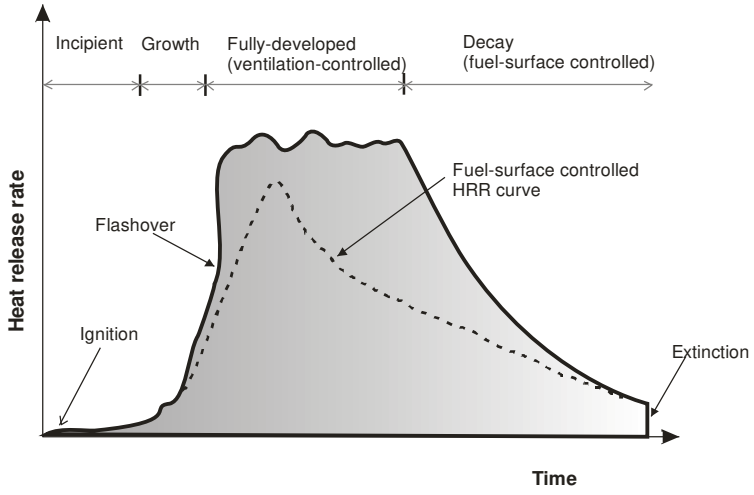

Figure 1. Stages of fire development in a room in the absence of an active suppression system [8].

The duration of the incipient phase depends on the strength and location of the source of ignition, ventilation conditions and the thermal properties of the combustible materials. In addition to these factors, fire development in a room is also understood to be influenced by the amount, type,

[2] Fire development is here defined as the progression of a fire from ignition to extinction.

[3] Full-room involvement is characterized by the burning of all exposed combustible surfaces and the burning rate (HRR) is limited by the size of the ventilation (window) opening.

position, spacing, orientation, and surface area of the fuel package, and the thermal inertia of the materials constituting the boundaries of the room [4].

The heat release rate during the growth stage is commonly approximated by the parabolic curves known as t-squared fires [8]. In a t-squared fire, the burning rate is assumed to vary proportionally to time squared. The NFPA t-squared design fires [10], given by Equation (2.1), are widely used and referenced in the literature:

$$\dot{Q} = \dot{Q}_o \left(\frac{t}{t_o} \right)^2 \tag{2.1}$$

where:

$\dot{Q}$ = rate of heat release (kW);

$\dot{Q}_o$ = reference heat release rate (kW), usually taken to be 1,055 kW.

t_o = time to reach reference heat release rate (s)

t = time after effective ignition (s)

The various categories of fire growth, which are commonly used, are given in Table 1 and illustrated graphically in Figure 2.

Table 1. Categories of t-squared Fires [7].

Growth Rate	**Design Fire Scenario**	**Characteristic time, t_o (s)**
Slow	Floor coverings	600
Medium	Shop counters, office furniture	300
Fast	Bedding, displays and padded work-station partitioning	150
Ultra-fast	Upholstered furniture, lightweight furnishings, non-fire-retarded plastic foam storage, cardboard, and plastic boxes in vertical storage arrangement.	75

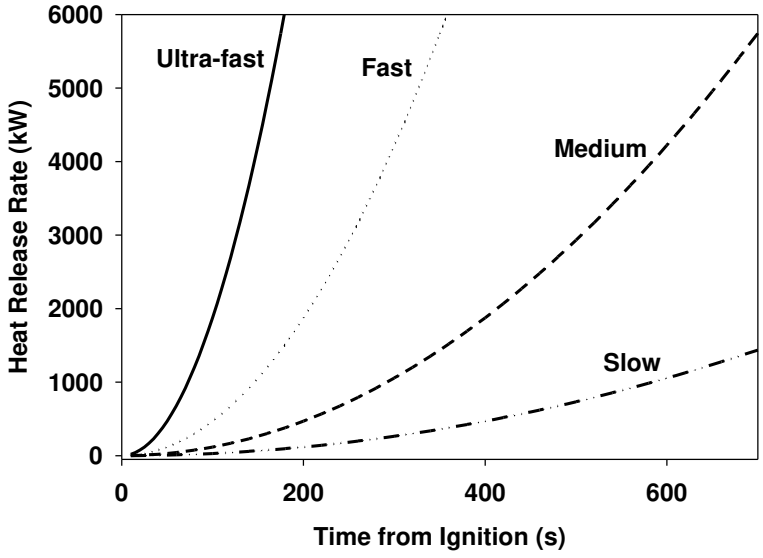

Figure 2. t-squared fires, rates of energy release [8].

Many studies have observed that the burning rate of fuel elements depends on the rate of flow of outside air into the enclosure. The flow of air through ventilation openings, such as windows and doors into a room, has been shown [6] to be proportional to the ventilation factor, F_v ($\mathrm{m}^{5/2}$), which is given by:

$$F_v = A_o \sqrt{H_o} \tag{2.2}$$

where A_o is the area of the opening and H_o is the height of the opening. For a room containing more than one opening, A_o and H_o are the total area of the openings and weighted height of the openings, respectively [4]. For n openings, H_o is given by Equation (2.3):

$$H_o = \frac{\sum_1^n A_n H_n}{A_o} \tag{2.3}$$

where:

n = number of openings

$A_o = \sum_1^n A_n$

The maximum air flow through a given room opening is given as [11]:

$$\dot{m}_{air} = 0.5 F_V \tag{2.4}$$

The dependence of the rate of burning on F_V is often expressed in terms of an opening factor, F_o ($\mathrm{m}^{1/2}$), given by:

$$F_o = \frac{F_V}{A_T} \tag{2.5}$$

where A_T (m^2) is the total internal surface area of the enclosing surfaces. F_V and F_o are used in many empirical fire correlations.

The maximum HRR is the value at which any one of the following events occurs [8]: a) the fire becomes ventilation-controlled and combustion proceeds at a relatively steady rate; b) a fire suppression system activates; c) the decay phase begins (in a fuel-controlled fire). Fires involving multiple combustibles, which become involved in the fire at different times, may exhibit a different behaviour such as having multiple HRR peaks.

The ventilation-controlled HRR (HRRv) is calculated by using Equation (2.6). For most fuels, the heat released per unit mass of air consumed is approximately equal to 3,000 kJ/kg [11]; therefore, the HRRv can be determined from:

$$HRRv = 1500\ F_v \tag{2.6}$$

2.2 Flashover

Flashover is a stage in the course of a fire during which exposed surfaces of most of the combustibles within the room suddenly ignite and the fire is no longer restricted to the first item ignited. At this stage, the HRR, temperature, smoke production and smoke toxicity increase rapidly until a further increase is restricted by the rate at which air flows through the available room openings [11]. The occurrence of flashover is generally believed to be promoted by hot-gas temperatures between 500°C and 600°C, and radiation heat flux levels of about 15 to 20 kW/m^2 at the floor level of the room [4]. The appearance of flames from an enclosure's openings is also said to indicate imminent flashover [4]. A more detailed discussion of flashover is provided by Poulsen et al. [12]

Simple correlations and more elaborate expressions are available in the literature [6, 11, 13, 14], which can be used to determine the likelihood of flashover and whether or not a fire will be ventilation-controlled or fuel-controlled, based on the knowledge of the HRR, size of the room, thermal properties of the materials forming the boundaries of the room, and the size and number of ventilation openings. Following flashover, fires usually progress rapidly to the fully-developed stage, where the rate of combustion is characterized by high HRRs and temperatures under ventilation-controlled conditions. Depending on the composition of the fuel load and room configuration, external combustion (and a degree of combustion inefficiency) is known to occur during the fully-developed stage, in which case the peak HRR measured outside the fire

compartment can exceed the ventilation-controlled value. When most of the combustible materials are expended, the HRR diminishes and the decay phase ensues.

2.3 Flashover Correlations

The following are three commonly used correlations for predicting flashover [11]. A more detailed discussion of these methods is provided by Poulsen et al. [12]:

2.3.1 Babrauskas' Correlation

Babrauskas' correlation [15] is given as:

$$\dot{Q}_{FO} = 750\, A_o \sqrt{H_o} \tag{2.7}$$

Where $\dot{Q}_{FO}$ (kW) is the heat release rate that will cause flashover to occur.

2.3.2 Thomas

The correlation by Thomas [16] is given as:

$$\dot{Q}_{FO} = 7.8\, A_T + 378\, A_o \sqrt{H_o} \tag{2.8}$$

2.3.3 McCaffrey, Quintiere and Harkleroad (MQH)

McCaffrey, Quintiere and Harkleroad [17] used a simple energy balance to develop the correlation given by the following equation:

$$\dot{Q}_{FO} = \left[\sqrt{g}\; c_p \rho_\infty T_\infty^2 \left(\frac{\Delta T_g}{480} \right)^3 \right]^{1/2} \left(h_k\; A_T\; A_o\; \sqrt{H_o} \right)^{1/2} \tag{2.9}$$

where:

ΔT_g Upper gas temperature rise above ambient (T_g - T_∞)

h_k is a heat transfer coefficient for the boundaries given by Equations (2.10) and (2.11) :

$$h_k = \sqrt{\frac{k \rho c_p}{t}} \; for\, t < \frac{\alpha \delta_w^{\,2}}{4} \tag{2.10}$$

$$h_k = \frac{k}{\delta_w} \; for\, t > \frac{\alpha \delta_w^{\,2}}{4} \tag{2.11}$$

where:

A_T total internal surface area of a room (m^2)

δ_w is the wall thickness (m)

α is the thermal diffusivity $\left({}^{k}/_{\rho c_p}\right)$ of the wall material (s^{-1})

k is the thermal conductivity of the boundary and (kW/m.k)

t is the time from fire start (s)

2.4 Calculating Temperatures in Post-Flashover Room Fires

The calculation of temperatures in post-flashover room fires has been studied for many decades and the thermal and fluid dynamics of the fires are well known [18] and documented in the published literature. Based on the existing theory [18], the following factors are known to determine the fire-induced temperature:

a) Fuel pyrolysis rate;
b) Size of ventilation openings (governs oxygen supply, radiation and convection losses);
c) Thermal properties of the room's wall and ceiling materials (governs conduction losses);
d) Calorific value of the combustibles (governs the heat release potential);
e) Combustion efficiency (governs amount of potential heat released in the room); and;
f) Effective emissivity of the fire gases (governs radiation heat transfer).

Many models for calculating temperatures in post-flashover fires are available in the published literature [11, 19]. The fundamental mathematical modelling approach that is employed to calculate the fire temperature involves conducting an energy balance on the room. Under ideal combustion conditions, achieved at 100% combustion efficiency with no heat losses, the absolute maximum theoretical temperature (also known as the adiabatic flame temperature) achieved by the combustion of most common materials in normal air is reported to be in the narrow range of 1,970°C – 2,070°C [18]. Each of the factors listed contribute to cause a reduction of the adiabatic flame temperature to its actual value in a room fire.

A common simplification (the so-called "well-stirred-reactor" model) in modelling post-flashover room fires is to assume that the combustion gases in the room behave as if they were well-mixed, i.e., their properties are uniform throughout the volume [6, 20]. Therefore, in the well-stirred-reactor model, the temperature during the post-flashover fully-developed phase is assumed to be uniform throughout the room, allowing it be modelled as a single control volume. The validity of the well-stirred-reactor model has been questioned before and found not to be accurate [21, 22]. The CFMRD research project presented an opportunity to further evaluate the accuracy of the well-stirred-reactor approximation using a more extensive set of realistic room fire tests.

The available correlations were reviewed and the following four methods were selected for use in this study for calculating room temperature and fire duration (fire severity) during the post-flashover phase.

2.4.1 Law's Correlation

Law's correlation [11] is given as:

$$T_{g(\max)} = 6000 \frac{\left(1 - e^{-0.1\Omega}\right)}{\sqrt{\Omega}} \tag{2.12}$$

where $T_{g(\max)}$ is the maximum gas (fire) temperature and Ω (the opening factor) is determined from:

$$\Omega = \frac{\left(A_T - A_o\right)}{A_o \sqrt{H_o}} \tag{2.13}$$

and ($A_T - A_O$) is the surface area of the room, which is exposed to heat. Equation (2.12) represents the upper limit of the temperature rise for a given Ω [11]. If the fuel load is low, this value may not be reached. The average fire temperature, T_g, is given by:

$$T_g = T_{g(\max)} \left(1 - e^{-0.05\Psi}\right) \tag{2.14}$$

where

$$\Psi = \frac{L}{\left[A_o \left(A_T - A_o\right)\right]^{0.5}} \tag{2.15}$$

where

L is the fuel load in (kg of wood) and the effective duration of the fire is given by:

$$\tau = \frac{L}{\dot{m}_f} \tag{2.16}$$

where $\dot{m}_f$ is the rate of burning in kg/s. This is obtained from the empirical correlation for wood:

$$\dot{m}_f = 0.18 A_o \sqrt{H_o (RW/RD)} \left(1 - e^{-0.036\Omega}\right) \quad \xi < 60 \tag{2.17}$$

where RW and RD are the width and depth of the room, respectively, and:

$$\xi = \frac{\dot{m}_f}{F_V} \left(\frac{RD}{RW}\right)^{0.5} \tag{2.18}$$

2.4.2 Ma and Makelainen's Correlation

Ma and Makelainen [23] developed a parametric temperature-time curve for structural fire design for small and medium room fires. The method was said to predict temperature history of fully-developed room fire with reasonable precision and applies to predominantly cellulosic fuels. The correlation is given as follows:

$$\frac{T_g - T_0}{T_{gm} - T_0} = \left[\frac{t}{t_m} \exp\left(1 - \frac{t}{t_m}\right) \right]^{\delta} \tag{2.19}$$

$$T_{gm} = 1240 - 11 \frac{A_T}{A_o \sqrt{H_o}} \tag{2.20}$$

For fuel surface controlled fire, the maximum gas temperature would be:

$$T_{gm} = 14.34 \Big/ knq \sqrt{\frac{A_T}{\eta_{cr} A_o \sqrt{H_o}}} \tag{2.21}$$

where:

k = ratio of floor area to the total surface area of the room

n = ration of fuel surface area to its mass.

q = fire load density per unit floor area (kg of wood / m^2)

t = time (min)

T_g = hot gas temperature (°C)

T_{gm} = maximum hot gas temperature (°C)

T_0 = reference temperature, taken to be 20°C.

t_m = time at which maximum hot gas temperature occurs (min)

δ = shape constant for the curve.

$\eta_{cr} = \dfrac{A_T}{A_o \sqrt{H_o}}$ (differentiates between fuel and ventilation controlled burning)

2.4.3 Tanaka's Correlation

According to Tanaka's correlation [24], the absolute temperature (K) is given as:

$$T = \beta_{F,1} \left(2.50 + \beta_{F,1}\right) T_\infty + T_\infty \qquad for \quad \beta_{F,1} \le 1.00 \tag{2.22}$$

$$T = \beta_{F,1} \left(4.50 - \beta_{F,1}\right) T_\infty + T_\infty \qquad for \quad \beta_{F,1} > 1.00 \tag{2.23}$$

where:

$$\beta_{F,1} = \left(\frac{A_O \sqrt{H_O}}{A_t} \right)^{1/3} \left(\frac{t}{k \rho C_p} \right)^{1/6}$$

T_∞ = ambient temperature = 300 K

t = time (s)

k = thermal conductivity of the enclosure lining (kW/m K)

ρ = density of the enclosure lining (kg/m^3)

C_p = specific heat capacity of the enclosure lining material (kJ/Kg K)

Calculation of burning rate using Sekine's [25] method:

$$\dot{m} = 0.1 A_O \sqrt{H_O} \quad (kg/s) \tag{2.24}$$

Therefore, the burnout time, $\tau_b(s)$, is computed as:

$$\tau_b = \frac{M}{\dot{m}} \tag{2.25}$$

where:

M = total mass of combustible material available for combustion (kg)

$\dot{m}$ = mass burning rate (kg/s)

2.4.4 Eurocode Parametric Curves

In the EUROCODE [26] parametric fire temperature equations for representing post-flashover temperatures, a time-temperature relationship is produced for any combination of fuel load, ventilation openings and wall lining materials. The time-temperature curves from which the equations were derived were produced by Magnusson and Thelandersson [27], and are shown in Figure 3.

Buchanan [3] and Karlsson and Quintiere [4] discuss the methodology employed by Magnusson and Thelandersson to produce the curves in greater detail. The effect of ventilation on the maximum temperature and duration of burning is apparent from Figure 3, and it can also be seen that the peak fire temperature increases with ventilation for any given fuel load.

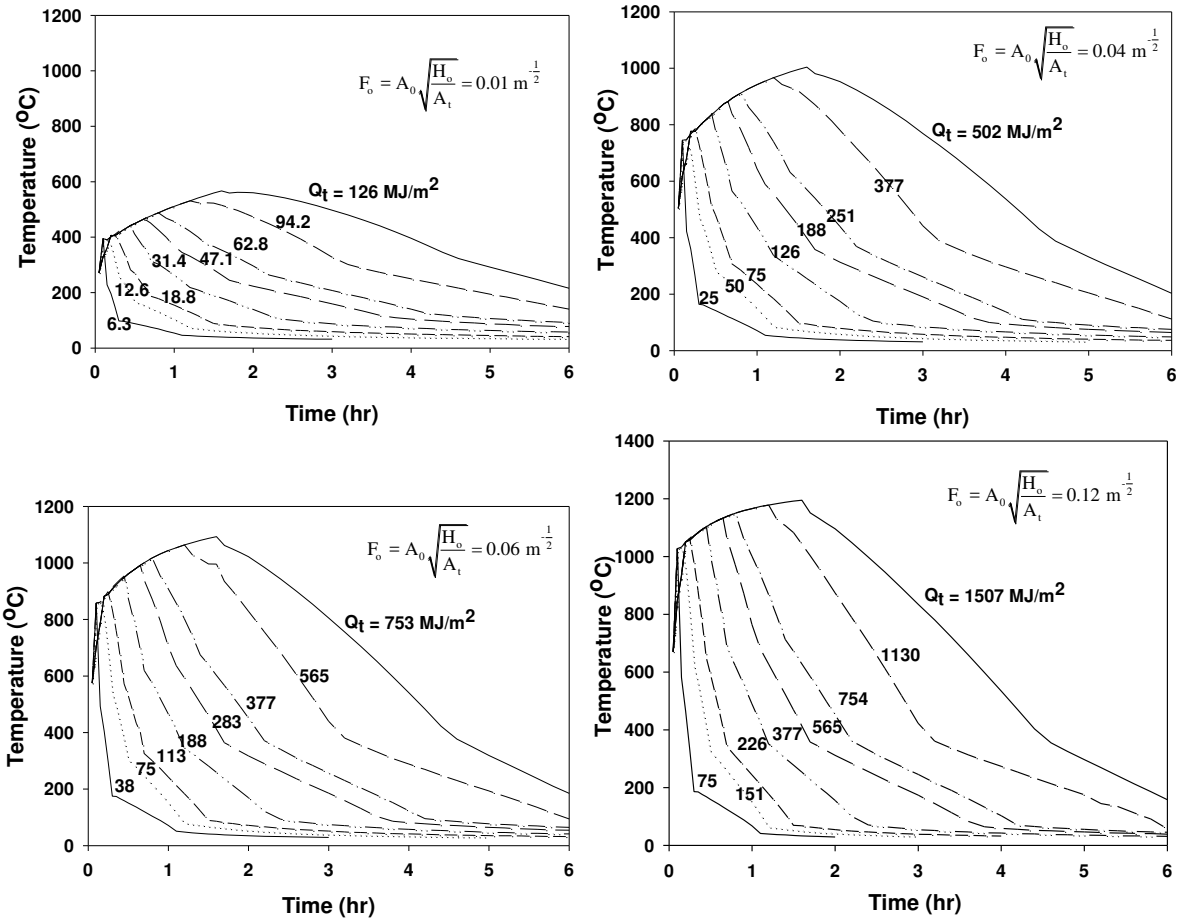

Figure 3. Time-Temperature Curves for Different Ventilation Factors and Fuel loads [27].

The EUROCODE method divides the fire development into two phases: the heating phase (full-developed phase) and the decay phase. The equation for the heating phase is:

$$T = 1325\left(1-0.324e^{-0.2t^*} -0.204e^{-1.7t^*} -0.472e^{-19t^*}\right) \tag{2.26}$$

where T is the temperature (°C) and t^* is a time parameter (in hours) that is given by:

$$t^* = t\left(\frac{(F_o/F_{ref})}{(b/b_{ref})}\right)^2 \tag{2.27}$$

where b is $\sqrt{k\rho C_p}$ (Ws$^{0.5}$/m^{2}K), F_o is the opening factor given by Equation (2.5), F_{ref} is the reference value of the opening factor, taken to be 0.04, $k\rho C_p$ is the thermal inertia, and b_{ref} is the reference value of $\sqrt{k\rho C_p}$, given the value of 1160. Therefore, Equation (2.27) can be rewritten as:

$$t^* = t\left(\frac{F_o}{\sqrt{k\rho C_P}}\right)^2\left(\frac{1160}{0.04}\right)^2 \qquad (2.28)$$

where t is the time (in hours).

The EUROCODE temperature-time curve in the decay phase is given by:

$$\begin{aligned} T_g &= T_{g,max} - 625(t^* - t_d^*) && \text{for } t_d \le 0.5 \\ T_g &= T_{g,max} - 250(3 - t_d^*)(t^* - t_d^*) && \text{for } 0.5 \le t_d^* \le 2.0 \\ T_g &= T_{g,max} - 250(t^* - t_d^*) && \text{for } t_d^* \ge 2.0 \end{aligned} \qquad (2.29)$$

where:

$T_{g,max}$ is the maximum temperature in the heating phase for $t^* = t_d^*$ and:

$$t_d^* = \frac{0.13\times10^{-3}Q_t''}{F_o}\left(\frac{F_o}{\sqrt{k\rho c_p}}\right)^2\left(\frac{1160}{0.04}\right)^2 \qquad (2.30)$$

The duration of the heating phase is given in terms of real time, by:

$$t_d = \frac{0.13\times10^{-3}Q_t}{F_o} \qquad (2.31)$$

therefore, the modified duration time can be rewritten as [4]:

$$t_d^* = t_d\left(\frac{F_o}{\sqrt{k\rho C_p}}\right)^2\left(\frac{1160}{0.04}\right)^2 \qquad (2.32)$$

3 Experimental Program

Fourteen room fire tests were conducted in a one-storey test facility, which was designed to represent a single storey of a multi-family dwelling, such as a main floor or second storey, having a floor area of approximately 48 m^2 (obtained from survey results [28]). The tests were based on the six base configurations, which are given in Table 2. Table 3 lists the window sizes and their corresponding theoretical ventilation-controlled HRRs, which varied from approximately 1,500 kW to 6,900 kW (ventilation factors ranging from 1 to 2.76). A detailed description of the following aspects of the experimental setup is provided in Part 1 of the report [1]:

1. <u>One-storey test facility:</u> Construction details of the facility, roof and ceiling assemblies, floor assemblies and test wall sections.

2. Design of room fire tests: Test matrix and related terminology, design fuel loads and test layouts.
3. Instrumentation: Data acquisition system and instrumentation plans.
4. Test procedures: Ignition, test duration and termination.
5. Data Processing: HRRs, temperatures, gas concentrations, smoke optical density, gas velocities and radiation heat flux.

The test matrix was formulated to address the following objectives:

1) Objective #1: Characterize fire behaviour for each of the six base configurations.
2) Objective #2: Evaluate the effect of the following parameters on fire characteristics: ventilation, fuel load composition and fuel load density (FLED).
3) Objective #3: Evaluate the effect of using a residential sprinkler.
4) Objective #4: Determine the repeatability of the measurements. (Repeatability is an assessment of the measurement variability found when the same test is repeated using the same apparatus under identical conditions. In many experimental studies, it is desirable to have less variability, i.e. good repeatability in the measurements is an indication of a good level of confidence in the results).
5) Objective #5: Determine the progressive mass loss during a test.

Table 4 provides the complete list of the tests conducted, indicating some of the key variables and details. Only one test (PRF-13) was conducted with load cells installed to measure the rate of mass loss during the test. Table 5 shows the status of Test Wall Section (TWS) installations in the tests.

Table 2. Base configurations of PRF Tests.

No.	Base configuration	Floor dimensions (floor area)	Tests
B1	Primary bedroom	3.8 x 4.2 m (16.0 m^2)	PRF-01, -02, -03, -04
B2	Secondary bedroom #1	3.2 x 3.5 m (11.2 m^2)	PRF-05, -07
B3	Secondary bedroom #2	3.2 x 3.5 m (11.2 m^2)	PRF-09
B4	Living room	3.8 x 4.2 m (16.0 m^2)	PRF-06, -11, -12, -13
B5	Secondary suite	Bedroom: 3.8 x 4.2 m (16.0 m^2) Living room: 3.4 x 6.3 m (21.4 m^2)	PRF-08
B6	Main floor (living/dining/kitchen)	7.3 x 6.3 m (46.0 m^2)	PRF-10, -14

Table 3. Window sizes used in the Tests.

Window ID	Dimensions Width x Height (m)		F_V ($m^{5/2}$)†	HRRv†† (kW)	Tests
	#1	#2			
V1	1.5 x 1.5	-	2.76	4,140	PRF-01, -03, -04, -06, -11, -12, -13
V2	1.4 x 1.2	-	1.84	2,760	PRF-02, -05
V3	1.0 x 1.0	-	1.00	1,500	PRF-09
V4	1.5 x 1.5	1.4 x 1.2	4.56	6,840	PRF-08, -10, -14
V5	1.4 x 1.2	0.7 x 1.2†††	2.76	4,140	PRF-07

† Ventilation factor ($F_v = A_o\sqrt{H_o}$) where A_o = sum of openings and Ho = average of heights;

†† Ventilation-controlled HRR calculated assuming a combustion efficiency of 100%: HRRv (kW) = 1,500 x F_v

††† Window in Room #2 was taken to be the governing opening size since it was smaller than the doorway in Room #2, which measured 0.9 m wide x 1.9 m height.

Table 4. Summary of the setup and variables for the tests.

Test ID	Config.†	Objective	Variables		
			Window	Floor finish	Additional details
PRF-01	B1	1	V1	Carpet	Base configuration
PRF-02	B1	2	V2	Carpet	Evaluated the effect of a reduced window size (compared to PRF-04).
PRF-03	B1	2	V1	Hardwood	Evaluated the effect of increased wood composition on fire behaviour • Achieved by replacing the carpet and under pad with hardwood flooring.
PRF-04	B1	1	V1	Carpet	Base configuration: Repeat of PRF-01, which was terminated prematurely.
PRF-05	B2	1 and 2	V2	Carpet	Base configuration and also evaluated effect of high FLED.
PRF-06	B4	1	V1	Carpet	Base configuration.
PRF-07	B2	2	V5	Carpet	Multi-room with door open to adjacent room (PRF-05 fuel load), studied: 1. Smoke flow and tenability conditions in Room #2. 2. Effect of increased ventilation (compared to Test PRF-05).
PRF-08	B5	1	V4	Carpet and OSB	Base configuration

Test ID	Config.†	Objective	Variables		
			Window	Floor finish	Additional details
PRF-09	B3	2	V3	Hardwood	Base configuration
PRF-10	B6	1	V4	Hardwood and vinyl	Base configuration
PRF-11	B4	3	V1	Carpet	Evaluated the effect of a residential sprinkler. Most of the SCFs were excluded since it was anticipated that the sprinkler would extinguish the fire before they ignited.
PRF-12	B4	4	V1	Carpet	Repeat of Test PRF-06.
PRF-13	B4	5	V1	Carpet	Based on configuration B4 with: 1. Load cells installed to measure mass loss. 2. Room surfaces lined with cement board to prevent corruption of mass loss measurements.
PRF-14	B6	2	V4	Hardwood and vinyl	Evaluated the effect of a kitchen fire started by a stove-top fire source.

† Base configuration.

Table 5. Status of TWS installations in the tests.

Specimen	GWB (single layer on each side)	Location	Installation status in PRF Tests ("X" denotes presence of a particular TWS)													
			1	2	3	4	5	6	7	8	9	10	11	12	13	14
TWS 01	12.7 mm Regular	East	X	X	X	X	X	X	-	X	-	X	-	X	-	X
TWS 02	15.9 mm Type X	East	X	X	X	X	X	X	-	X	-	X	-	X	-	X
TWS 03	12.7 mm Regular	West	-	-	X	X	X	-	X	-	X	-	-	-	-	-
TWS 04	15.9 mm Type X	West	-	-	X	X	X	-	X	-	X	-	-	-	-	-

Details of the fuel load, such as total mass, estimated FLED and material composition, are given in Table 6. Where applicable, calorific values measured in Phase 1 of the project [2] were used to calculate the FLED. Fuel load quantities included combustible structural elements (such as, OSB sub-floor and wood framing for test wall sections) that were expected to be involved in the fire.

Table 6. Quantity and composition of the design fuel load used in the tests.

Test no.	Window	Material Mass Composition (%)					Total Mass	FLED	HC_{avg}
		W	P	T	TP	NC	Kg	MJ/m^2	MJ/Kg
PRF-01	V1	58.6	2.4	26.5	10.1	2.5	790.5	869.0	18.0
PRF-02	V2	60.1	2.3	25.5	9.7	2.4	809.2	910.6	18.1
PRF-03	V1	73.6	1.8	16.4	6.2	1.9	1,000.8	976.1	15.8
PRF-04	V1	62.2	2.2	23.7	9.5	2.3	831.4	914.5	17.7
PRF-05	V2	59.9	3.5	19.1	14.1	3.3	677.8	999.3	17.1
PRF-06	V1	60.3	11.7	6.2	17.4	4.4	714.2	689.4	16.0
PRF-07	V5	57.7	3.7	20.1	14.9	3.5	642.8	962.6	17.4
PRF-08	V4	65.6	7.0	16.3	10.6	2.0	1,403.2	617.3	16.6
PRF-09	V3	79.7	0.8	9.4	6.8	3.3	618.5	750.7	14.1
PRF-10	V4	89.1	4.2	0.1	5.7	0.9	1,878.5	535.2	13.5
PRF-11	V1	70.1	0.0	5.7	9.9	4.3	414.6	404.9	16.4
PRF-12	V1	61.0	11.3	5.8	18.5	3.5	707.0	682.6	16.0
PRF-13	V1	61.1	11.3	5.8	18.4	3.5	710.0	685.6	16.0
PRF-14	V4	89.9	4.3	0.1	5.7	0.9	1,882.3	535.2	13.5

FLED: Fuel load density; W: Wood P: Paper; T: Textiles; TP: Thermo-plastics; NC: Non-combustible, e.g. Metal; HC_{avg}: Mean theoretical heat of combustion.

The fire was initiated on the first-ignited-item using the appropriate ignition method given in Table 7. The first-ignited-item and ignition sources were selected in Phase 1 of the project [2]. The planned duration of each test was 1 hour.

Table 7. Ignition sources used in the tests.

First ignited item	Tests (PRF no.)	Ignition source	Strength	Reference Standard
Bed assembly	01, 02, 03, 04, 05, 07, 09, 08	T-burner	9 kW (6.6 L/min) for 50s positioned 0.47 m from the head-side	Developed in Phase 1 [2].
Two-seat sofa (loveseat)	06, 11, 12, 13	Square-burner	19 kW (13.0 L/min) for 80s	ASTM 1537 [29]
Oil pan simulating stove-top fire	14	Heated cooking oil in oval roaster	Approximately 60 kW	Ad hoc

It is acknowledged that the ignition sources listed in Table 7 are severe in comparison to realistic igniters such as matches, cigarette lighters and candles, which are often mentioned in many fire

statistics as the major causes of residential fires. However, it is common practice in the fire research community to use ignition sources similar to those listed in Table 7 for the benefit of standardization and repeatability. Weaker ignition sources may affect the time to ignition; however, it is believed that the post-ignition phase, during which the fire becomes self-sustaining, is the most important period in studying fire behavior and hence the reason for selecting stronger ignition sources that ensure ignition. A study on the influence of ignition sources on HRR in a furniture calorimeter [30] compared propane burners with ignition strengths ranging from 1.7 kW to 30 kW and found that the burning behavior of the burning items was similar regardless of the type of burner used. As well, the repeatability was better when a stronger ignition source was used. In that study they considered a HRR of 50 kW to be the fire size that can be detected by persons who are not fully alert or those who are further away from the burning item or a fire detector. Therefore, the period before sustained ignition occurs is considered to be relatively unimportant to the assessment of burning behavior and can be accounted for by appropriately modifying the time to ignition or attainment of the experimental HRR at ignition. The above methods have also been supported by Babrauskas and Peacock [31] who stated that although fire deaths are mainly caused by the inhalation of toxic gases, HRR was still the best indicator of fire hazard and that the relative toxicity of combustion gases, and delays in the ignition time as measured by small flame tests, had been shown to have a minor effect on the fire severity.

4 Results and Analysis

Apart from the HRR vs. time graphs that are provided in Appendix A, none of the data discussed in this report were smoothed. The use of smoothing techniques, such as running time averages was considered, but was not pursued since there is a possibility of damping out some real features.

4.1 Summary of Quantitative Results

Table 8 summarizes the test results: HRR, total heat released, mean maximum hot layer temperatures and peak heat flux. Five tests (PRF-01, -05, -10, -13 and -14) were terminated early due to safety concerns caused by temperatures in the roof joist space exceeding 300°C. The graphical results for all of the measurement points in each test are given in Appendix C (Figures C-1 to C-334) in Part 1 of the report [1]. In Table 8, the mean maximum temperature ($\bar{T}_{\max}$) is defined as the mean of the temperatures measured at a location in the hot layer that is calculated over the duration of the post flashover phase (stage R4, which is defined later in the report). The mean maximum temperature is calculated either for a zone in a single quadrant of the room or for the entire room (four zones associated with the four quadrants of the room).

In 12 of the tests (excluding Test PRF-11, which had an active sprinkler system installed), where the first-ignited-item was a PCF (either a bed assembly or a sofa), the fires developed rapidly and flashover (full room involvement) occurred within five minutes of ignition.

Table 8. Summary of the test results.

Test ID	Peak HRR (kW)	THR (MJ)	$\bar{T}_{max}$ (°C)	q''_{mf} (kW/m^2)	q''_{mwc} (kW/m^2)	T_∞ (°C)	Test Date	Test Duration (min)
PRF-01	6,752 (232)†	9,912	1,061	288	315	25.0	24-Jun-2009	42
PRF-02	3,642 (262)	8,650	1,060	89	279	6.6	27-Oct-2009	64
PRF-03	6,103 (303)	9,821	1,202	251	285	-15.0	4-Feb-2010	63
PRF-04	6,014 (239)	10,225	1,129	189	298	-1.0	3-Mar-2010	61
PRF-05	3,782 (928)	7,136	1,140	262	239	19.1	31-May-2010	56
PRF-06	5,133 (255)	8,214	1,119	239	276	20.0	20-Jul-2010	60
PRF-07	4,134 (636)	7,219	1,142	X†††	293	12.5	13-Oct-2010	64
PRF-08	9,230 (1,212)	14,460	1,118	203	276	-14.0	14-Dec-2010	61
PRF-09	2,793 (841)	5,911	1,039	200	295	-6.0	23-Feb-2011	60
PRF-10	8,776 (1,241)	16,660	1,163	236	270	20.0	11-May-2011	45
PRF-11	110 (47)	28	117††	X	4.4	21.0	22-June-2011	30
PRF-12	5,084 (515)	8,402	1,066	179	261	24.0	13-Sept-2011	64
PRF-13	5,474 (546)	7,750	1,084	X	280	13.0	9-Nov-2011	44
PRF-14	9,090 (1,337)	12,725	1,036	224.	266	-3.0	14-Feb-2012	40

$\bar{T}_{max}$ – Mean maximum hot layer temperature (of four zones) in stage R4 of the fully-developed phase; q''_{mf} – Maximum heat flux at floor level; q''_{mwc} – Maximum heat flux on the walls and ceiling; THR – Total heat release.

†Time to reach the peak HRR (s); †† Measured at a single point; ††† Data acquisition or instrument failure.

In one other test, PRF-14, the first-ignited-item was a kitchen cabinet that was ignited by a simulated stove-top ignition source (an oval roaster containing two litres of cooking oil). This resulted in a slower rate of fire growth (since the wooden cabinets did not ignite and spread flames

readily, which is typical of wood-based furnishings). In Test PRF-14, flashover of the entire space was not observed until about 13 minutes after ignition.

In Test PRF-11, the ceiling-mounted sprinkler activated at 45 s after ignition and was very effective in preventing further fire growth; the HRR did not exceed 110 kW and the maximum temperature recorded at a single point in the room was only 117°C.

4.2 Qualitative Results (Dynamics of Fire Development)

The pictorial sequences of fire progression (from ignition to extinguishment) for each test are provided in Appendix D in Part 1 of the report [1]. Photographs are given at one-minute intervals for the first 14 min of each test and at three-minute intervals for the remaining duration. Photographs showing the aftermath of the tests are given in Appendix D in Part 1 of the report [1].

Due to the complexity of the test series and the voluminous data generated, analysis of the data and formulation of technical opinions of fire development was an ongoing process. In this report, the opinions are presented as a new understanding of fire development ahead of the discussion of test data since it is considered important in the overall analysis of the quantitative results presented in Section 4.3: “Quantitative Results and Analysis”.

4.2.1 Novel Understanding

While the conventional portrayal of fire development (Figure 1; discussed in Section 2.1) is true to a certain extent, the opinion (from observations, data analysis and literature reviews) developed in this research is that the ventilation-controlled phase was actually composed of two distinct phases: a transitional “unsteady” phase (R3) and a conventional “steady” phase (R4), which are depicted in Figure 4. The unsteady phase occurs immediately after the flashover. The duration of Stage R3 was determined based on a combination of:

1. The magnitude of the HRR with respect to the theoretical ventilation-controlled HRR value (HRRv): The measured HRR significantly exceeded the HRRv during Stage R3.
2. Visual observations from test videos: In Stage R3, the room environment appeared to be a sporadic mosaic of bright orange and dark turbulent flames and dense smoke that extended out into the exhaust duct.
3. Temperature gradient: During Stage R3, the measured hot layer temperatures typically increases from the values in the range of 500 – 700°C at flashover to values above 1,000°C, which results in a steep temperature gradient during this period. The end of Stage R3 was determined by a qualitative examination of temperature gradient of the temperature vs. time graphs, i.e. there was a discernible change in the temperature

gradient (from steep to gradual or flat) that was collaborated with features of the HRR profile and video observations.

The end of Stage R4 (beginning of the decay phase) was taken to be the time when the HRR begun to consistently decline below the HRRv value. Based on this approach, the results show that the standard deviation of the mean hot layer temperature (measured with TCs located at either 1.4 m or 2.4 m height) in Stage R4 was generally less than 100°C.

Theoretically, combustion efficiency could be another distinguishing feature for Stage R3 since it is assumed that poor combustion inefficiency due to excessive supply of fuel volatiles contributes to a decrease in the fire temperature. However, since there was no means if measuring combustion efficiency directly, it was inferred from a visual assessment of the colour of the flames, i.e. dark flames are indicative of poor combustion efficiency in the tests. An additional reason for the lower temperatures in Stage R3, than those in Stage R4, is likely due to heat losses from the fire gases to the room boundaries (walls and ceiling), which are at a lower temperature. Therefore, this research identifies five distinct stages of fire development, which are depicted in Figure 4 as R1 to R5, and the conventional portrayal (shown in Figure 1) becomes a special case of the new portrayal (Figure 4), in which there is no unsteady phase. All of the discussion of fire development in this report will be referenced to this new understanding of fire development.

For the fuel loads used in the tests, this research hypothesises that following the flashover there was an excessive liberation of fuel volatiles (likely due to the pyrolysis of thermoplastic fuels) from the surfaces of exposed combustibles upon their exposure to sufficiently high radiant heat flux (caused by hot layer temperatures higher than 500°C). This resulted in a fuel-rich combustion atmosphere, since there was insufficient oxygen (i.e. less than the stoichiometric requirement) for efficient combustion to occur. Hence, Stage R3 is thought to undergo inefficient (unsteady) combustion and a large amount of un-burnt fuel volatiles left the fire room and ignited (completed burning) outside where fresh air with sufficient oxygen was entrained into the exhaust stream. Increased production of fuel volatiles and external combustion resulted in the peak HRR occurring immediately after the flashover and its magnitude was significantly greater than the ventilation-controlled HRR value. The duration of Stage R3 is considered to depend on factors such as window size, heat losses to the room boundaries (room size) and the quantity and composition of the fuel load (particularly the thermoplastic content), as will be shown later in this report.

Stage R4 was considered to have occurred when most of the excess fuel volatiles from thermoplastic combustibles had been consumed and the ventilation-regulated pyrolysis of wood-based combustibles (the majority of the fuel load) predominated. At this stage, the fuel/air ratio likely approached stoichiometric conditions and the flames inside the room and those flowing out of the window opening were characterized by an increasingly orange colour punctuated by sporadic

streaks of dark smoke. External combustion is also believed to occur in Stage R4, to a lesser extent, and it is known that actual heat release in the room can be less than the theoretical maximum (ventilation-controlled) value supported by the available window [20], i.e. less than 100% combustion efficiency.

The combustion behaviour described in Stage R3 has long been known and documented in the literature; however, the novelty alluded to here lies in this research's emphasis on the importance of Stage R3 as a distinct phase that has a significant effect on initial post-flashover temperatures and, consequently, the destructive impact of a fire, as will be shown when room temperature data are discussed.

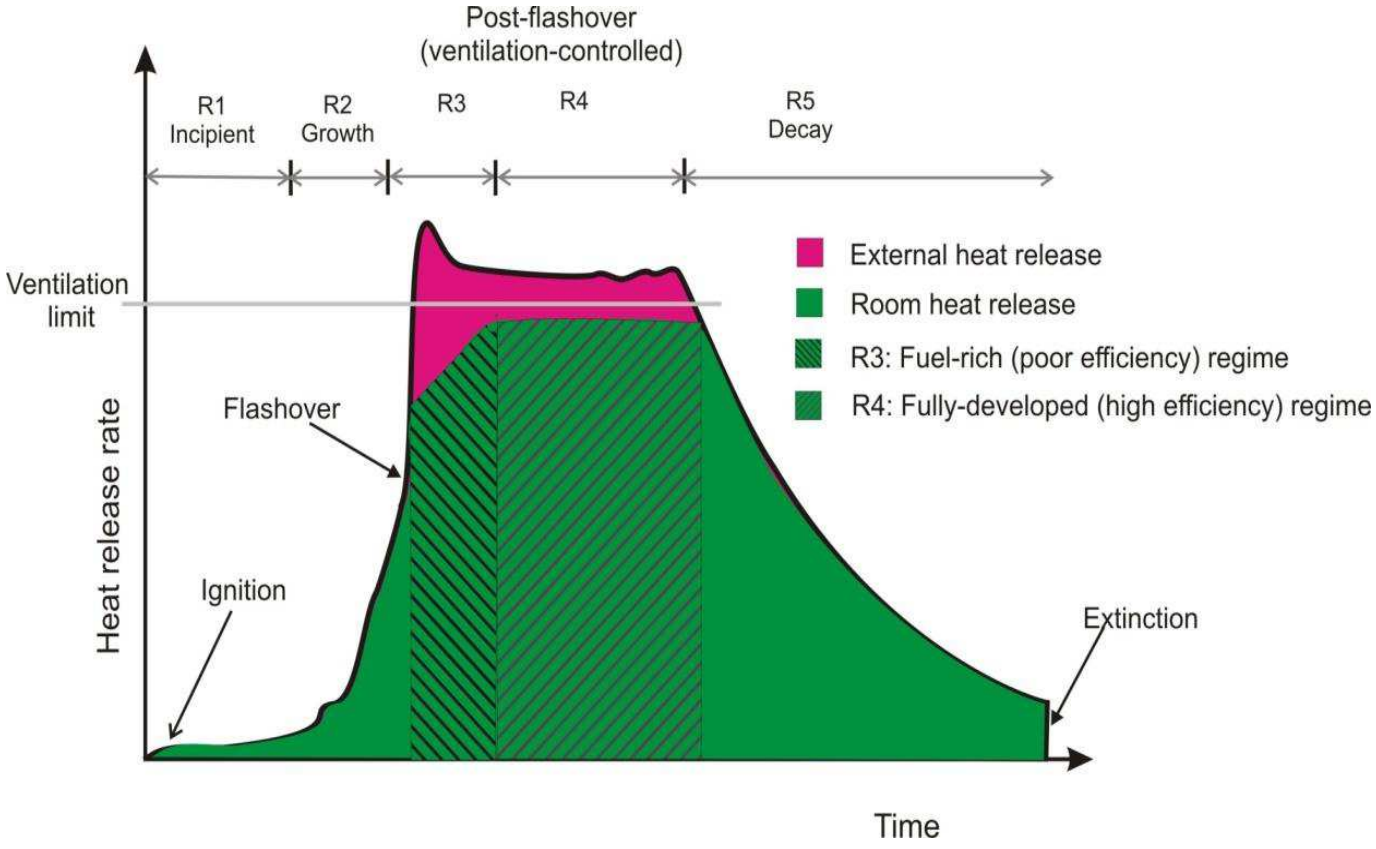

Figure 4. Novel division of stages of fire development based on CFMRD test results.

4.2.2 Characteristics of Fire Development

Except for Test PRF-14 (stove-top ignition source), all tests in this research had practically no incipient phase; fire growth (stage R2) began immediately since, by design, the strong ignition sources guaranteed rapid ignition of the first-ignited-item.

4.2.2.1 Observations of Key Features of Fire Behaviour

All of the observations presented here describe features of the fires that could be seen from outside the fire room through the windows and, therefore, may not be true for areas located further inside the room that were not visible from that vantage point due to smoke obscuration. Two important observations were made:

1. **Transition to flashover:** There were two patterns of fire development depending on the size of the fire room, whether small- to medium-sized (floor area not more than 16 m^2, with a single window) or large-sized (floor area greater than 16 m^2 with two windows). These were characterized by the type of transition to flashover, whether it was complete or partial, as observed from outside the fire room:

   a) **Single flashover:**
   - Occurred in tests conducted in small- and medium-sized rooms (configurations B1, B2, B3 and B4);
   - Conformed to the norm that radiant heat from a hot upper layer causes flashover to occur in the entire room when hot layer temperatures and floor-level heat flux thresholds of about 600°C and 20 kW/m^2 [3, 17], respectively, are attained.

   b) **Multiple flashovers:**
   - Occurred in large rooms (configurations B5 and B6);
   - Did not conform to the pattern of single flashover; the room appeared to be split in two halves (zones), with flashover first occurring in the zone containing the first-ignited item (Zone 1 in Figure 5) followed by the distant zone (Zone 2 in Figure 6), after a noticeable time delay.

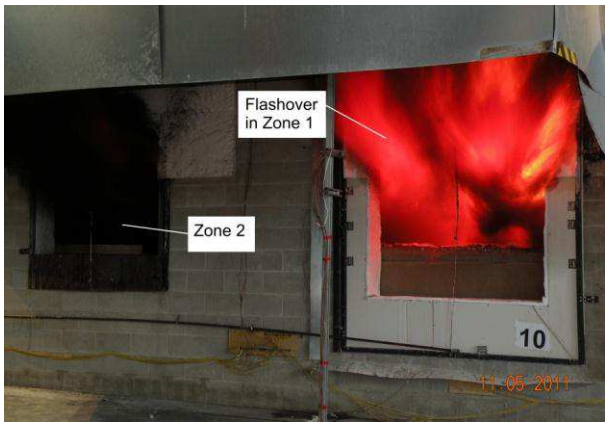

Figure 5. Multiple flashover case (Test PRF-10): Flashover in Zone 1.

Figure 6. Multiple flashover case (Test PRF-10): Flashover in Zone 2.

2. **Zonal burning phenomenon:** Tests that experienced multiple flashovers showed complex zonal burning behaviour in the transition to Stages R3 and R4, i.e. there were two different

zones visible from outsides the test room. Test data supports the notion that each visible zone appeared to undergo different stages of combustion with Zone 2 lagging Zone 1 by an appreciable time period. Figure 7 demonstrates the phenomenon: Zone 1 was undergoing Stage R4 combustion while Zone 2 was undergoing Stage R3 combustion. Figure 8 also demonstrates zonal burning, where Zone 1 was undergoing Stage R5 combustion while Zone 2 was undergoing Stage R4 combustion.

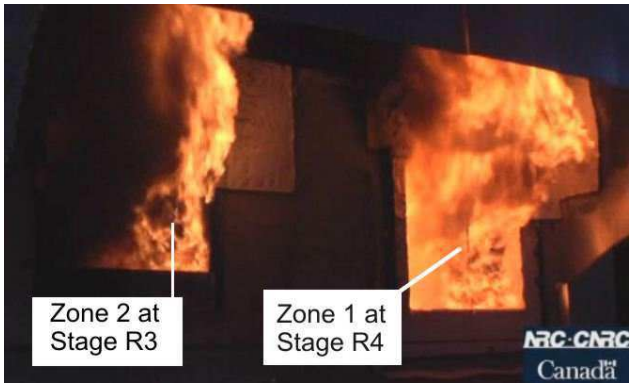

Figure 7. Zonal burning phenomenon in Test PRF-10): Zone 1 undergoing Stage R4 combustion.

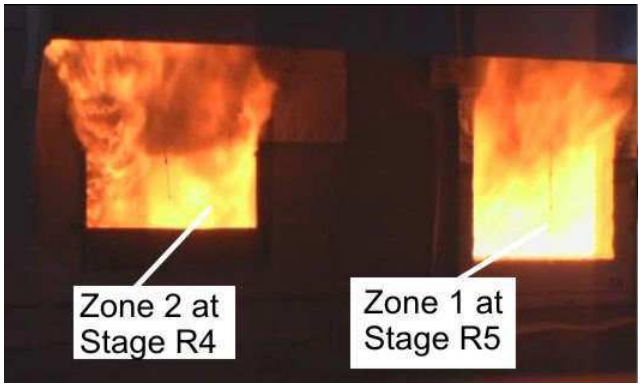

Figure 8. Zonal burning phenomenon in Test PRF-10: Zone 1 undergoing Stage R5 combustion.

4.2.2.2 General Description of Fire Development

Base configuration B1 (primary bedroom, Test PRF-03) with window V1 (1,500 mm x 1,500 mm) is used as the reference case for a general description of fire development below. Following is the sequence of fire development based on review of the test videos:

1. **Incipient phase (Stage R1):** Did not exist since a flaming ignition source was used.
2. **Growth phase (Stage R2;** Figure **9):** After igniting the bed assembly in Tests PRF-01, -03 and -04, the fires in each test developed rapidly, with flames spreading over the surface of the bed while dense dark smoke flowed out of the window soffit. Flames began flowing out of the top left corner of the window.
3. **Transition to flashover (end of Stage R2;** Figure **10):** Flames began to flow out of the entire width of the window, with increasing intensity and turbulence of gas movement inside the room. There was increasing production of dark dense smoke in the west side (lower half) of the room. There was limited visibility into the room.
4. **Single Flashover (Interface of Stages R2/R3;** Figure **11):** Spontaneous ignition of visible combustible surfaces near the window (there was no visibility into the room).
5. **Poor efficiency post-flashover ventilation-controlled phase (Stage R3;** Figure **12):** Room environment appeared to be a sporadic mosaic of bright orange and dark turbulent flames and smoke that extended out of the window and into the calorimeter hood.

6. **High efficiency post-flashover ventilation-controlled (Stage R4;** Figure **13):** Characterized by an increasingly orange colour consistency of the flames with sporadic streaks of dark smoke likely due to burning of thermoplastic materials.
7. **Decay Phase (Stage R5;** Figure **14):** Decreasing turbulence of gas movement and outflow; flames were less dense and the inside of the room became increasingly visible.
8. **Termination:** Extinguishment of fire with water.

Figure 9. Test PRF-03: Flames flowing out of the top left corner of window (130 – 160 s).

Figure 10. Test PRF-03: Transition to flashover – flames flowing out of entire with of window.

Figure 11. Test PRF-03: All visible combustible surfaces igniting (flashover: 190 – 270 s).

Figure 12. Test PRF-03: Poor efficiency post-flashover (270 – 510s; no visibility inside room).

Figure 13. Test PRF-03: High efficiency post-flashover – flames vigorously flowing and extending out of the window (no visibility inside room).

Figure 14. Test PRF-03: Onset of decay phase – flames flowing out of the window with decreasing vigour (inside room becoming visible).

4.2.2.3 Visual Assessment of Fire Development

The visual assessment of fire development for all of the tests that experienced a single flashover is presented Table 9 and shown graphically in Figure 15. Since the observations were based on test videos, it was difficult to visually discriminate between some stages of fire development, particularly during the post-flashover phase, such as the transition to Stages R4 and R5. Observations relating to the onset of flashover (i.e. flames emerging from the windows and ignition of surfaces) were more clearly distinguishable. This qualitative assessment shows that flashover was observed to occur between three and five minutes after ignition in those tests that experienced a single flashover. As well, the effect of reduced window size (lower ventilation) on the duration of the post-

flashover phase manifested itself in the longer times it took for the decay phase to begin in tests PRF-02 and -05.

Table 9. Approximate timeline of observed stages of fire development in tests with a single window in configurations B1, B2, B3 and B4.

Test No.	Flames emerge from window #1 (Stage R2) (min)	All surfaces ignite (Stage R2/R3) (min)	Flames in room have consistent orange colour (Stage R3/R4) (min)	Decay begins (Stage R4/R5) (min)	Termination (min)
PRF-01	2.5	3.8	7.8	22.0	42
PRF-02	2.7	4.9	16.5	41.0	64
PRF-03	2.2	3.2	8.5	28.0	63
PRF-04	2.2	3.3	7.5	25.5	61
PRF-05	2.9	4.3	14.0	35.0	56
PRF-06	2.3	3.3	9.0	26.0	60
PRF-07	2.5	3.2	6.0	20.0	64
PRF-12	3.0	3.3	9.0	22.0	64
PRF-13	3.6	4.3	13.0	23.0	44

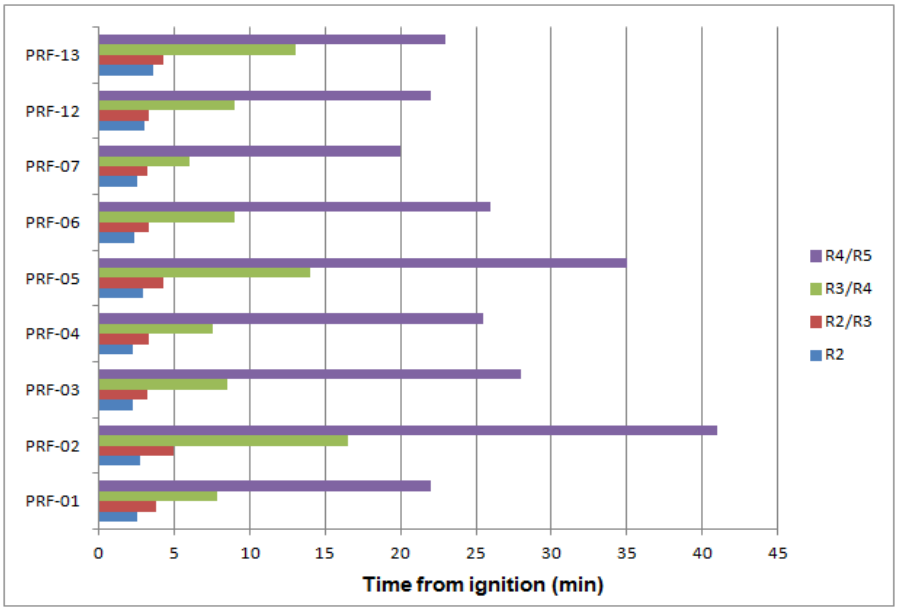

Figure 15. Bar chart presentation of the data in Table 9.

Table 10 summarizes the observations for tests in which multiple flashovers occurred. According to observations, these tests experienced multiple flashovers and a zonal burning phenomenon likely due to a complex combination of several (many of which could not be determined through visual observation) factors, such as:

a) High rates of localized heating and pyrolysis in the ignition zone;
b) Predominant flow of fresh air from both windows towards the fire centered around the first-ignited item, depriving other areas of oxygen (i.e. conditions in other areas could not sustain ignition even though flashover thresholds had been reached) ; and,
c) Differences in pyrolysis rates between areas with relatively high thermoplastic fuel load (e.g. living room in Test PRF-10), and those with wood-based materials, e.g. the kitchen). This is believed to be the reason that Zone 1 (living room) became the dominant combustion zone in Test PRF-14 even though the fire originated in Zone 2 (kitchen), i.e. Zone 1 with largely thermoplastic combustibles (upholstered sofas) consumed the available oxygen.

Table 10. Approximate timeline (in minutes) of observed stages of fire development for multiple flashover tests with two windows in configurations B5 and B6.

Test No.	Stage R2: Flames emerging from window #		Stage R2/R3: All surfaces ignite		Stage R3/R4: Flames in room have consistent orange colour	Stage R4/R5: Decay begins	Termination
	1	2	Zone 1[††]	Zone 2[†††]			
PRF-08	3.6[†]	6.5	4.4	7.3	Zone 1- 6.0 Zone 2 - 19.0	Zone 1 - 22.0 Zone 2 - 29.0	61
PRF-10	2.7	8.0	3.0	8.2	Zone 1- 3.7 Zone 2 - 20.5	Zone 1 - 20.0 Zone 2 - 28.0	45
PRF-14	13.0	9.1	13.1	9.8	Zone 1- 15.0 Zone 2 - 19.0	Zone 1 - 25.0 Zone 2 - 38.0	40

[†]Time from ignition (in minutes); [††]Zone 1: area near window #1; [†††]Zone 2: area near window #2

4.3 Quantitative Results and Analysis

4.3.1 Primary Bedrooms (Configuration B1)

Four tests (PRF-01 to PRF-04) were conducted using configuration B1. However, the results of Test PRF-01 are not suitable for comparison with the other three tests because the test was terminated abruptly after 42 min, due to failure of the test room's ceiling and floor assemblies. These assemblies were modified in all subsequent tests. Test PRF-04 was conducted to replace Test PRF-01. Table 11 lists the window size and fuel load composition in each test.

Tests PRF-02, -03 and -04 are used to formulate the initial understanding of post-flashover fire behaviour, which will be the basis for discussing subsequent tests.

The following variables were evaluated in Test PRF-02, -03 and -04:

1. Effect of ventilation (Test PRF-02): A smaller window (V2; Table 3), with a ventilation-limited HRR of about 2,793 kW, was used compared to 4,140 kW in tests PRF-01, 03 and 04.

2. Effect of fuel load composition (Test PRF-03): The floor was finished with oak hardwood instead of the carpet and under pad used in tests PRF-01 and -04. This resulted in an increase in fuel load mass of about 26% (791 kg in PRF-04 vs. 1,000 kg in PRF-03). However, this translated into a small increase in the FLED because wood has a much lower calorific value than carpet and under pad, which are thermoplastics. Therefore, the actual energy content was virtually unchanged. However, the major difference was in the composition of wood, which increased to 73% (by mass) in Test PRF-03 vs. 62.2% in Test PRF-04, while the composition of thermo-plastics was reduced to 6.2% in Test PRF-03 vs. 9.5% in Test PRF-04.

Table 11. Quantity and composition of the design fuel load used in the tests.

Test no.	Window	Material Mass Composition (%)					Total Mass	FLED	HC_{avg}
		W	P	T	TP	NC	Kg	MJ/m^2	MJ/Kg
PRF-01	V1	58.6	2.4	26.5	10.1	2.5	790.5	869.0	18.0
PRF-02	V2	60.1	2.3	25.5	9.7	2.4	809.2	910.6	18.1
PRF-03	V1	73.6	1.8	16.4	6.2	1.9	1,000.8	976.1	15.8
PRF-04	V1	62.2	2.2	23.7	9.5	2.3	831.4	914.5	17.7

FLED: Fuel load density; W: Wood P: Paper; T: Textiles; TP: Thermo-plastics; NC: Non-combustible, e.g. Metal; HC_{avg}: mean theoretical heat of combustion.

4.3.1.1 Heat Release Rate

Figure 16 shows the graph of HRR vs. time for the tests. Figure 17 illustrates the stages of fire development using the results of Test PRF-03. Table 12 gives the estimated time duration of each stage of fire development. The rate of fire growth of the fires was identical during the first 120 s of the tests. The fires developed rapidly and flashover occurred within 2.5 min of ignition.

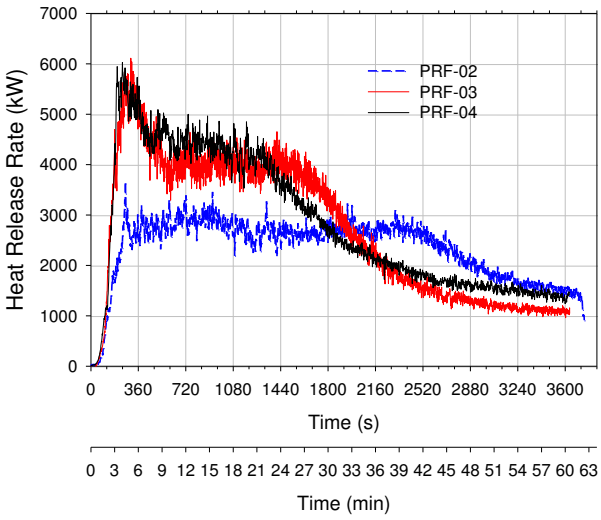

Figure 16. HRR vs. time for Test PRF-02 to -04.

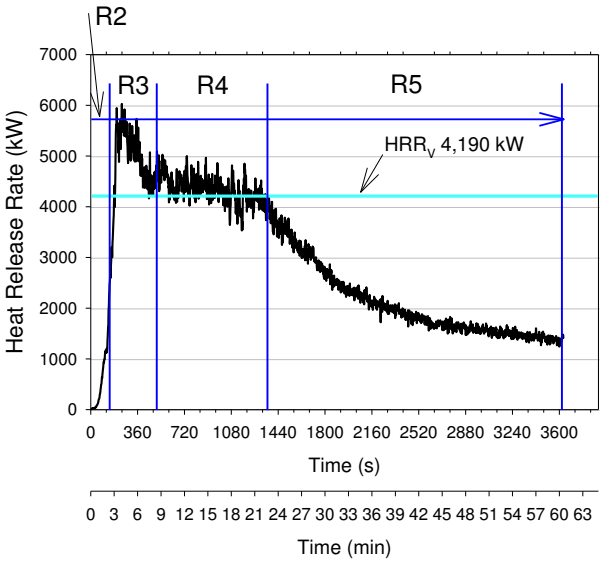

Figure 17. Illustration of the stages of fire development in Test PRF-03.

Following flashover, the fires quickly (within about 1 min) reached the ventilation-limited HRR value (HRR_V). Despite reaching the ventilation limit, generation of pyrolysis gases appears to have continued and all tests reached the peak HRR in Stage R3. The peak HRR was significantly greater than the HRRv: about 45% for Tests PRF-03 and -04, and 30% for Test PRF-02. In the test facility, there was no means to measure the amount of heat release that occurred inside the room vs. outside the room. There was a rapid decline from the peak HRR value towards the ventilation-controlled value, which is especially noticeable in Tests PRF-03 and -04. Test PRF-02 had a lower peak HRR and longer fully-developed phase ($\Delta t_{R3} + \Delta t_{R4}$; Table 12) due to the reduced window size (Table 3), which had a lower HRRv of 2,760 kW.

Table 12. Duration of stages of fire development for Tests PRF-02, -03 and -04.

Test ID	Peak HRR (kW)	t_{HRRv} (min)	Δt_{R2} (min)	Δt_{R3} (min)	Δt_{R4} (min)	Δt_{R5} (min)	$\overline{HRR}_{R4}$ (kW)	$\sigma X_{HRR_{R4}}$ (kW)
PRF-02	3,642 (4.4) †	4.2	2.5	17.1	20.3	23.5	2,676	150
PRF-03	6,103 (5.1)[1]	3.2	2.2	6.7	17.5	36.6	3,977	209
PRF-04	6,014 (4.0)[1]	3.1	2.4	4.3	15.7	38.6	4,330	269

† time to reach peak HRR (min), t_{HRRv} – time to reach HRRv; Δt_{RX} – duration of fire development Stage RX, where X= 2 to 5.

$\overline{HRR}_{R4}$ - Mean HRR in Stage R4; $\sigma X_{HRR_{R4}}$ - Standard deviation of HRR at Stage R4.

4.3.1.2 Evaluation of the Correlation for the Ventilation Controlled HRR

The theoretical ventilation-controlled HRRv (maximum room HRR for given window size) was given in Table 3. The values for windows V1 and V2 are 4,140 kW and 2,793 kW, respectively. Focusing on Stage R4, the average HRRs for Tests PRF-03 and -04 are 3,977 kW and 4,330 kW, respectively, which is within +/- 5% of the theoretical value. The theoretical values were calculated assuming 100% combustion efficiency, which cannot be expected to occur in reality since a number of factors detract from ideal combustion conditions. Therefore, the expected peak room HRR should be less than the ideal value, in which case the average value of 3,977 kW in Test PRF-03 would represent about 95% efficiency, if all the heat release occurred in the room. At this point, it is not known whether this was the case since visual observations suggest that there was external combustion. In the case of Test PRF-04, the mean value of 4,330 kW is only greater than the ideal value by about 3%, which does not fully confirm that there was external combustion. However, at this point there is no further information that can be used to determine combustion efficiencies.

In Test PRF-02, the measured mean peak HRR in Stage R4 is also within 5% of the theoretical value. Therefore, it is concluded that the correlation for HRRv provides excellent estimates.

4.3.1.3 Summary of HRR Results

1. The rate of fire growth was identical for all of the tests until after flashover had occurred.
2. There was an initial spike in the HRR that occurred immediately after flashover, which is believed to be due to external combustion of excess fuel (including flashing of the paper layer on the gypsum boards). For tests PRF-03 and -04, the peak HRRs (respectively, 6,103 kW and 6,014 kW) were significantly greater than the theoretical peak ventilation-controlled HRR of 4,140 kW by about 45%.
3. The correlation for estimating the ventilation-controlled HRR does not yield good results for the multi-window setup in this test. The difficulty of evaluating the correlation is compounded by the complex shape of the HRR profile caused by compartmentation (presence of a door and destructible partition wall), disparity in FLEDs between zones 1 and 2 and other unknown aspects of the complex fire dynamics in this configuration.

4.3.1.4 Effect of Variables

1. Reduced ventilation (Test PRF-04 vs. Test PRF-02): Test PRF-02 had a lower peak HRR and longer fully-developed phase (Stages R3 + R4) due to the reduced window size (Table 3), which had a lower HRRv of 2,760 kW.
2. Fuel load composition (Test PRF-04 vs. Test PRF-03): The increased composition of wood in Test PRF-03 led to a reduction in the peak HRR in Stage R4 (3,977 kW vs. 4,330 kW in Test PRF-04) and about 11% longer time duration of Stage R4. Stages R2 and R3 were

relatively unaffected. The rate of HRR decay in Stage R5 was slower in Test PRF-03 than in Test PRF-04.

4.3.1.5 Room Temperatures

The temperature conditions in the fires proved to be harsh for the 0.51 mm diameter, glass-fibre insulated, Type K thermocouple (TC) wires used to make the thermocouples. The specified operating temperature range for this type of TC wire is up to 1,250°C with an uncertainty of 0.4%, and it is believed they were operating near the upper limit of their operating temperature, which frequently caused erroneous readings (likely due to spurious hot junctions caused by shorting of TC wires after the protective sheath was destroyed) during the tests. However, it was not always possible to filter out the erroneous data due to the lack of a consistent and efficient method for identifying the affected periods. Therefore, the approach taken in this work was only to correct the obvious errors (e.g. open circuit periods) and other doubtful data were left to be subject to a cautious interpretation.

Figures 18 to 21 show the room temperatures measured by the four TC trees in Test PRF-04. The results show that the temperature environment was different in each of the four quadrants (zones) of the room where the TC trees were located. There is greater temperature variation between the TC trees (across zones), but the floor-to-ceiling variations at each TC tree are small, which suggests a better agreement with the well-mixed-reactor assumption in each zone. However, across the entire room, the assumption does not hold as it has been shown here and elsewhere by other researchers [21, 22].

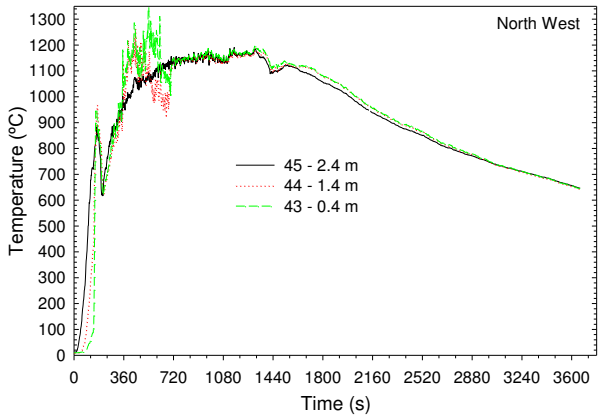

Figure 18. Test PRF-04: North West TC tree.

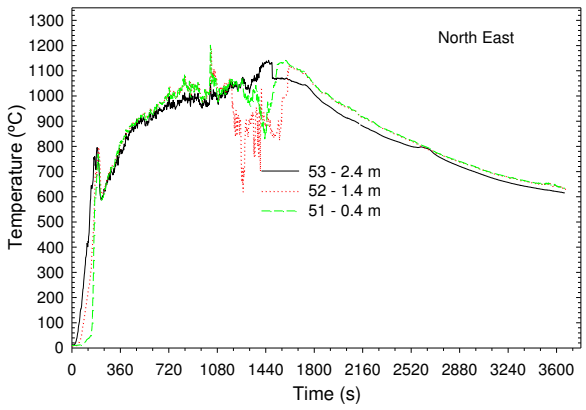

Figure 19. Test PRF-04: North East TC tree.

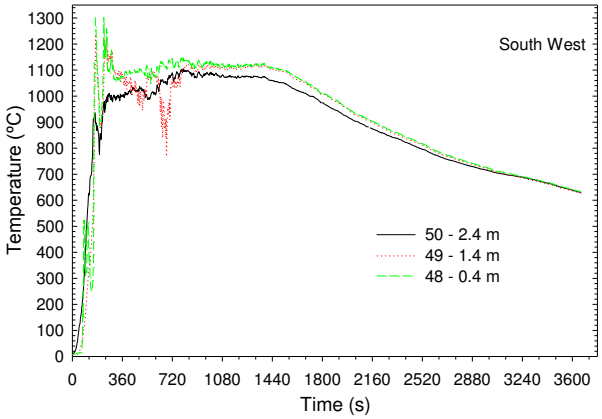

Figure 20. Test PRF-04: South West TC tree.

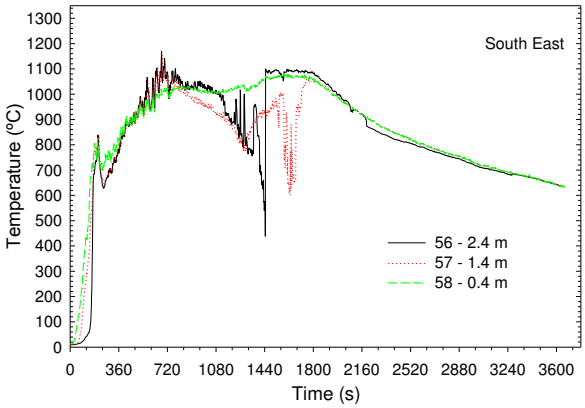

Figure 21. Test PRF-04: South East TC tree.

There was a sharp temperature drop of approximately 100°C to 300°C immediately after flashover followed by a temperature rise at rates that were different in each zone. The temperature rise was quickest in the SW zone and slowest in the NE zone. The data from the TC at 1.4 m shows signs of corruption between 720 s and 1800 s from ignition; especially in the SE zone. The data also shows numerous temperature spikes, which reduces the significance of instantaneous maximum values of individual TCs, e.g. taking the maximum values at 1.4 m in the SW, SE, NW and NE zones gives maximum temperature values of 1240°C, 1230°C, 1299°C and 1319°C, respectively. However, these instantaneous values likely correspond to temperature spikes and are therefore not representative of the prevailing conditions in Stage R4, which is the most significant portion of the fully-developed phase of the fire. Therefore, statistical values (mean and standard deviation) in Stage R4 would be more meaningful in describing the post-flashover temperatures - this is the approach taken in this research. The mean temperatures given in Tables 13 and 14 are considered to be the appropriate representation of the conditions in Stage R4 since they are average values calculated over the indicated durations of Stage R4. Therefore, a mean maximum temperature is defined as follows: The average of the instantaneous peak temperatures measured at a location in the hot layer that is calculated over the duration of the Stage R4 in the post flashover phase. The mean maximum temperature is calculated either for a single measurement location (zone) or the entire room (four zones).

To provide further insight and support this research's conclusion that there are five distinct stages of fire development (Figure 4), the temperature profiles measured at 2.4 m in each of the four zones are plotted on the same graph as the HRR in Figure 22. The results are quite telling:

1) The peak HRR occurs in Stage R3 (poor efficiency post-flashover) and coincides with a rapid temperature drop (to about 600°C) that follows flashover:

- Rationale: Poor combustion efficiency due to excessive pyrolysis products (i.e. fuel-rich atmosphere) causes temperatures to drop since the actual room HRR is lower, but the excess pyrolysis products still burn outside the room resulting in the high measured value of peak HRR (~ 6,000 kW). Given the strong correlation of HRR and room temperature, a temperature of about 700°C correlates with a HRR of about 3,000 kW, which represents about 50% combustion efficiency for a peak HRR of about 6,000 kW. Room temperatures increase as the excess fuel is expelled from the room and the fuel/air mixture ratio approaches stoichiometry conditions (i.e., combustion efficiency improves).

2) Maximum temperatures (in all sections, except for at the NE TC tree) occurred in Stage R4 (the high efficiency fully-developed phase);
   - Rationale: Lower heat losses through the heated walls and improved combustion efficiency as the fuel/air mixture ratio is less rich resulting in increased room HRR and consequently higher temperatures. As explained earlier, once a significant proportion of thermoplastic materials are consumed, the pyrolysis rate of the remaining materials, which are largely wood, is better regulated by available ventilation. At the NE TC tree, the peak temperatures occurred later due to the Zonal burning phenomenon

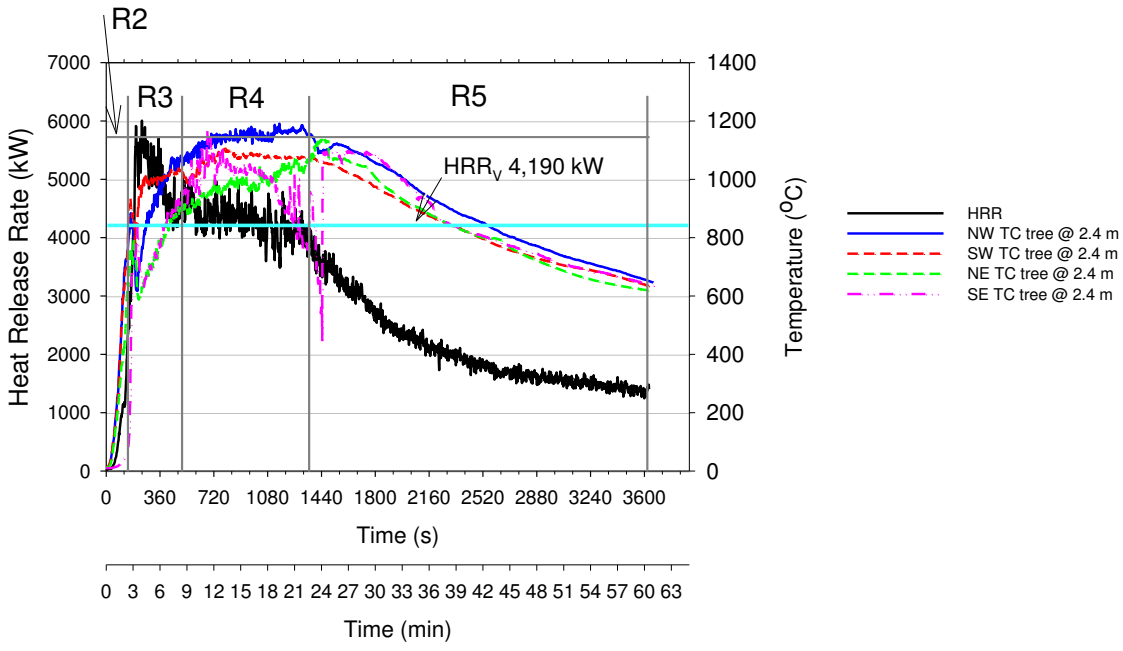

Figure 22. Graph of HRR and zonal temperatures at 2.4 m vs. time for Test PRF-04.

Figures 23 to 26 show the room temperatures measured by the four TC trees in Test PRF-03. The differences in room temperature profiles are evident in the NW and NE zones: after flashover had occurred, the rate of temperature rise (especially at 0.4 m height) was slower than in Test PRF-04. A slow temperature rise as shown in Figures 23, 254 and 26 indicates the existence of oxygen-deficient combustion conditions (i.e. poor combustion efficiency). Despite the slower rise, temperatures in the NE zone eventually exceed 1,000°C before they begin to decline in the decay phase.

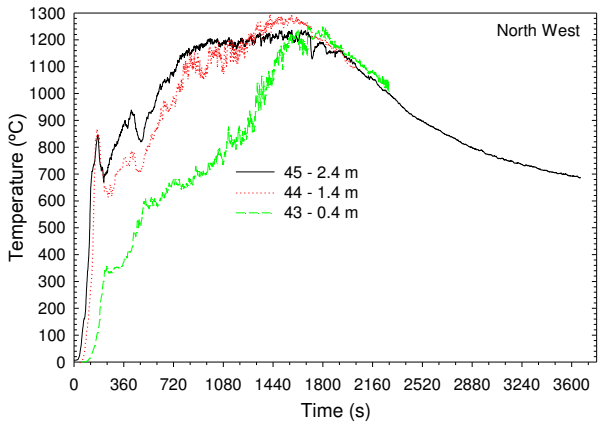

Figure 23. Test PRF-03: North West TC tree.

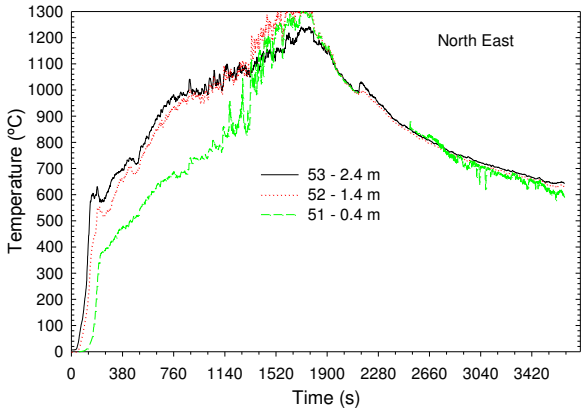

Figure 24. Test PRF-03: North East TC tree.

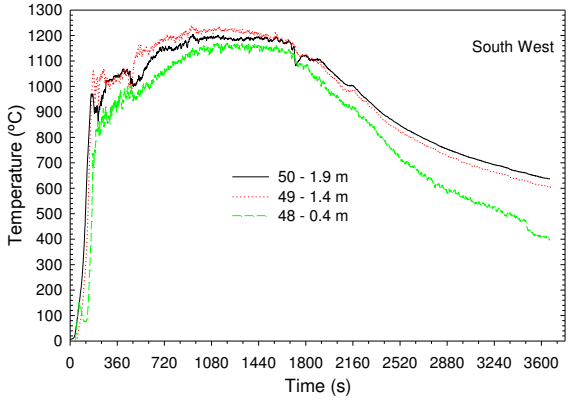

Figure 25. Test PRF-03: South West TC tree.

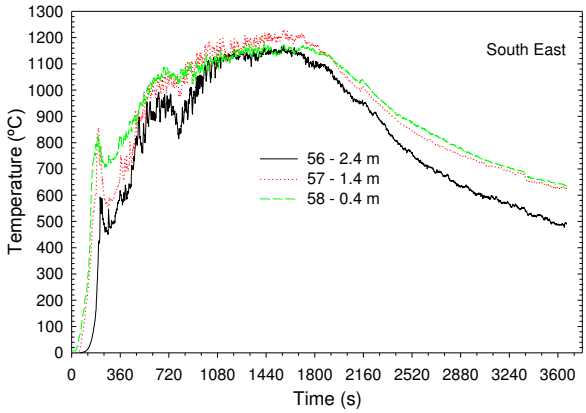

Figure 26. Test PRF-03: South East TC tree.

Figures 27 to 30 show the room temperatures measured by the four TC trees in Test PRF-02. Overall, all zones show a slow temperature rise during Stage R3 reaching steadier temperatures of about 1,100°C after 1,080 s. In this test, there appears to be less variation in temperature between the zones (i.e. room temperatures were more uniform throughout the room). The temperature dip after flashover is more pronounced in the SW zone.

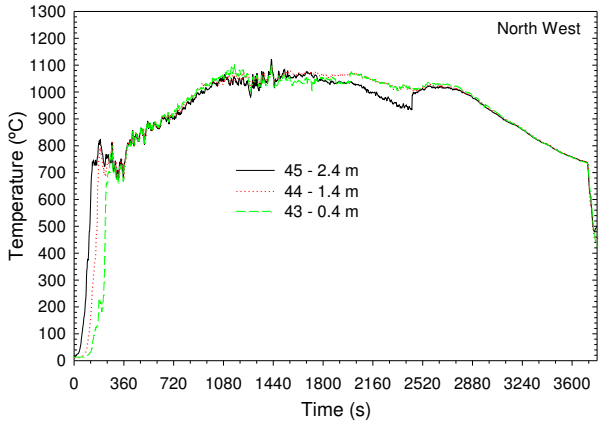

Figure 27. Test PRF-02: North West TC tree.

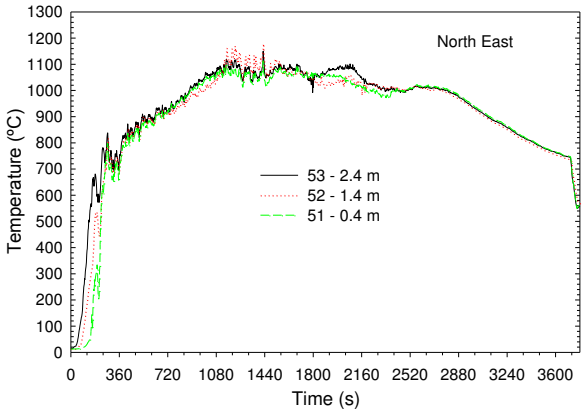

Figure 28. Test PRF-02: North East TC tree.

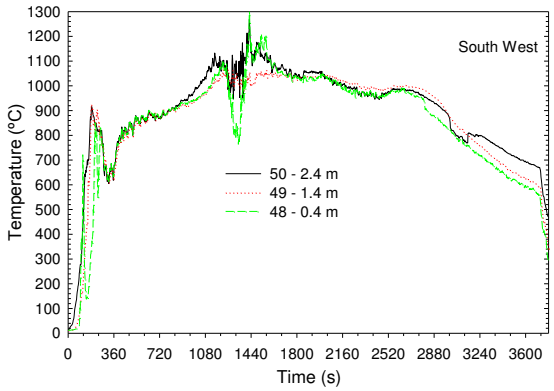

Figure 29. Test PRF-02: South West TC tree.

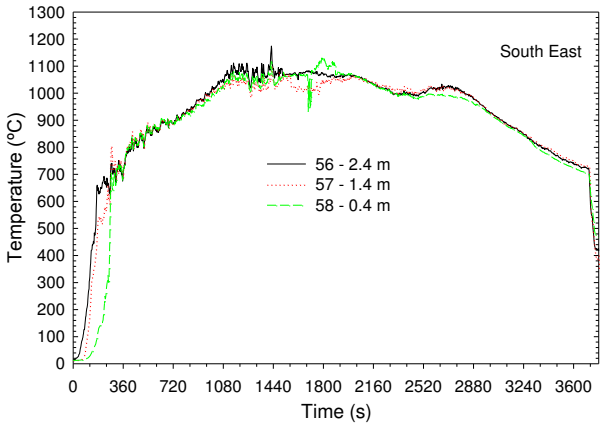

Figure 30. Test PRF-02: South East TC tree.

Tables 13 and 14 summarize the temperature results in Stages R3 and R4, respectively, for Tests PRF-02, -03 and -04. As stated earlier, the complexity of the fires requires a statistical analysis to provide more information on the temperature environment. The results were calculated assuming the five stages of fire development were uniform in all zones. However, this assumption is not necessarily correct for the SE and NE zones, which experienced prolonged periods of oxygen starvation and, hence, temperature profiles clearly show that the duration of Stage R3 was longer than in the SW and NW zones. As a result, Stage R4 was also shorter since pyrolysis products were likely being drawn out and burned in the SW and NW zones. The results show strong zonal burning behaviour, suggesting that the contribution of each zone to the total room HRR is likely not the same: SW and NW zones (the zones of fire origin) are the dominant combustion areas (based on temperature results) during the initial post-flashover phase and the bulk of the oxygen is drawn to these areas causing severe under ventilation in the SE and NE zones. Active combustion appeared to switch to the SE and NE zones after a while; likely once a significant portion of combustibles in the SW and NW zones were consumed.

Table 13. Temperatures at 1.4 m height (measured by a single TC) in each of the four zones of the room during Stage R3.

Test ID	Peak HRR (kW)		Temperature values in zone NW (°C)	NE (°C)	SW (°C)	SE (°C)	Duration of Stage R3 (min)
PRF-02	3,642	Min-Max	469-1,073	327-1,163	600-1,031	382-1,068	
		Mean	897	877	861	864	17.1
		SD †	126	162	100	149	
PRF-03	6,103	Min-Max	505-872	319-769	562-1,171	357-996	
		Mean	726	606	1025	701	6.7
		SD	63	101	86	134	
PRF-04	6,014	Min-Max	623-1,221	419-868	704-1,240	516-864	4.3
		Mean	868	721	1076	735	
		SD	147	89	87	74	

†SD – Standard deviation

Table 14. Temperatures at 1.4 m height (measured by a single TC) in each of the four zones of the room during Stage R4.

Test ID	Peak HRR (kW)		Temperature values in zone NW (°C)	NE (°C)	SW (°C)	SE (°C)	Duration of Stage R4 (min)
PRF-02	3,642	Min-Max	1,005-1,096	984-1,181	979-1,067	985-1,105	20.3
		Mean	1,056	1,060	1,030	1,036	
		SD †	18	39	79	19	
PRF-03	6,103	Min-Max	801-1,299	764-1,304	1,120-1,240	873-1,230	17.5
		Mean	1,125	1,032	1,203	1,118	
		SD	126	35	25	77	
PRF-04	6,014	Min-Max	921-1,264	621-1,188	770-1,125	776-1,158	15.7
		Mean	1,129	959	1,080	947	
		SD	53	57	57	72	

†SD – Standard deviation

For Stage R3, Table 13 shows that there is a wide variation in the temperatures measured at 1.4 m height: Mean and standard deviation, respectively, for all the four zones for each test are: PRF-02 (875°C and 134°C); PRF-03 (765°C and 96°C) and PRF-04 (850°C and 100°C). The temperature graphs show that the temperature rise is approximately linear. Table 14 gives the results for stage R4; there is less variation in temperatures at 1.4 m compared with Stage R3: Mean and standard deviation, respectively, for all the four zones for each test are: PRF-02 (1,046°C and 36°C); PRF-03 (1,120°C and 66°C) and PRF-04 (1,029°C and 60°C). It can be seen that the mean temperature of all four zones was more uniform in Test PRF-02. The mean temperatures in Test PRF-02 are only

marginally lower than those in Tests PRF-03 and -04, which suggests that the main effect of reduced ventilation was to prolong Stage R3. The extended duration of the post-flashover phase (R3+R4) is a direct consequence of the reduced burning rate imposed by the smaller size of the window.

Comparing the results of PRF-03 and -04, temperatures in Stage R4 were higher in Test PRF-03. Figure 31 compares the temperatures measured at the SW TC tree at 1.4 m and 2.4 m in tests PRF-03 and -04 and it can be seen that the temperatures in PRF-03 (during Stage R4) were higher than in PRF-04 by about 100 – 150°C. Review of heat flux data (Figures 32 to 35) supports these results since the heat flux values recorded at walls were higher in PRF-03. These results suggest that combustion efficiency was higher in PRF-03 than in PRF-04 since the fuel load in PRF-03 had a higher composition of wood (since carpet was replaced with hardwood) and hence there was less excess pyrolysis products.

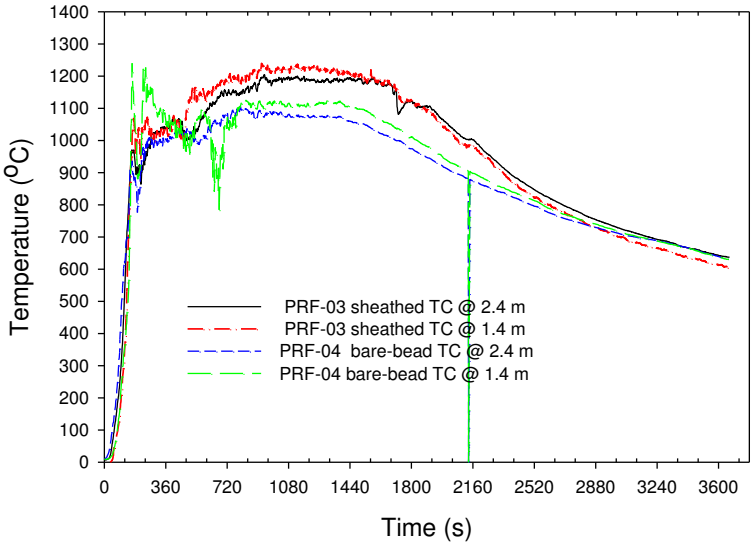

Figure 31. Temperatures in Test PRF-03 compared to Test PRF-04.

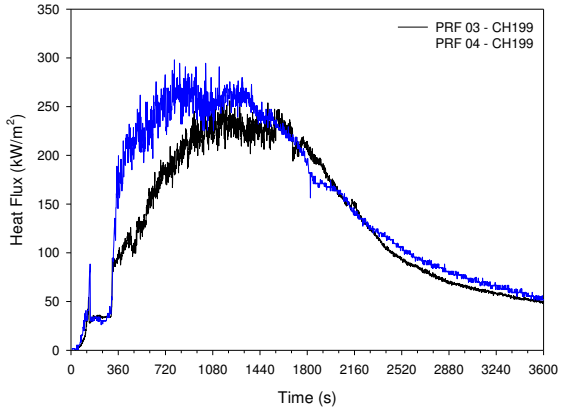

Figure 32. Heat flux at the ceiling in tests PRF-03 and -04.

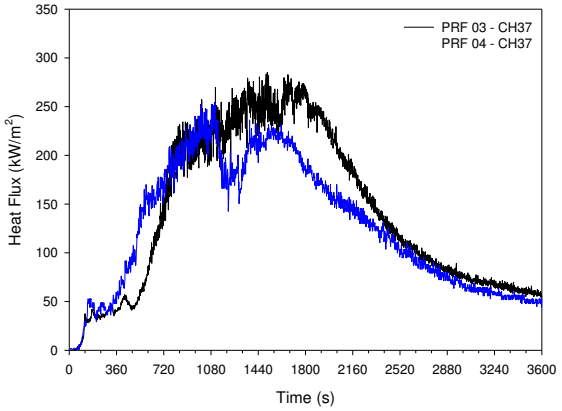

Figure 33. Heat flux at the north wall in tests PRF-03 and -04.

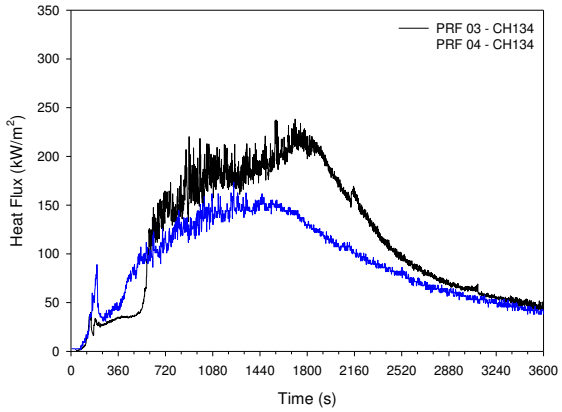

Figure 34. Heat flux at the east wall in tests PRF-03 and -04

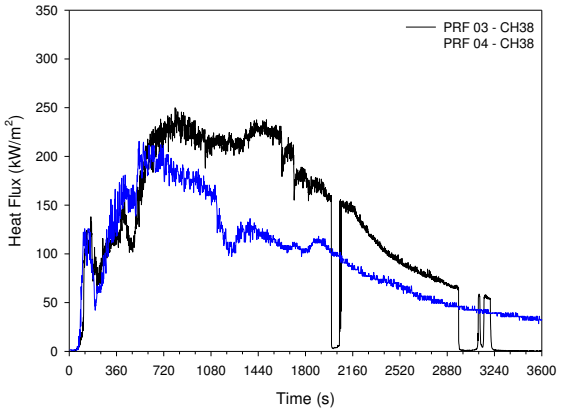

Figure 35. Heat flux at the west wall in tests PRF-03 and -04.

4.3.2 Flashover

Table 15 gives the results of the assessment of the flashover conditions that were carried out using three criteria:

1. **F_600°C:** attainment of an average temperature of 600°C in the hot layer (based on the average of the TC tree measurements at heights of 1.4 m and 1.9 m);
2. **F_20 kW/m^2:** attainment of heat flux reading of 20 kW/m^2 at floor level, and;
3. **F_flames out:** visual observations of flames flowing out of the room window.

Three correlations were used to estimate the theoretical value of HRR required to cause flashover in the test room and the values obtained for window V1 were: Thomas [16]– 1,600 kW; Babrauskas [15] – 2, 100 kW; MQH [17] – 1,700 kW. For window V2 values are: Thomas – 1,244 kW; Babrauskas – 1, 380 kW; MQH – 1,062 kW.

For tests PRF-03 and -04 (window V1), Babrauskas' correlation provides the best agreement with test results. For Test PRF-02 (window V2), Thomas and Babrauskas' correlations are in agreement with the results. The MQH correlation consistently gives lower estimates, but given the rapid rate of fire growth around flashover, time difference is not significant.

Table 15. Flashover results.

	Peak HRR	Time to peak HRR	Time to flashover based on various criteria (s)			
Test ID	(kW)	(s)	F_600°C	HRR (kW)	F_20 kW/m^2	F_flames out
PRF-02	3,642	262	152	1,252	198	198
PRF-03	6,103	303	133	1,970	102	168
PRF-04	6,014	239	141	2,107	156	162

F_600°C: hot layer temperature of 600°C; **F_20 kW/m^2**: heat flux of 20 kW/m^2 at floor level; **F_flames out**: flames emerge from window

4.3.2.1 Thermal Radiation

Table 16 lists the peak heat flux recorded by Gardon gauges at various locations. Gardon gauges are designed to measure the total radiation flux ($Q"(W/m^2) \propto T_{fire}^4$) from a field of view of 180 degrees, which may include both radiation and convection components. However, it is presumed that at high temperatures the radiation component becomes dominant. In this report, the term "heat flux" is used to refer to radiation flux for simplicity and when mentioned in relation to room surfaces, radiation exposure will be the implied meaning rather than the quantitative measure of actual heat flow through the surfaces (i.e. true heat flux). The true heat flux through a room surface is expected to be less than the value measured by the gauge since it is a function of the temperature difference, i.e. $Q"(W/m^2) \propto (T_{fire}^4 - T_{wall}^4)$.

Since radiation is the dominant heat transfer mechanism in the fires under consideration, the measurements are expected to indicate the emissive power of the source (fire temperature; assuming convection to be less significant), which is proportional to the fourth power of temperature as defined by the radiation power law (Stefan-Boltzmann law):

$$Q'' = \varepsilon \sigma T^4 \tag{4.1}$$

where:

$Q'' - heat\ flux\ \left(kW/m^2\right)$; $\varepsilon - emissivity$;

σ – Stefan-Boltzmann`s constant ($5.66 \times 10^{-8}\ W\,m^{-2}K^{-4}$); $T - absolute\ temperature\ (K)$

Therefore, the source temperature can be estimated from the measured values of the radiation flux.

Table 16. Peak radiation flux at various locations in Tests PRF-02, -03 and -04.

Test ID	Peak heat flux at various surfaces (kW/m^2)						
	Floor	West wall	East wall	Ceiling center	North wall	Ext-2.4†	Ext-4.8††
PRF-02	198	274	194	253	220	28	7
PRF-03	271	250	238	257	269	45	12
PRF-04	189	252	173	298	260	42	12

†Heat flux gauge located at 2.4 m from window #1; ††Heat flux gauge located at 4.8 m from window #1

Figure 36 shows the idealized relationship (assuming an emissivity of 0.98) of heat flux to temperature according to the radiation power law.

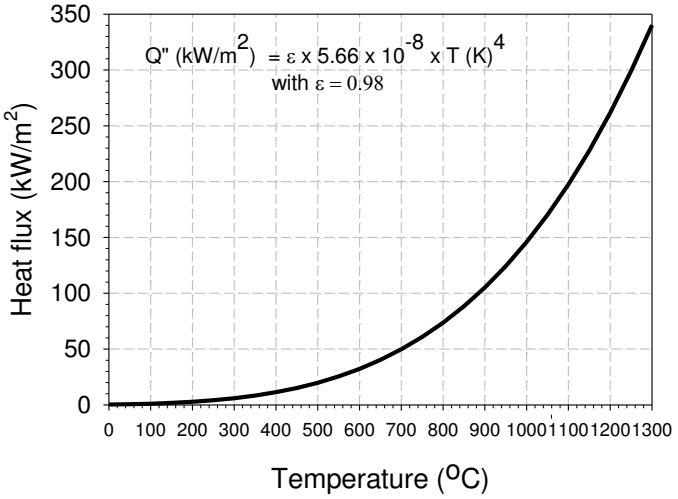

Figure 36. Ideal heat flux vs. Temperature.

In the tests, the highest value of 298 kW/m^2 (approximately 1,250°C inverse temperature), was recorded at the ceiling in Test PRF-04. As with temperatures, a single value cannot describe the heat flux profile. Furthermore, unlike temperatures, which appear to be semi-steady during Stage R4, heat flux behaves otherwise since it is driven by the fourth power of absolute temperature – a seemingly small change in temperature results in a significant change in heat flux magnitude, as can be seen in Figure 36. Therefore, the results will be discussed with recourse to graphs since statistical values such as mean and standard deviation are not useful in describing the heat flux profiles measured in these tests.

Figures 37 to 42 show the heat flux profiles measured in Tests PRF-02, -03 and -04. Two graphs are given for each test. The profiles are typically bell-shaped and hence peak values are short-lived. The results show the complexity of the fire environments and confirm existence of the strong zonal burning behaviour discussed earlier – for the most part, all surfaces experience moderate to

vastly different heat fluxes. In all of the tests, the west wall experiences significantly higher heat fluxes earlier than the east and north walls (Figures 37, 39 and 41), which is likely because the first-ignited-item was located on the west side, in addition to other yet unknown factors. This is consistent with the zonal burning behaviour seen in the temperature data (since temperature drives heat flux), which showed that the west half of the test rooms (where the fire originated) had higher temperatures and fire development was ahead of the eastern half.

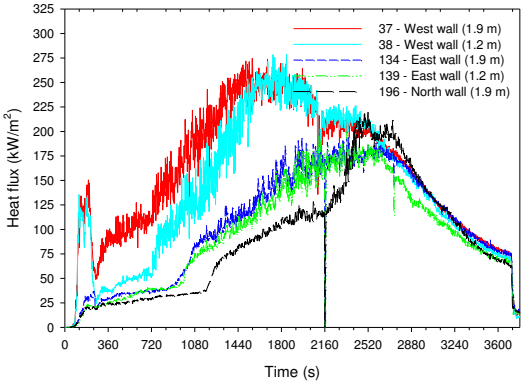

Figure 37. Test PRF-02: Heat flux at wall surface locations.

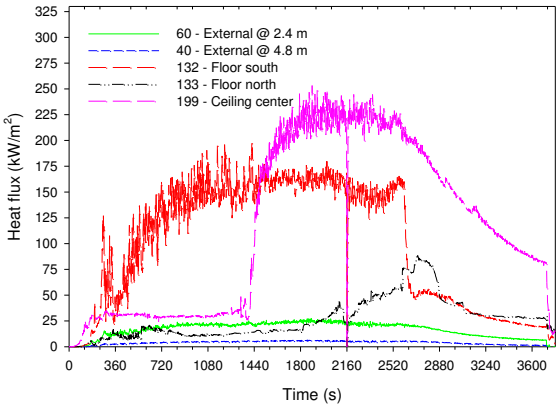

Figure 38. Test PRF-02: Heat flux at ceiling, floor and external locations.

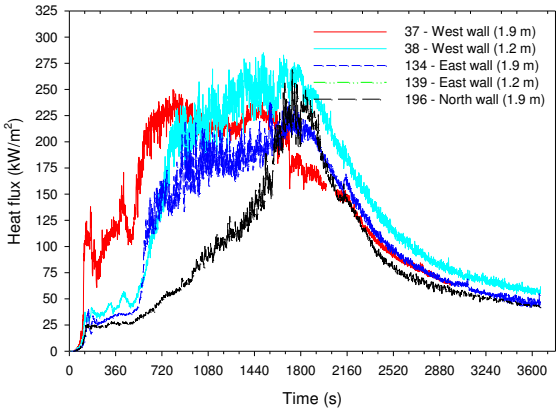

Figure 39. Test PRF-03: Heat flux at wall surface locations.

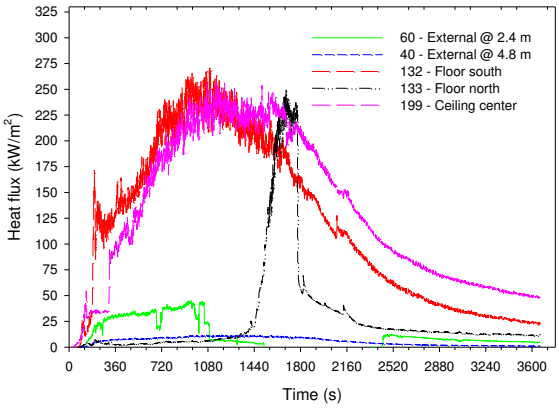

Figure 40. Test PRF-03: Heat flux at ceiling, floor and external locations.

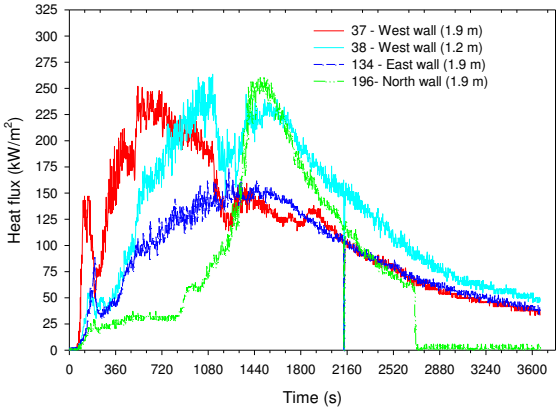

Figure 41. Test PRF-04: Heat flux at wall surface locations.

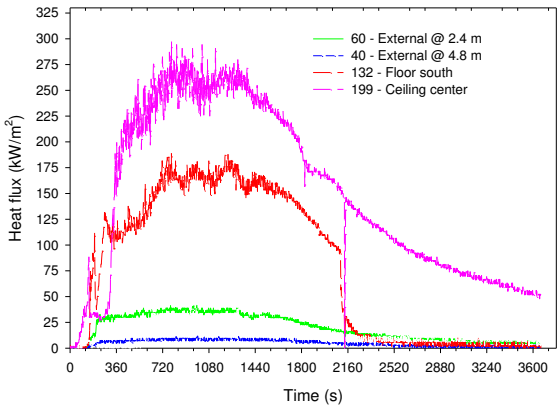

Figure 42. Test PRF-04: Heat flux at ceiling, floor and external locations.

4.3.2.2 Comparison with ASTM E119 and CAN/ULC S101 Furnace Conditions

A comparison of the temperature and heat flux conditions in the room fire tests with those in standard ASTM E119 test furnaces, is of interest since the fire performance of the Test Wall Sections will be evaluated using the performance criteria that are utilized in the widely-used ASTM E119 and CAN/ULC S101 test protocols. It is generally believed that real fires are more severe than the standard test fire exposure and other researchers [32] have provided experimental evidence. Standard tests are convenient for regulatory purposes and have a long history of use, which on the one hand inspires a degree of confidence and on the other causes a reluctance to change. The comparison of the performance of wall assemblies in real fires vs. standard tests that is carried out here is intended to provide information that would be useful in performance-based design approaches and in no way attempts to discredit standard tests, which serve an entirely different purpose. Therefore, the phrase “fire performance” is used in this work to differentiate from the phrase “fire resistance”, which is commonly associated with standard furnace tests. In making this comparison, it is acknowledged that, apart from the fire environment, the following deviations from the ASTM E119 and CAN/ULC S101 wall furnace test configurations may have an impact on the results:

a) The size (dimensions and exposed area) of each TWS did not conform to the ASTM E119 and CAN/ULC S101 test protocols. The exposed area of each TWS was only 30% of the value of at least 9 m^2 that is required in the test protocols.
b) The unexposed side of each TWS was not open to ambient conditions as is the case in the test protocols, but rather was exposed to a closed cavity. Therefore, the rate of heat loss from the TWS surface would be expected to be lower due to reduced convection heat transfer. However, it is noted that the TCs on the unexposed TWS surface were installed

under insulation pads, as is the practice in standard tests. Therefore, in both configurations, the TCs on the unexposed surface were insulated from ambient conditions, but there could be differences in lateral heat transfer gradients due to differences in convention heat losses, which was not considered in this work.

Figure 43 shows the average heat flux and temperature measured in a full-scale wall furnace [33]. It can be seen that the temperature and heat flux are considerably lower than those in test PRF-01, which was conducted in this research. A comparison of the furnace average temperature to that measured in the fire tests can only be made with test PRF-01 since it was the only test in which a shield TC (similar to the ASTM E119 and CAN/ULC S101 TC) was installed. It is noted that:

a) The furnace temperature does not reach 1,000°C until after 120 min whereas in the real fires temperatures exceeded this value within 6 min;
b) Since heat flux is a derivative of the fourth power of absolute temperature, as shown in the ideal relationship in Figure 36 and confirmed by actual measurements in Figure 43, the heat flux in furnaces only reaches150 kW/m^2 after 120 min, whereas values of approximately 200 kW/m^2 are reached (and exceeded at some locations) in the Test PRF-01 within 18 min.

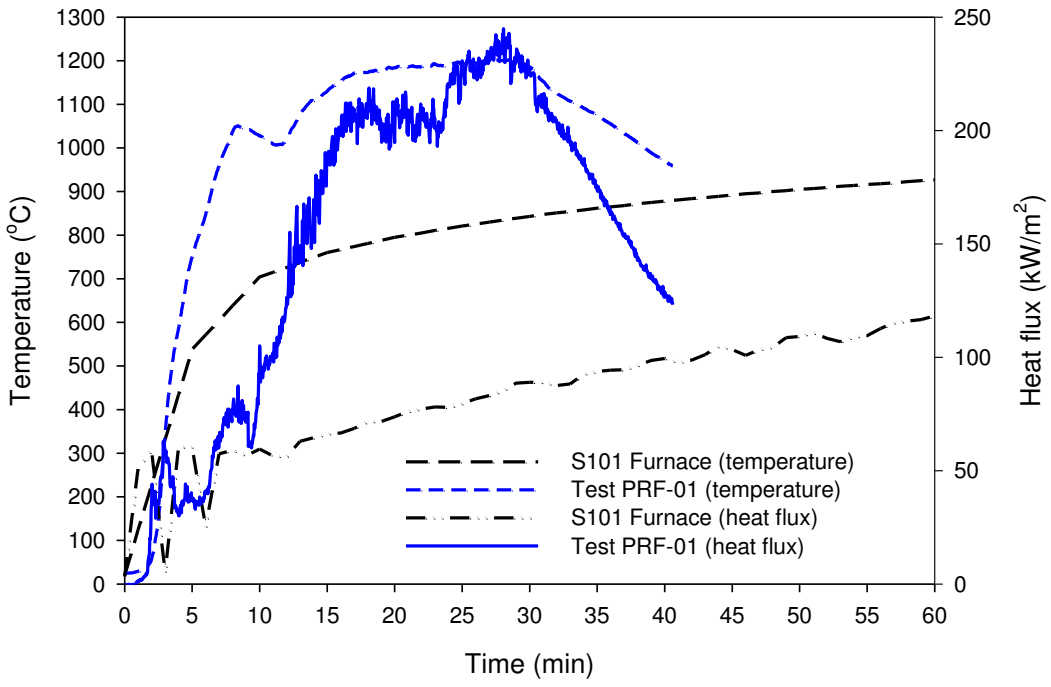

Figure 43. Heat flux and temperature measurements in an ASTM E119 full-scale wall furnace [33] compared with the results of Test PRF-01.

Therefore, the temperature conditions in the real fires considered here appear to be more severe—within the first 30 min—than in standard test furnaces. The fires studied here had relatively short fully-developed phases and were well into the decay phase by the time 60 min had elapsed. Evaluation of the fire performance of Test Wall Sections will determine the significance, if any, of early severe temperature exposure vs. the prolonged and gradually increasing exposure in standard test furnaces and other potential fire scenarios.

4.3.2.3 Fire performance of Test Wall Sections

Test Wall Sections (TWSs), each measuring approximately 1,180 mm wide and lined with a single layer of either regular or type X GWB on each side of the framing were installed in many of the tests. The installation schedule for the TWSs is given in Part 1 of this report [1]. The TWSs were constructed with non-load bearing wood-frame wall specimens and provided a means to evaluate the impact of the fires on realistic boundaries. One pair of TWSs (TWS 01 and 02) was inserted in the east wall and the other pair (TWS 03 and 04), if installed, was on the west wall of the test room, as described in Part 1 of this report [1].

In Tests PRF-01 and -02 the TWSs were only installed on the east side. Upon reviewing the test results, the non-uniformity in the heat flux measured at interior surfaces became apparent and necessitated the installation of a second set of test wall sections (TWS 03 and 04) on the west side in Tests PRF-03 and -04.

Table 17 gives fire performance results for TWSs installed in Tests PRF-02, -03 and 04. The failure times were determined using the ASTM E119 and CAN/ULC S101 [34, 35] single point insulation failure criterion, i.e. that the maximum temperature rise at any single TC (single-point) on the unexposed surface does not exceed 180°C above ambient. The results show that the lowest fire performance times for a simulated 1 h assembly (TWS-03) were recorded on the west side, with the lowest value (28 min) being recorded in Test PRF-04. The lowest failure time obtained for a regular partition assembly was 19 min for TWS-03 in Test PRF-04. Therefore, the fire environment in Test PRF-04 appears to have been more severe than in Test PRF-03.

Table 17. Fire performance results for TWSs in Tests PRF-02, -03 and 04

Test ID	Duration (min)	Peak HRR (kW)	TWS Time to Temperature Rise of 180°C			
			TWS-01 (RGWB) (min)	TWS-02 (XGWB) (min)	TWS-03 (RGWB) (min)	TW-04 (XGWB) (min)
PRF-02	64	3,642	40	54	None	None
PRF-03	63	6,103	29	44	20	35
PRF-04	61	6,014	24	53	19	28

RGWB: Regular gypsum board (12.7 mm thick); XGWB: Type X gypsum board (15.8 mm thick)
None: Test section was not installed; NULL: ATSTM E119/ULC-S101 failure criteria were not reached.

On the east side, the fire performance times for both TWS-01 (regular interior partition) and TWS-02 (1 h partition) were longer, with TWS-02 achieving a fire performance time of 53 min in Test PRF-04. Fire performance times for TWS-01 in Test PRF-03 and -04 are comparable to the results in standard CAN/ULC S101 furnace test [36]. In Test PRF-02, the effect of reduced ventilation manifests itself in the longer fire performance times for both TWSs, confirming that the fire environment in Test PRF-02 was less severe than in Tests PRF-03 and -04. Therefore, in this case, it was found that reducing ventilation for the same fuel load results in a less severe fire environment based on the CAN/ULC S101 insulation failure criteria. However, a definitive conclusion is deferred until all of the tests addressing the issue of ventilation have been discussed. Based on the knowledge developed thus far, it seems that reducing ventilation while maintaining the same fuel load extends the duration of Stage R3 of the fire and thereby lessens the initial thermal assault on the boundaries since R3 is a lower-temperature phase. In tests with a shorter R3 (PRF-03 and -04), the initial thermal assault was more severe and failure occurred even though the duration of the fully-developed phase was shorter than that in Test PRF-02.

The impact of these results on fire spread to adjacent areas was not explicitly addressed. However, analysis of the results shows that integrity failure (due to large cracks and / or fall off of gypsum board) of the unexposed gypsum surface occurred 3 to 5 min after insulation failure had occurred. Following integrity failure, fire spread to adjacent spaces can occur.

4.3.2.4 Uncertainty of Temperature Measurements

In addition to their inherent uncertainty, bare-bead thermocouples are known to be subject to errors (believed to be due to radiation and conduction) in measuring gaseous temperatures in fires and numerous studies have been carried out by other researchers in an attempt to develop methods for correcting readings [37 - 39].

To evaluate the accuracy of the temperature measurements, two common approaches [37] for correcting TCs for radiation heat transfer errors, the use of aspirated thermocouples and multiple bare-bead TCs of different diameters, were attempted. It was reported [37] that the use of multiple-bare bead TCs could not be used for temperature corrections when there are significant temperature fluctuations (with time scales comparable to the response times of the TCs) in the fire environment.

Temperatures measured with bare-bead TCs are compared with those measured with an ASTM E119 shielded TC, 20 AWG (0.812 mm diameter) bare-bead TCs and inverse temperature derived from near-by heat flux gauges. In some tests, two TCs of different bead sizes were installed at the

same location to determine whether the method of Pitts et al. [37] could be used to correct for radiation errors. Figure 44 is a photograph of the west side of the test room showing the location of the ASTM E119 shielded TC, 2.4 m and 1.4 m TC on the SW TC tree, and the heat flux gauge located at 1.9 m on the west wall, in Test PRF-01. Figure 45 (Test PRF-01) shows that the TCs on the tree (at 1.4 m and 2.4 m) measured considerably lower temperatures (by about 150°C) than the ASTM E119 TC during the full-develop phase (Stage R4). The ASTM E119 TC measured maximum temperatures of about 1,200°C during Stage R4. Although the ASTM E119 TC has as a slow response time constant due to its large thermal mass, the TC (inside the tube) is shielded and may not be subject to radiation errors. The inverse temperatures derived from heat flux measurements at the ceiling (center) and west wall are in reasonably good agreement with bare-bead TCs up to about 800°C. Thereafter, the disagreement is considerably larger during the fully-developed phase. However, the inverse temperatures are in fairly good agreement with the ASTM E119 TC during the post-flashover phase. Therefore, it appears that the bare-bead TC was subject to considerable radiation error in fire temperatures exceeding 1,100°C. It is recognized that there is a degree of uncertainty with the value of the emissivity used in the inverse temperature calculated since it is unknown. A value of 0.98 was assumed. Figure 46 shows a similar comparison for Test PRF-02. In this case, a pair of TCs with different diameters was installed at 1.9 m height. The analysis for Test PRF-03 and -04 is shown in Figures 47 and 48, respectively.

Figure 44. Test PRF-01: Location of ASTM E119 shield TC, SW TC tree and west wall heat flux gauge.

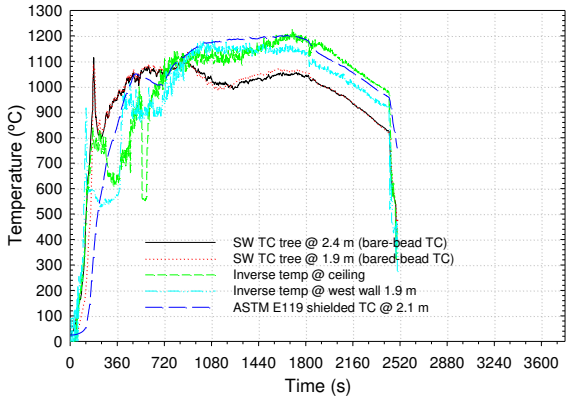

Figure 45. Test PRF-01: Temperatures measured by two different TCs and heat flux gauges.

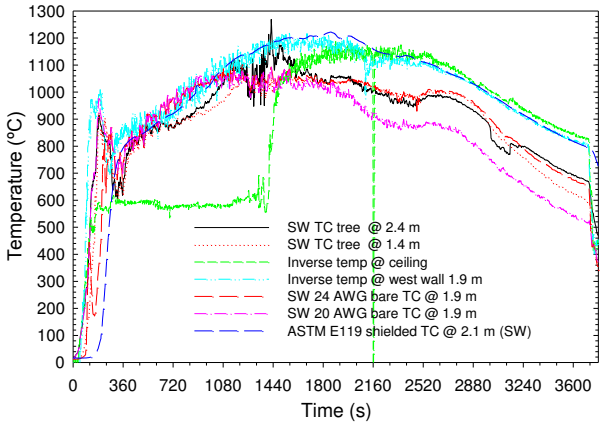

Figure 46. Test PRF-02: Temperatures measured by three different TCs and heat flux gauges.

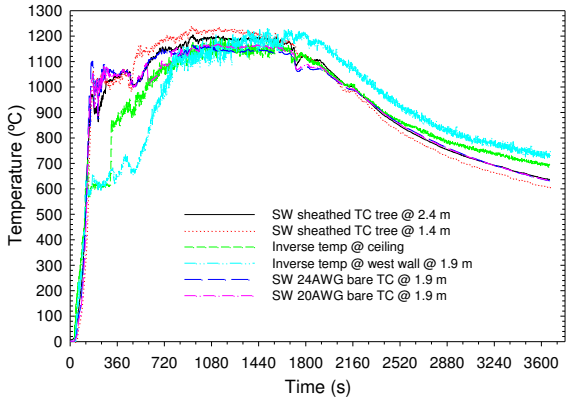

Figure 47. Test PRF-03: Temperatures measured by two different TCs and heat flux gauges (Note: The ASTM E119 TC was defective in this test).

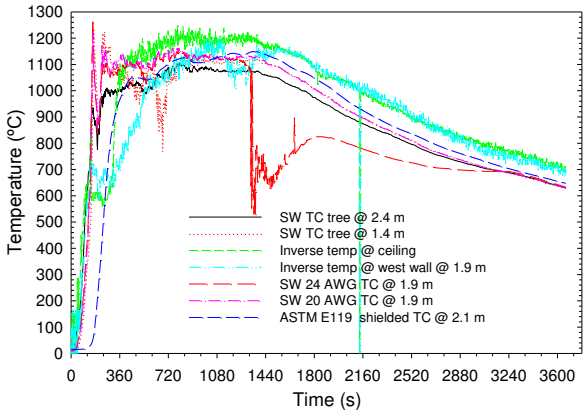

Figure 48. Test PRF-04: Temperatures measured by three different TCs and heat flux gauges.

Figure 49 shows the results for Test PRF-05. Peak temperatures are lower than those in Tests PRF-01 to -04 and there is good agreement between all measurement instruments.

The maximum inverse temperatures are around 1,100°C and are consistent with the TC measurements. This seems to confirm the earlier suggestion that TC errors were considerably larger above 1,100°C. For Test PRF-06, Figure 50 shows that the inverse temperatures are within the range of the TC measurements and the agreement is as good as in Test PRF-05.

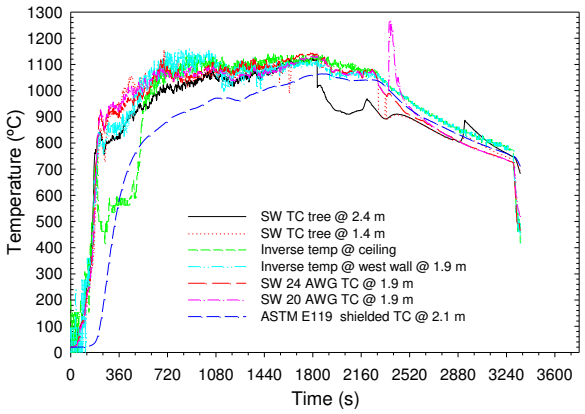

Figure 49. Test PRF-05: Temperatures measured by two different TCs and heat flux gauges.

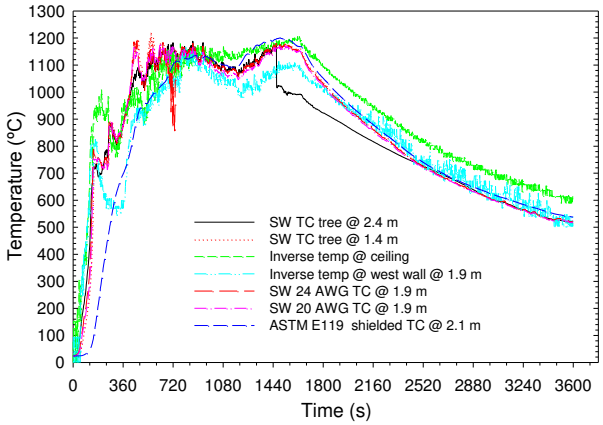

Figure 50. Test PRF-06: Temperatures measured by two different TCs and heat flux gauges.

An aspirated TC probe was first used in Test PRF-07; the results are shown in Figure 51 – the aspirated TC measurement was in very good agreement with the bare-bead TC until it was removed from the fire environment at about 1,200 s. As well, it can be seen that the aspirated TC does not experience rapid temperature fluctuations. Figure 52 shows the results of inverse temperature calculations. The results are in good agreement with bare-TCs until about 1,320 s when the inverse temperatures are about 50°C higher. Similar results (Figures 53 and 54) were obtained in Test PRF-08: the aspirated TC had fewer fluctuations and temperature measurements were in excellent agreement with the bare-bead TCs until it was removed from the fire.

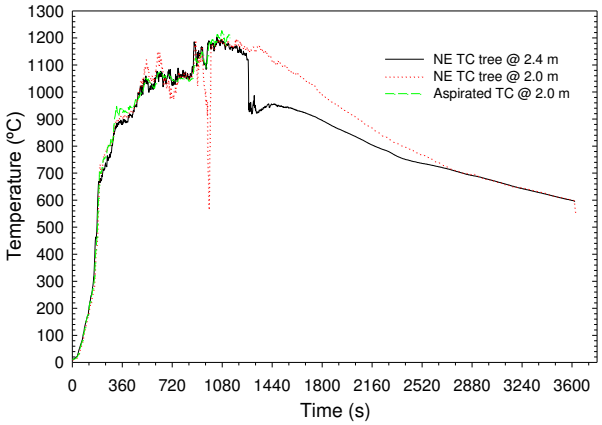

Figure 51. Test PRF-07: Temperatures measured by bare-bead and aspirated TCs in the NW section.

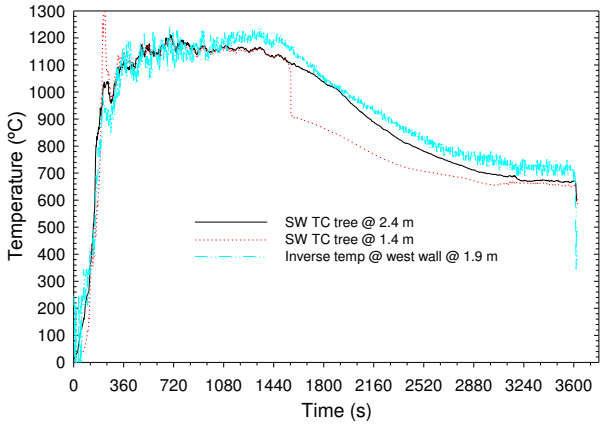

Figure 52. Test PRF-07: Temperatures measured by bare-bead TCs and west wall heat flux gauge (ceiling heat flux gauge was defective).

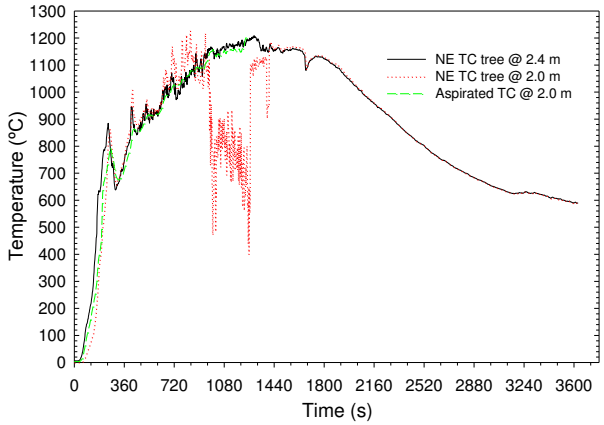

Figure 53. Test PRF-08: Temperatures measured by bare-bead and aspirated TCs in the NW section.

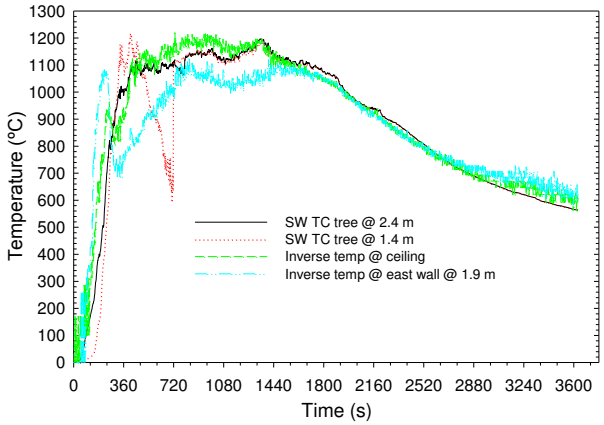

Figure 54. Test PRF-08: Temperatures measured by bare-bead TCs and west wall heat flux gauge (ceiling heat flux gauge was defective).

4.3.2.4.1 Conclusions

Temperature measurements using bare-bead TCs were analyzed to evaluate the level of accuracy. The results show that the TCs gave consistently accurate results with no evidence of there being any significant radiation errors up to about 1,100°C. For temperatures higher than 1,100°C, there appears to be significant errors in some tests. Methods of correcting bare-bead TC errors based on measurements using an aspirated TC probe and TC beads of different diameters could not be used in these tests. Crosschecking the temperature measurements against inverse temperatures derived from heat flux measurement confirmed that maximum instantaneous temperatures were approximately 1,200°C. Temperature spikes above 1,200°C which occurred in many of the tests can be considered to be less significant since they only existed for very short durations.

Overall, the complex flow dynamics in the fires and data corruption caused by the destruction of bare-bead TCs at very high temperatures made it difficult to implement a consistent error correction method.

4.3.2.5 Fire performance of ceiling and floor assemblies

Evaluation of the fire performance of floor and ceiling assemblies was not explicitly addressed in the tests. However, TCs were installed at various floor and ceiling cross-sections to provide information about the impact of the fires on the floor and ceiling. Although this discussion is only provided for Test PRF-02, -03 and -04, graphs for the entire test series were provided in Part 1 of the report.

Figures 55 to 60 show the temperature profiles across ceiling and floor cross-sections in Tests PRF-02, -03 and -04. The temperature profiles provide insight into the duration of various processes, such as calcination of gypsum board. In PRF-02, Figure 55 shows that it took about

1,080 s (period with small temperature gradient) to drive out moisture for the first layer of gypsum board on the ceiling to undergo calcination. The temperature spike that occurred at about 2,640 s (~ 600°C) likely indicates fall-out of some parts of the exposed layer. At that time the exposed layer falls off, the second layer begins to experience a rapid temperature rise. The times are considerably shorter in Tests PRF-03 and -04 with calcination of the first layer occurring around 840 s and fall-out at about 1,680 s. For the floor cross sections, the fire penetrated the OSB sub-floor at around 840 s in Test PRF-04 whereas it took 360 s longer in Test PRF-03 due to the presence of hardwood. The impact of the fire is less severe in the northern section of the fire room and fire penetration was therefore slower.

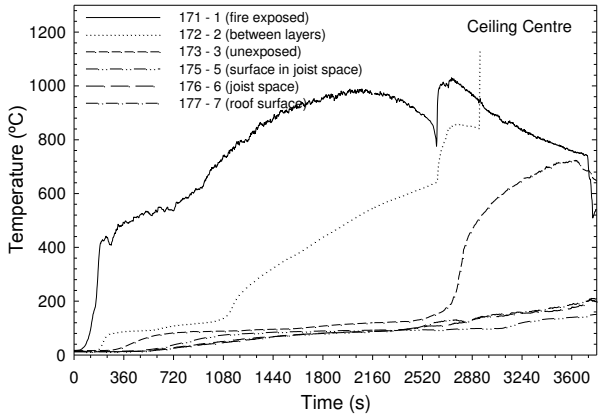

Figure 55. Temperature measurements at the ceiling (center cross-section) in Test PRF-02.

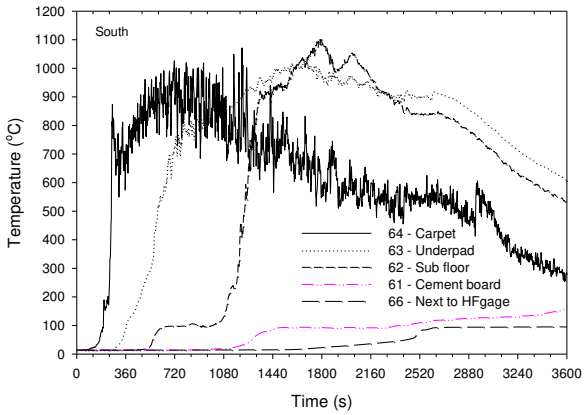

Figure 56. Temperature measurements at the floor (south cross-section) in Test PRF-02.

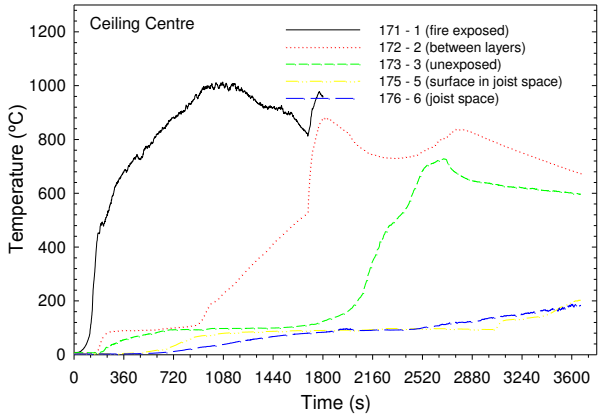

Figure 57. Temperature measurements at the ceiling (center cross-section) in Test PRF-03.

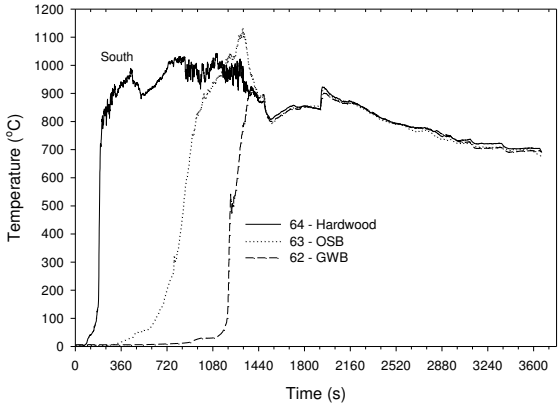

Figure 58. Temperature measurements at the floor (south cross-section) in Test PRF-03.

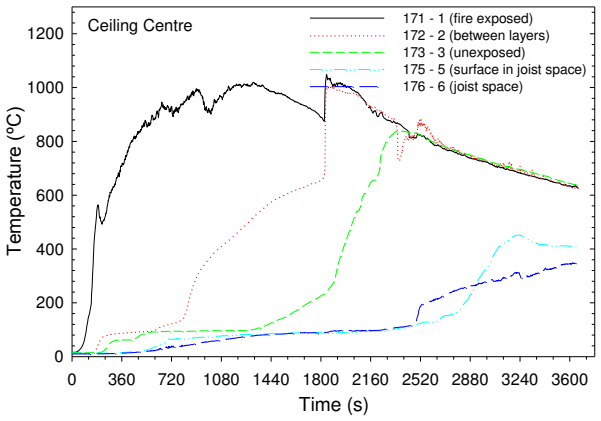

Figure 59. Temperature measurements at the ceiling (center cross-section) in Test PRF-04.

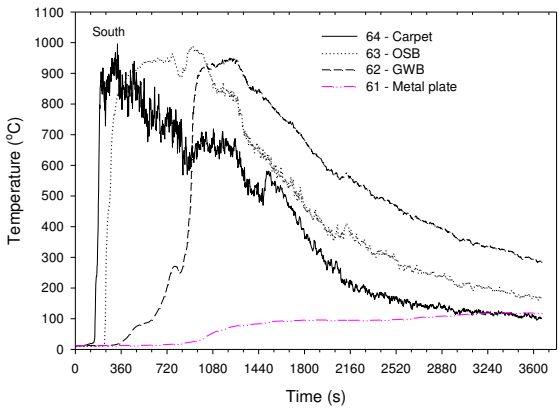

Figure 60. Temperature measurements at the floor (south cross-section) in Test PRF-04.

These results show that the fire burned through the floor finish and sub-floor at a fast rate. However, these results may not be indicative of the performance of a real assembly since both the floor and ceiling were constructed with additional layers of XGWB to better withstand the fires i.e. two layers of XGWB were installed under the OSB sub-floor and therefore the heat loss characteristics were different than in a real assembly. As well, the ceiling was reinforced with screws at 200 mm o.c. in addition to having three layers of XGWB as described in Part 1 of the report [1].

4.3.3 Secondary Bedroom (Configurations B2 and B3)

Three tests (PRF-05, -07 and -09) were conducted in this category. The results of Test PRF-05 will be compared with those for Test PRF-02 (Primary bedroom with the same window size) to evaluate the effect of a different fuel load composition, a slightly higher FLED (911 MJ/m^2 in Test PRF-02 vs. 999 MJ/m^2 in Test PRF-05) and smaller room size (16.0 m^2 in Test PRF-02 vs. 11.2 m^2 in Test PRF-05). Although the FLED in Test PRF-05 is 10% greater than that in Test PRF-02, the heat energy content (in MJ) of the fuel load in PRF-02 (14,647 MJ) is significantly greater (by about 26%) than that in PRF-05 (11,594 MJ). Earlier in this research, a fuel load survey was conducted and it was concluded that the fuel load density alone does not provide a complete picture of the associated fire hazard since parameters such as floor area and composition of the fuel load can affect the total heat energy content and its rate of release during a fire, assuming that other parameters remained identical [40]. Test PRF-05 presented an opportunity to evaluate the effect of fuel load density and room size on room fire behaviour.

Figure 61 shows the graphs of HRR for Tests PRF-02 and -05. While both fires follow the five stages of fire development established earlier, there are distinct differences: higher peak HRR and shorter post-flashover duration (Stages R3+R4) in PRF-05. There is less total energy released

(area under the HRR curve) in PRF-05 and hence the shorter duration of Stage R4 (Table 18), which is in agreement with theoretical estimates of heat content. PRF-05 shows a slightly slower initial fire growth, but the rate of fire growth is identical to PRF-02. The differences are likely due to the fact the furnishings were different and, specifically, the composition of thermoplastics was higher in Test PRF-05 (14.1% by mass in PRF-05 vs. 9.5% in PRF-02). However, the relative compositions of wood, which was the bulk of the fuel load, were comparable (60.1% by mass in PRF-02 vs. 59.9% in PRF-04; see Table 6). The higher peak HRR and external combustion, in PRF-05 is likely due to the increased composition of thermoplastics. It is not possible to make a definitive conclusion regarding this aspect of the fire behaviour since tracking of mass loss of individual furnishings was beyond the scope of this research; what is presented here is the overall perspective of fire behaviour based on observations and measurements of HRR, heat fluxes and temperatures.

Figure 62 shows the temperature measurements at 1.4 m and 2.4 m taken in the South West zone of the compartment for both tests. The differences mirror the HRR profiles: PRF-05 has higher temperatures in Stage R3, but ultimately both fires reach comparable mean maximum temperature levels of approximately 1,100°C in Stage R4 as can be seen in Table 19. Based on the features of the HRR profile immediately after flashover had occurred, it appears that there were more excess pyrolysis products in PRF-02 leading to the initial HRR spike and simultaneously-occurring temperature dip at around 360 s (also observed in tests based on configuration B1), which is absent in PRF-05. This suggests that there was better combustion efficiency (less excess pyrolysis products) immediately after flashover in PRF-05.

Analysis of temperatures at 1.4 m (on the TC trees) in the four zones of the room shows that the temperature environment was largely non-uniform in Test PRF-05 (Figure 63) compared to PRF-02 (Figure 64). The lower temperatures in Stage R3 in the northern zones (further inside the room) suggest that there was poor combustion efficiency (due to oxygen starvation) in those zones. Again, the differences in the types and arrangement of furnishings are a plausible explanation for these results: review of the fuel load schematics presented in Part 1 of the report shows that in PRF-05 there was a computer work station in the northern section of the room with a quantity of other plastic materials, which were absent in PRF-02.

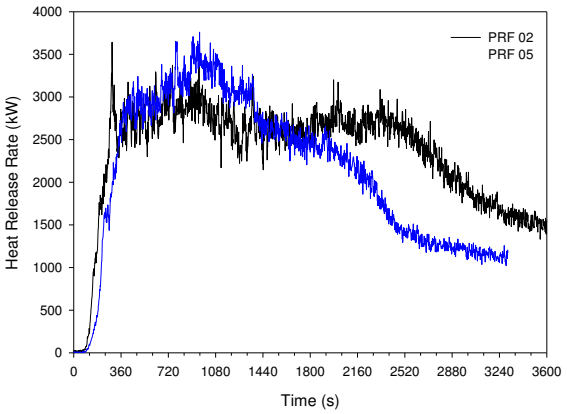

Figure 61. Comparison of HRRs for Tests PRF-02 and PRF-05.

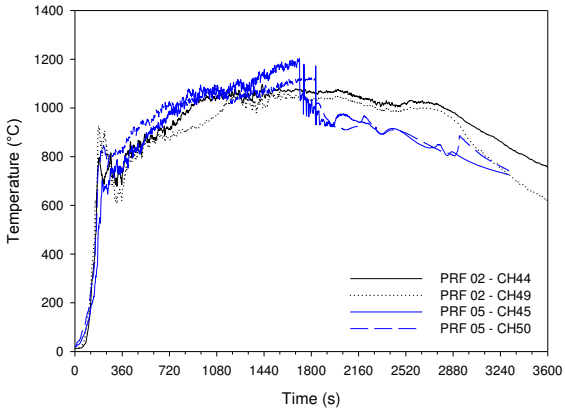

Figure 62. Comparison of temperatures at 1.4 m (CH44 & 49) and 2.4 m (CH45 & 50) on South West TC trees for Tests PRF-02 and -05.

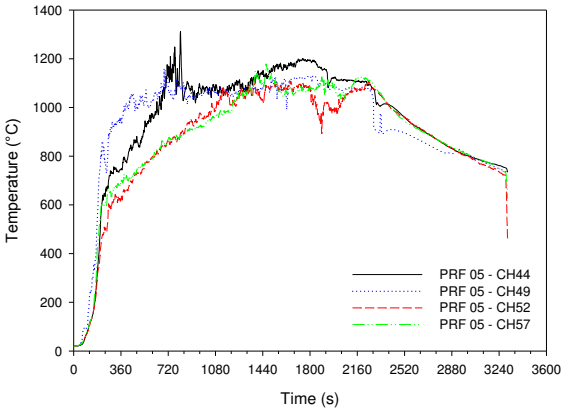

Figure 63. Temperatures at 1.4 m in the four zones of the room in tests PRF-05 (CH44 NW; CH49: SW; CH52: NE; CH57: SE).

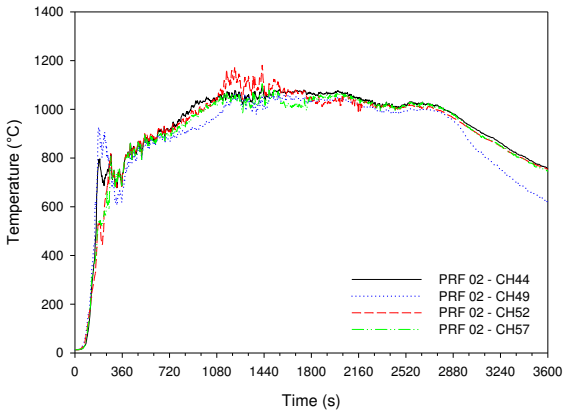

Figure 64. Temperatures at 1.4 m in the four zones of the room in tests PRF-02.

Table 18. Duration of stages of fire development for Tests PRF-02, and -05.

Test ID	Peak HRR (kW)	t_{HRRv}	Δt_{R2}	Δt_{R3}	Δt_{R4}	Δt_{R5}	$\overline{HRR}_{R4}$ (kW)	$\sigma_{HRR_{R4}}$ (kW)
PRF-02	3,642 (4.4) †	4.2	2.5	17.1	20.3	23.5	2,676	150
PRF-05	3,782 (15.5)[1]	5.6	3.5	17.4	16.0	19.1	2,455	265

† time to reach peak HRR (min); t_{HRRv} – time to reach HRRv; Δt_{RX} – duration of fire development Stage RX, where X= 2 to 5.

$\overline{HRR}_{R4}$ - Mean HRR in Stage R4; $\sigma_{HRR_{R4}}$ - Standard deviation of HRR at Stage R4.

Table 19. Temperatures at 1.4 m height (measured by a single TC) in each of the four zones of the room during Stage R4.

Test ID	Peak HRR (kW)		Temperature values in zone NW (°C)	NE (°C)	SW (°C)	SE (°C)	Duration of Stage R4 (min)
PRF-02	3,642	Min-Max	1,005-1,096	984-1,181	979-1,067	985-1,105	20.3
		Mean	1,056	1,060	1,030	1,036	
		SD †	18	39	79	19	
PRF-05	3,782	Min-Max	1,064-1,204	891-1,114	992-1,130	1,035-1,179	16.0
		Mean	1,140	1,053	1,090	1,085	
		SD	36	39	22	28	

† SD – Standard deviation

4.3.3.1 Fire performance of Test Wall Sections (Tests PRF-02 and PRF-05)

Table 20 compares the fire performance of TWS-01 and -02. The results show that TWS-01 had longer fire performance in Test PRF-02 than in PRF-05. This could be due to the smaller room size in PRF-05 and the fact that temperatures were higher in the west side of the room than in PRF-02 (Figures 63 and 64). In Test PRF-05, specimen TWS-02 did not reach the insulation failure criteria, which indicates that the fire was less severe than that in PFR-02 since it had a lower fuel load (resulted in a shorter duration of Stage R4).

Table 20. Fire performance results for TWSs in Tests PRF-02, and -05.

Test ID	Duration (min)	Peak HRR (kW)	TWS Time to Temperature Rise of 180°C TWS-01 (RGWB) (min)	TWS-02 (XGWB) (min)	TWS-03 (RGWB) (min)	TW-04 (XGWB) (min)
PRF-02	64	3,642	40	54	None	None
PRF-05	56	3,782	31	NULL	22	40

RGWB: Regular gypsum board (12.7 mm thick); XGWB: Type X gypsum board (15.8 mm thick)
None: Test section was not installed; NULL: ATSTM E119/ULC-S101 failure criteria were not reached.

4.3.3.2 Summary

1. In the context of Tests PRF-02 and -05, the FLED had no significant effect on peak temperatures and the duration of Stage R4. However, the fuel load (MJ) had a significant effect on the duration of Stage R4. Although, PRF-02 had a slightly lower FLED, it had more fuel load (MJ) since the floor area was greater than that in PRF-05.
2. The temperatures in Stage R4 were higher in PRF-05 than in PRF-02, which is likely due to lower heat losses through the room boundaries since the room was smaller than that in PRF-02.

4.3.3.3 Effect of Ventilation (Tests PRF-05, -07 and -09)

The effect of ventilation was further investigated in Tests PRF-05, -07 and -09 (all based on a room with a floor area of 11.2 m^2) with window sizes V2, V3 and V5 (refer to Table 3 for window dimensions), and FLEDs 999 MJ/m^2, 963 MJ/m^2 and 751 MJ/m^2, respectively. The fuel load quantity and composition in Test PRF-09 was altered to simulate bedrooms in residential care dwellings, which typically have lower FLEDs, smaller windows and hardwood floor finish [28]. Figure 65 shows the graphs of HRR vs. times for all three tests. The effect of ventilation on peak HRRs in both stages R3 and R4 is clearly shown:

a) With reduced ventilation, peak HRR values decrease while external heat release increases. The proportion of external heat release for Tests PRF-05, -07 and -09 was estimated to be 13%, 0% and 15%, respectively (with PRF-07 having the highest ventilation and PRF-09 having the lowest). The proportion of external heat release was calculated by dividing the total heat release above the ventilation limited HRR value (i.e. area above) by that below it (i.e. area below the ventilation HRR value);
b) Test PRF-09 had a faster rate of fire growth;
c) In Test PRF-09, there is a good agreement with the theoretical HRRv in Stage R4 (Figure 65), but Tests PRF-05 and -07 do not show good agreement. The lack of agreement could be due to the fact that the second window in Test PRF-07 was not directly in the original room, but rather connected to the room through an open doorway.

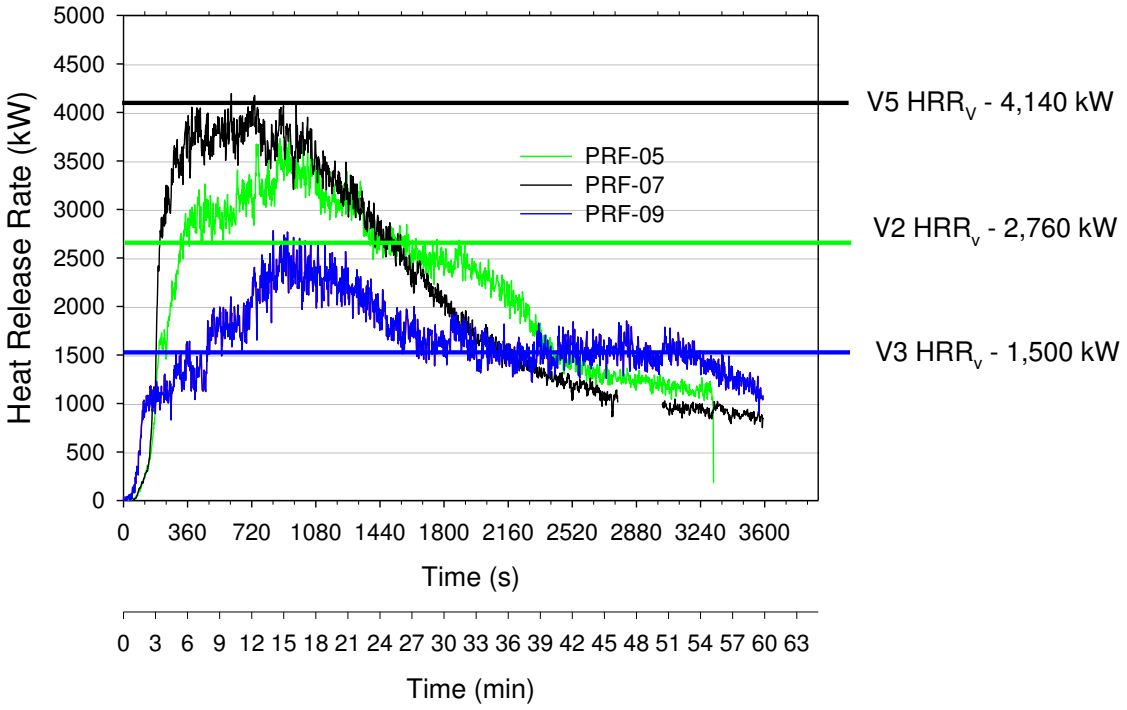

Figure 65. Graphs of HRR vs. time for Tests PRF-05, -07 and -09.

Figures 66 to 68 show the results of temperature measurements, while heat flux results are shown in Figures 69 to 71. Table 21 gives the analysis of temperatures in all four zones in Stage R4. Peak heat flux values are given in Table 22. The results are summarized as follows:

a) Higher and faster-occurring post-flashover temperatures (Figure 66) in Test PRF-07 due to increased ventilation compared to PRF-05 and -09, but the higher burning rate resulted in a shorter fully-developed phase; Test PRF-09 had the lowest post-flashover temperatures in Stage R3 (Table 21) and the longest duration of the decay phase (Stage R3). In PRF-09, the temperature reached a mean maximum value (during Stage R4) of 1,039°C in the SE zone (Table 21).
b) Consistent with previous findings, temperatures in the northern zones were lower in all of the tests (Figures 63, 67 and 68)
c) Heat flux results are consistent with temperature measurements: higher heat flux at the ceiling in PRF-07, the floor and on the east wall. Lowest peak heat flux in PRF-09 indicated lower maximum temperatures. Tests PRF-05 and -07 had higher peak heat readings flux at the floor shortly after flashover since the gauge was located in the south of the room near the window.

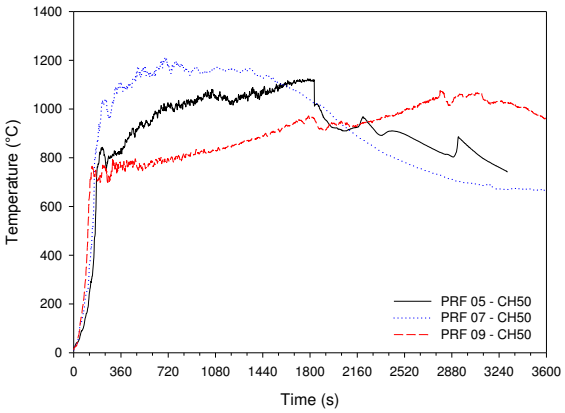

Figure 66. Temperatures at 2.4 m in the SW zone of the room in Tests PRF-05, -07 and -09.

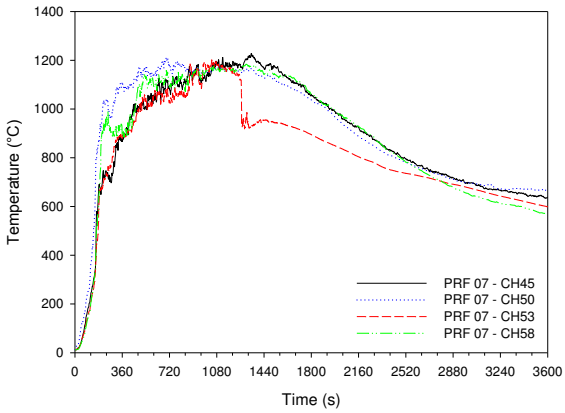

Figure 67. Temperatures at 2.4 m in the four zones of the room in Test PRF-07 (CH50-SW; CH53-NE; CH45-NW; CH58-SE).

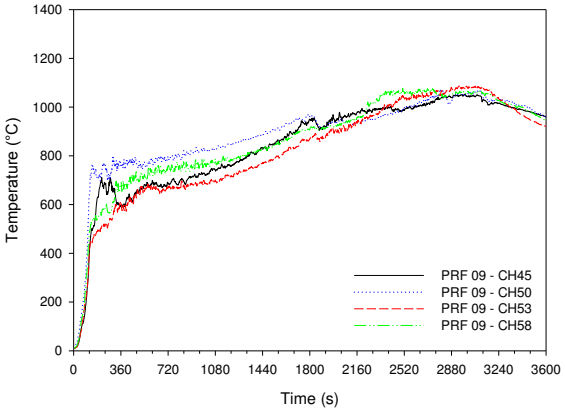

Figure 68. Temperatures at 2.4 m in the four zones of the room in Test PRF-09 (CH50-SW; CH53-NE; CH45-NW; CH58-SE).

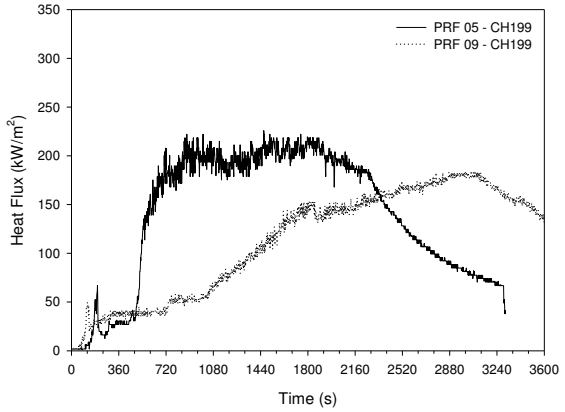

Figure 69. Heat flux the center of the ceiling (CH199) in Tests PRF-05 and -09 (No data for PRF-07 due to instrument malfunction).

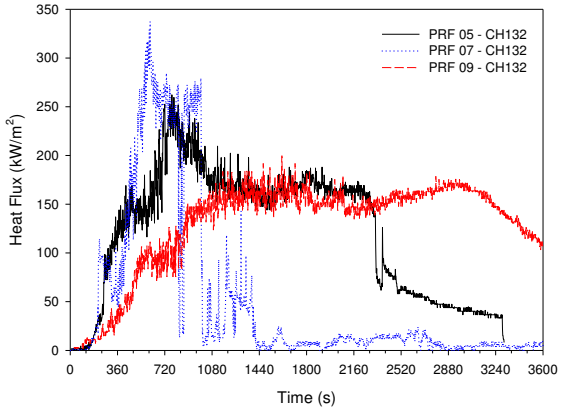

Figure 70. Heat flux on the floor (CH132) in PRF-05, -07 and -09 (instrument malfunction in Test PRF-07 after 800 s).

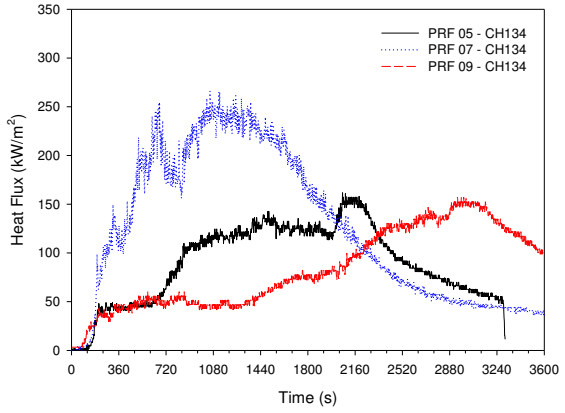

Figure 71. Heat flux at east wall (CH134) in Tests PRF-05, -07 and -09.

Table 21. Temperatures at 1.4 m height (measured by a single TC) in each of the four zones of the room during Stage R4.

Test ID	Peak HRR (kW)		Temperature values in zone NW (°C)	NE (°C)	SW (°C)	SE (°C)	Duration of Stage R4 (min)
PRF-05		Min-Max	1,064-1,204	891-1,114	992-1,130	1,035-1,179	16.0
	3,782	Mean	1,140	1,053	1,090	1,085	
		SD †	36	39	22	28	
PRF-07		Min-Max	760-1,315	565-1,196	979-1,353	916-1,267	14.5
	4,134	Mean	1,066	999	1,142	1,081	
		SD	130	123	48	73	
PRF-09		Min-Max	964-1,054	916-1,092	956-1,133	980-1,066	14
	2,793	Mean	1,005	1,027	1,021	1,039	
		SD	19	47	41	23	

† SD – Standard deviation

Table 22. Peak radiation flux at various locations in Tests PRF-05, -07 and -09.

Test ID	Floor	Peak heat flux at various surfaces (kW/m^2) West wall	East wall	Ceiling center	North wall	External @ 2.4 m	External @ 4.8 m
PRF-05	262	239	161	225	228	34	<7
PRF-07	337	293	266	X	None	35	9
PRF-09	200	295	157	183	X	18	<5

4.3.3.4 Fire performance of Test Wall Sections (Tests PRF-05, -07 and -09)

Table 23 gives the fire performance results. PRF-05 was the most severe fire given the shorter failure times for TWS-03 and TWS-04, while PRF-09 was the least severe with TWS-04 achieving almost 60 min fire performance. It is interesting to note that in this case, the higher ventilation in PRF-07 did not create the most severe impact on the wall specimens (as was seen in Test PRF-02 vs. -05) since the duration of the fully-developed phase was slightly shorter than that in Tests PRF-5 and -09. However, in PRF-09, the much lower ventilation caused an extended period of low temperatures in Stage R3, while Stage R4 was of shorter duration and had lower mean maximum temperatures of around 1,000°C. Therefore, it is concluded that either a longer duration (lower ventilation and initial post-flashover temperatures) or shorter duration (higher ventilation and initial post-flashover temperatures) can create the most severe temperature conditions for the room boundaries depending on the specific combinations of fuel load and ventilation. In order for the higher ventilation scenario to create severe fire conditions, there has to be enough of a fuel load to

support a fully-developed phase of a given duration otherwise the higher initial temperature will not be sustained for a long enough time to challenge the room boundaries. It was beyond the scope of this research to establish analytical methods of quantifying the thermal response of room boundaries under various fire scenarios. Rather, this research characterizes specific fire scenarios (based on a limited number of tests) and develops the understanding of room fire behaviour to facilitate further analytical work.

Table 23. Fire performance results for TWSs in Tests PRF-05, -07 and 09.

Test ID	Duration	Peak HRR	TWS Time to Temperature Rise of 180°C			
			TWS-01 (RGWB)	TWS-02 (XGWB)	TWS-03 (RGWB)	TWS-04 (XGWB)
	(min)	(kW)	(min)	(min)	(min)	(min)
PRF-05	56	3,782	31	NULL	22	40
PRF-07	64	4,134	NULL	NULL	27	51
PRF-09	60	2,793	None	None	37	59

RGWB: Regular gypsum board (12.7 mm thick); XGWB: Type X gypsum board (15.8 mm thick)
None: Test section was not installed; NULL: ATSTM E119/ULC-S101 failure criteria were not reached.

4.3.3.5 Flashover

Table 24 gives the results of the assessment of the flashover conditions. The results show that Test PRF-07 has the shorter time to flashover, which is likely due its faster rate of fire growth as can be seen in Figure 67. Three correlations were used to estimate the theoretical value of HRR required to cause flashover in the test room and the values obtained for window V2 were: Thomas [16] – 1,244 kW; Babrauskas [15] – 1, 380 kW; MQH [17] – 1,062 kW.

In this case, none of correlations were in good agreement with the test results; Babrauskas's correlation provides the better overall prediction given that the Thomas and MQH correlations largely under predicted flashover in Test PRF-05.

Table 24. Flashover results.

Test ID	Peak HRR (kW)	Time to peak HRR (s)	Time to flashover based on various criteria (s)			
			F_600°C	HRR (kW)	F_20 kW/m^2	F_flames out
PRF-05	5,133	255	210	1,699	222	174
PRF-07	4,134	636	180	1,189	186	150
PRF-09	2,793	841	192	1,021	240	240

F_600°C: hot layer temperature of 600°C; **F_20 kW/m^2**: heat flux of 20 kW/m^2 at floor level; **F_flames out**: flames emerge from window

4.3.4 Living Room (Configuration B4)

The tests discussed thus far have established many characteristics of room fires with real furnishings. Three tests (PRF-06, -12, and -13) were conducted under configuration B4. Test PRF-06 was conducted to characterize a living room fire while the other two tests addressed the issues of repeatability and measurement of progressive mass loss.

To evaluate the effects of fuel load composition PRF-06 (living room configuration B4) is compared to PRF-04 (primary bedroom configuration B1), both tests had the same window configuration (V1) and had a carpet floor finish. Test PRF-06 had a significantly lower FLED (689.4 MJ/m^2) than Test PRF-04 (914.5 MJ/m^2). Figure 72 shows the graphs of HRR vs. time for both tests. There are noticeable differences in the HRR profiles in Stages R3 and R5: lower peak HRR followed by a dip, and a more rapid decay in PRF-06. While both tests have similar fire growth rates, after flashover Test PRF-06 had a lower peak HRR (5,133 kW vs. 6,014 kW in PRF-04) and a pronounced dip in HRR to about 3,500 kW followed by a rapid climb to values around the HRRv. Table 25 summarizes the results: shorter duration of the post-flashover phase (R3+R4), but PRF-06 appears to be more severely under-ventilated immediately after flashover, judging by the lower temperatures in Stage R3 (Figure 73). The variation of temperatures in the four zones of the room (Figure 74) is consistent with previous observations: that fire development in the north and eastern zones lag the western zones.

Figures 75, 76 and 77 show the graphs of heat flux vs. time at the ceiling, west wall and east wall. The heat flux profiles clearly reflect the fact that Test PRF-04 had higher temperatures earlier on in Stage R3 as shown in Figure 73, but the heat flux in PRF-06 eventually became higher than that in PRF-04 later on during the test, such that both tests appear to have comparable thermal exposure (area under the curves). Table 26 gives the analysis of temperatures in all four zones in Stage R4 for Tests PRF-04 and -06.

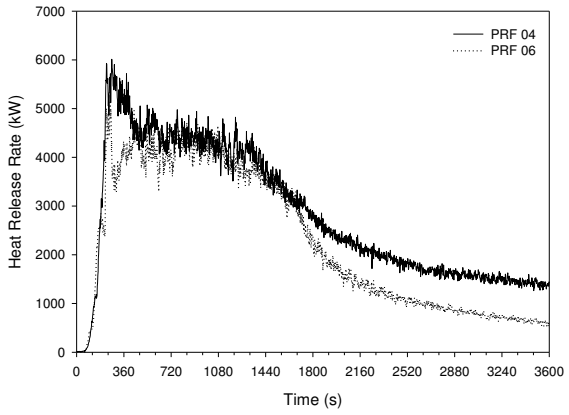

Figure 72. HRR vs time for Tests PRF-04 and -06.

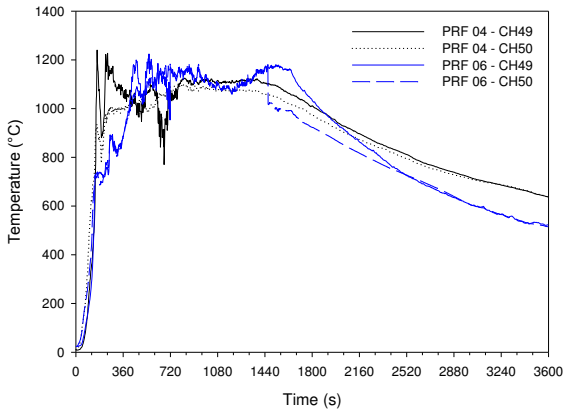

Figure 73. Temperatures at 1.9 m (CH49) and 2.4 m (CH50) in the SW Zone in Tests PRF-04 and -06.

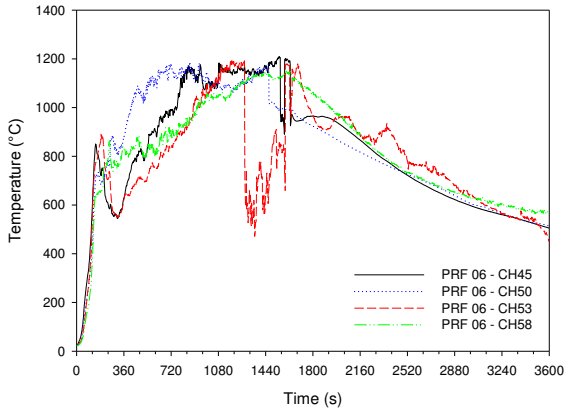

Figure 74. Temperatures at 2.4 m in the four zones of the room in Tests PRF-06 (CH50-SW; CH53-NE; CH45-NW; CH58-SE).

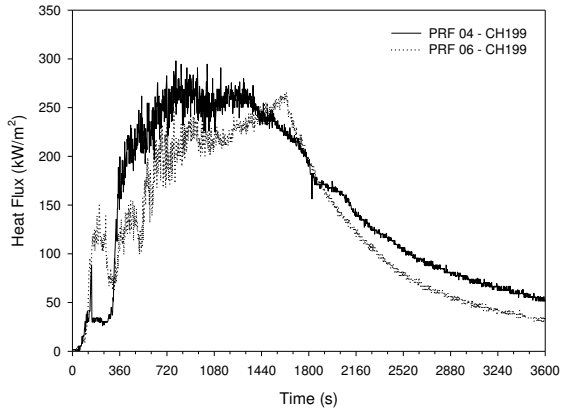

Figure 75. Heat flux at the ceiling in Tests PRF-04 and -06.

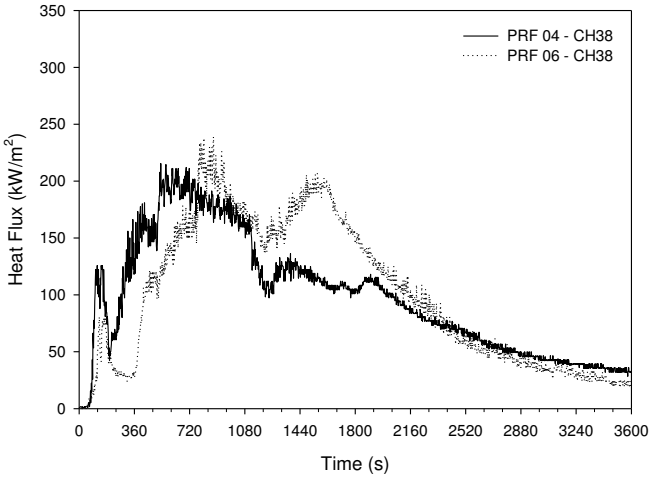

Figure 76. Heat flux on west wall in Tests PRF-04 and -06.

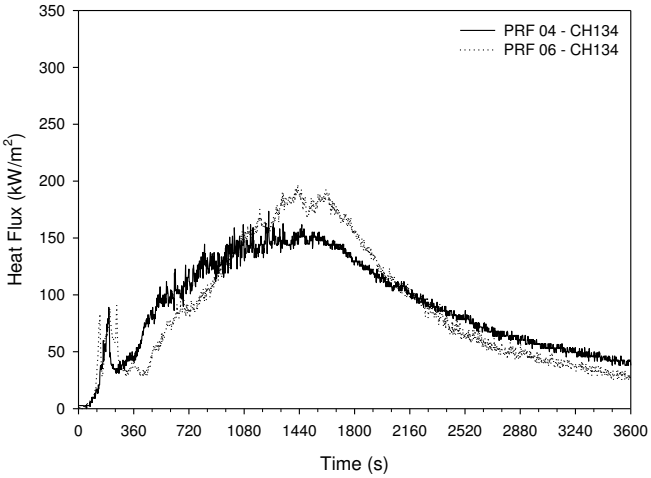

Figure 77. Heat flux on east wall in Tests PRF-04 and -06.

Table 25. Duration of stages of fire development for Tests PRF-04 and -06.

Test ID	Peak HRR (kW)	t_{HRRv} (min)	Δt_{R2} (min)	Δt_{R3} (min)	Δt_{R4} (min)	Δt_{R5} (min)	$\overline{HRR}_{R4}$ (kW)	$\sigma X_{HRR_{R4}}$ (kW)
PRF-04	6,014 (4.0) †	3.1	2.4	4.3	15.7	38.6	4,330	269
PRF-06	5,133 (4.3)	3.2	2.3	5.1	12.8	39.8	4,130	258

† time to peak HRR (min); t_{HRRv} – time to reach HRRv; Δt_{RX} – duration of fire development Stage RX, where X= 2 to 5.; $\overline{HRR}_{R4}$ - mean HRR in Stage R4; $\sigma X_{HRR_{R4}}$ - Standard deviation of HRR at Stage R4.

Table 26. Temperatures at 1.4 m height (measured by a single TC) in each of the four zones of the room during Stage R4.

Test ID	Peak HRR (kW)		Temperature values in zone NW (°C)	NE (°C)	SW (°C)	SE (°C)	Duration of Stage R4 (min)
PRF-04	6,014	Min-Max	921-1,264	621-1,188	770-1,125	776-1,158	15.7
		Mean	1,129	959	1,080	947	
		SD †	53	57	57	72	
PRF-06	5,133	Min-Max	743-1,202	663-1,307	953-1,224	860-1,064	12.8
		Mean	1037	966	1,119	971	
		SD	137	199	40	46	

† SD – Standard deviation

4.3.4.1 Fire performance of Test Wall Sections

The fire performance results (given in Table 27) for TWS-01 and -02 show that the fire performance of TWS-01 in PRF-04 was less than that in PRF-06 by 4 min, whereas the results show an opposite trend for TWS-02: the fire performance was shorter in PRF-06. The heat flux measurements (Figures 76 and 77) support these trends. Based on heat flux results and Temperatures in region R4, the severity (heat flux, temperatures and impact on boundaries) of the two fires (PRF-04 and -06) are comparable although fuel load mass and the total heat released in PRF-04 was significantly greater than that in PRF-06 (10,225 MJ in PRF-04 vs. 8,214 MJ in PRF-06). There was a greater amount of the external and decay-phase heat release in Test PRF-04.

Table 27. Fire performance results for TWSs in Tests PRF-04 and 06.

Test ID	Duration (min)	Peak HRR (kW)	TWS Time to Temperature Rise of 180°C			
			TWS-01 (RGWB) (min)	TWS-02 (XGWB) (min)	TWS-03 (RGWB) (min)	TW-04 (XGWB) (min)
PRF-04	61	6,014	24	53	19	28
PRF-06	60	5,133	28	48	None	None

RGWB: Regular gypsum board (12.7 mm thick); XGWB: Type X gypsum board (15.8 mm thick)
None: Test section was not installed

4.3.4.2 Repeatability

Repeatability was evaluated in Test PRF-12. Fuel load masses were 714 kg for PRF-06 and 707 kg for PRF-12. Figure 78 shows that the HRR profiles are in good agreement for most of the fire duration except for the peak HRR spike in PRF-06 (not repeated in PRF-12) and towards the end of the test where PRF-12 shows a slightly slower rate of decay. Temperature results are compared in Figure 79. There was good agreement until after about 600 s: temperature drop in PRF-12, which is likely related to a drop in combustion efficiency. Reproducibility of the temperature environment is not consistent after 1,380 s (going into the decay phase) with PRF-06 showing higher measured values of heat flux at the west wall, east wall and ceiling (Figures 80 to 82).

The duration of the various stages of fire development is compared in Table 28. Although the times to reach flashover are identical, there are some differences in duration of various stages. Table 29 summarizes the Temperatures in Stage R4.

The peak values of heat flux measured in Tests PRF-06, -12 and -13 are summarized in Table 30. At this point, there is no clear indication as to which factors or fire phenomena were responsible for the lack of repeatability during the decay phase.

The fire performance results are presented in Table 31. The results show that the performance of TWS-01 was the same in both tests, but TWS-02 had a shorter fire performance (by 6 min) in PRF-06. This result is consistent with heat flux results, which show higher heat fluxes in Test PRF-06 in the decay phase.

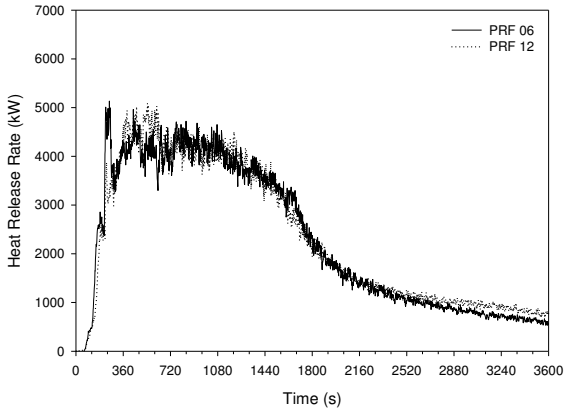

Figure 78. HRR vs time for Tests PRF-06 and -12.

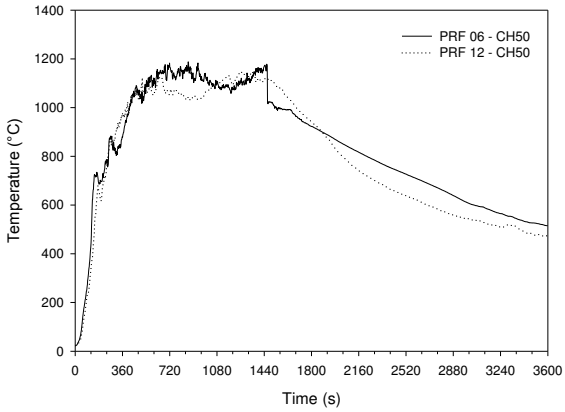

Figure 79. Temperatures at 2.4 m (CH50) in the SW Zone in Tests PRF-06 and -12.

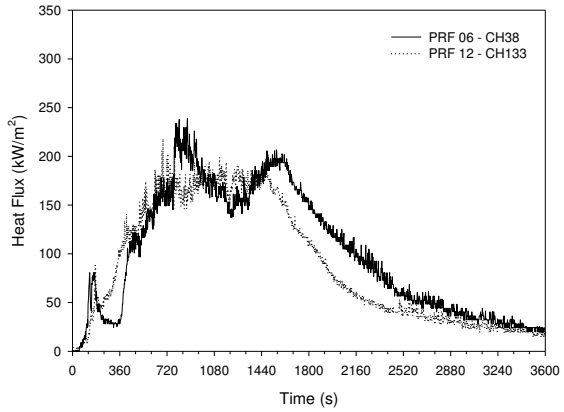

Figure 80. Heat flux at the west wall in Tests PRF-06 and -12.

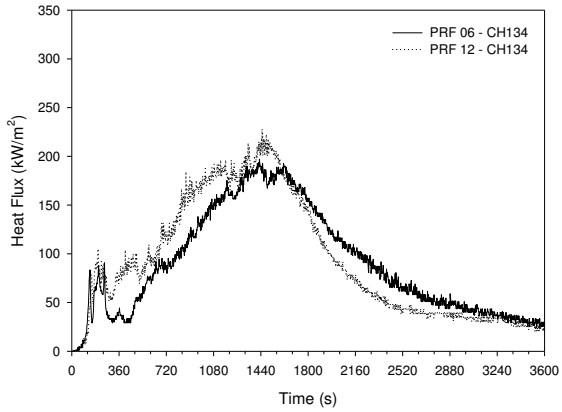

Figure 81. Heat flux at the east wall in Tests PRF-06 and -12.

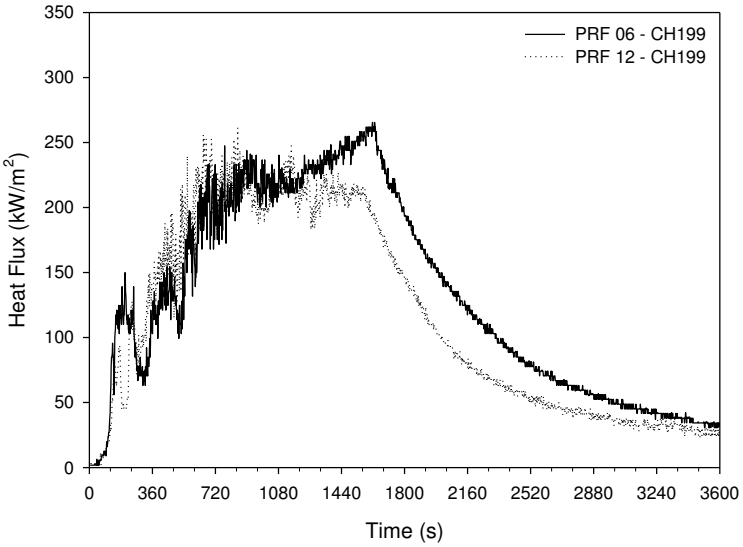

Figure 82. Heat flux at the ceiling in Tests PRF-06 and -12.

Table 28. Duration of stages of fire development for Tests PRF-06 and -12.

Test ID	Peak HRR (kW)	t_{HRRv} (min)	Δt_{R2} (min)	Δt_{R3} (min)	Δt_{R4} (min)	Δt_{R5} (min)	$\overline{HRR}_{R4}$ (kW)	$\sigma X_{HRR_{R4}}$ (kW)
PRF-06	5,133 (4.3) †	3.2	2.3	5.1	12.8	39.8	4,130	258
PRF-12	5,084 (8.5)	5.3	2.5	7.6	11.1	42.8	4,006	379

† time to peak HRR; t_{HRRv} – time to reach HRRv; Δt_{RX} – duration of fire development Stage RX, where X= 2 to 5.; $\overline{HRR}_{R4}$ - mean HRR in Stage R4; $\sigma X_{HRR_{R4}}$ - Standard deviation of HRR at Stage R4.

Table 29. Temperatures at 1.4 m height (measured by a single TC) in each of the four zones of the room during Stage R4.

Test ID	Peak HRR (kW)		Temperature values in zone NW (°C)	NE (°C)	SW (°C)	SE (°C)	Duration of Stage R4 (min)
PRF-06	5,133	Min-Max	743-1,202	663-1,307	953-1,224	860-1,064	12.8
		Mean	1037	966	1,119	971	
		SD †	137	199	40	46	
PRF-12	5,084	Min-Max	722-1,273	785-1,207	876-1,202	949-1,209	11.1
		Mean	974	1,060	1,024	1,066	
		SD	151	135	65	42	

† SD – Standard deviation

Table 30. Peak radiation flux at various locations in Tests PRF-06, -12 and -13.

Test ID	Floor	Peak heat flux at various surfaces (kW/m^2) West wall	East wall	Ceiling center	North wall	External @ 2.4 m	External @ 4.8 m
PRF-06	276	239	197	266	255	37	11
PRF-12	179	218	228	261	X†	37	X
PRF-13	198	206	280	265	X	37	X

† X – No data

Table 31. Fire performance results for TWSs in Tests PRF-06 and 12.

Test ID	Duration (min)	Peak HRR (kW)	TWS Time to Temperature Rise of 180°C TWS-01 (RGWB) (min)	TWS-02 (XGWB) (min)	TWS-03 (RGWB) (min)	TW-04 (XGWB) (min)
PRF-06	60	5,133	28	48	None	None
PRF-12	64	5,084	28	54	None	None

RGWB: Regular gypsum board (12.7 mm thick); XGWB: Type X gypsum board (15.8 mm thick)

None: Test section was not installed

4.3.4.3 Measurement of Mass Loss

Test PRF-13 was conducted to measure the mass loss during the test. While the HRR vs. time profile is identical to that in tests PRF-06 and -12 (Figure 83), the temperature environment was quite different (Figure 84) since the exposed wall lining material used in PRF-13 was 12.7 mm cement board, while 15.8 mm XGWB was used in PRF-06.

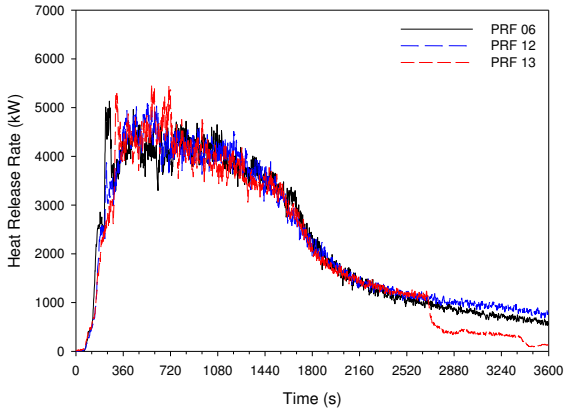

Figure 83. HRR vs. time for tests PRF-06, -12 and -13.

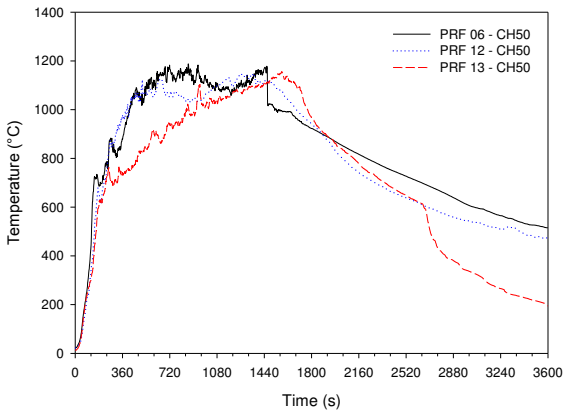

Figure 84. Temperatures at 2.4 m (CH50) in the SW Zone in tests PRF-06, -12 and -13.

Figure 85 shows the graph of mass loss (kg) vs. time (s). From about 240 s, the mass loss trend is approximately linear until at about 1,440 s when the readings begin to show some distortion, which was likely due to falling debris from the walls and ceiling. Temperatures at a cross-section located at the center of the ceiling shows evidence of TC breakage on CH171 (Figure 86) and a rapid temperature rise on CH173 (behind the second layer of the wall lining), which suggests that the first layer of cement board had fallen off. Therefore, mass loss measurements after that point were no longer usable since they had been corrupted by falling debris.

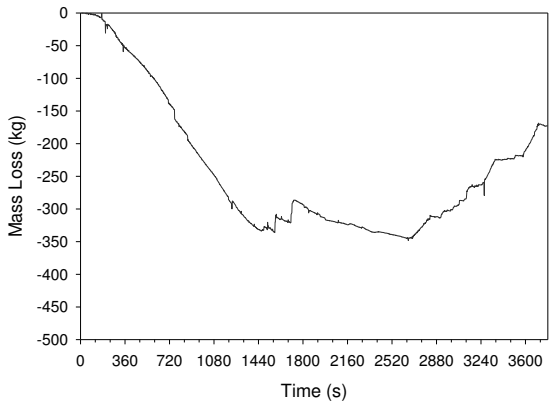

Figure 85. Mass loss vs. time for tests PRF-13.

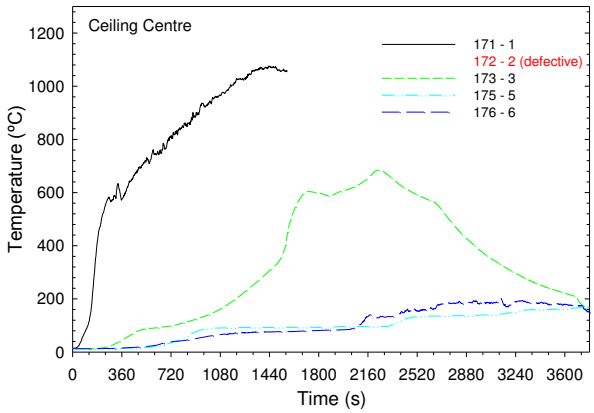

Figure 86. Cross-section temperatures at the center of the ceiling in Test PRF-13 (171 – exposed surface; 172 – between layers; 173 – behind second layer on cavity side).

The analysis of mass loss data was focused on the period before 1,440 s. About 40% of the mass (272 kg) was consumed during the growth and fully-developed stages (R2-R4) of the fire. A detailed breakdown of the results in Stages R2-R4 is given in Table 32. The results show that the total heat release from 272 kg of consumed mass is approximately 4,112 MJ (based on HRR measurements), giving a mean net calorific value (HC) of 15.1 MJ/kg during this period. This compares favourably (within about 6%) with the theoretical value of 16.0 MJ/kg that is estimated by using the weighted average of the fuel load's constituent materials.

Table 32. Mass loss results for Test PRF-13.

	t_{HRRv} (min)	Δt_{R2} (min)	Δt_{R3} (min)	Δt_{R4} (min)	Δt_{R5} (min)
Stage time (s) †	4.5	3.2	8.4	7.8	24.6
Mass loss (kg)	28.7	12.8	115.2	144	-
HC (MJ/kg) ††	11.3	9.7	18.0	13.3	-
Measured HR (MJ) †††	324	124	2078	1,910	3,660
% of Ideal HR††††	3.0	1.1	19.0	17.4	33.3

† Duration of each stage of fire development; †† Net calorific value; ††† Total heat release calculated from HRR measurements; †††† Theoretical total heat release (10,969 MJ).

4.3.4.4 Test with a Residential Sprinkler

Test PRF-11 was conducted in a living room configuration to evaluate the effect of a Reliable® Model F1Res 49 residential pendent sprinkler as shown in Figure 87. The line pressure was set to 15 PSI. The smoke alarm sounded at 30 s and the sprinkler activated at 47 s and effectively controlled the fire.

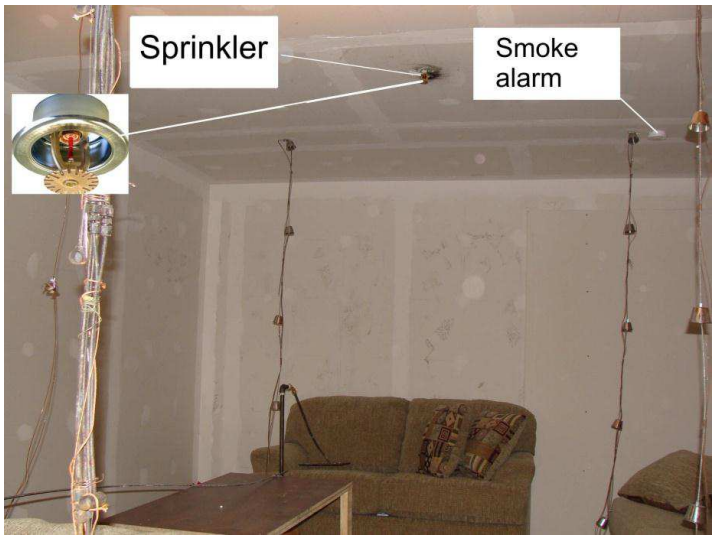

Figure 87. Position of the sprinkler on the ceiling.

Figures 88 and 89 show the HRR and temperature profiles, respectively: the peak HRR was 110 kW at 47 s and the peak temperature at a single measurement point was 117°C, which is well below the flashover threshold of 600°C. The total heat energy released was only 27.6 MJ, which is only 0.4% of the total fuel load of 6,478 MJ.

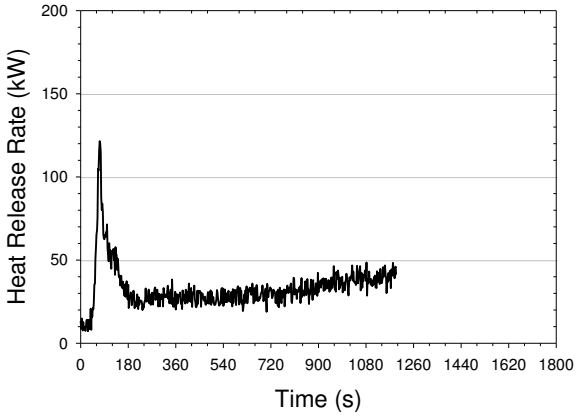

Figure 88. HRR vs. time for Test PRF-11.

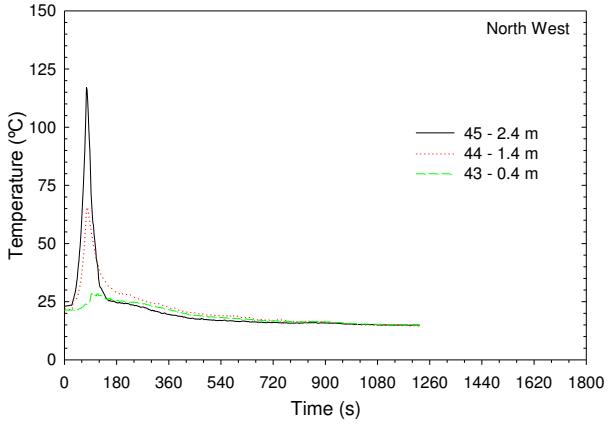

Figure 89. Temperature profiles measured by the TC tree in the North West quadrant in Test PRF-11.

The fire produced enough dense dark smoke to fill the upper half of the room and there was diminished visibility into the room after sprinkler had activated. The fire was not completely extinguished after the sprinkler activated – there was a small fire that continued to burn for about 10 min in a gap between two cushions that were located near the ignition source. However, the initial discharge of water from the sprinkler was able to significantly reduce the size of the fire from 110 kW to about 30 kW within 120 s of activating, as shown in Figure 88. The test was terminated at 20 min when the fire was completed extinguished by NRC staff.

4.3.5 Secondary Suite (Configuration B5)

Test PRF-08 was a multi-room setup simulating a secondary suite. The setup consisted of a bedroom and living room separated by an interior gypsum partition wall that had a door connecting the two rooms. The door was closed during the test; the fire was started in the bedroom as was done in the tests based on configuration B1. The instrumentation plan is shown in Figure 90.

In Test PRF-08, the fire only spread to the living room after it burnt through the door at about 4.5 min. Figure 91 shows the picture of the door at the time when the fire began to burn through it and Figure 92 shows the situation at 6.5 min when the fire had completely burnt through the door. Therefore, the fire had spread past the door within 3 min of flashover occurring in the bedroom (room of origin).

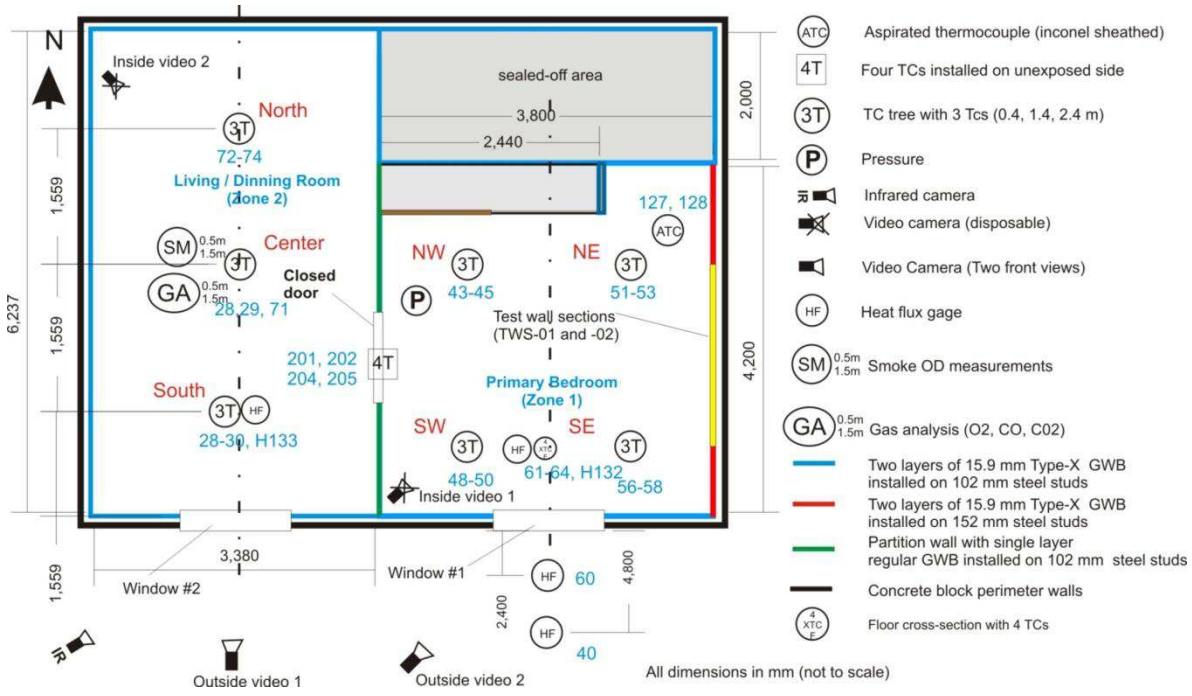

Figure 90. Test PRF-08 - Instrumentation floor plan showing location of TC trees.

Figure 91. Test PRF-08: Fire starting to burn through the door at 4.5 min.

Figure 92. Test PRF-08: Fire burns through the door at 6.5 min.

Figure 93 shows the graph of HRR vs. time. The multiple peaks in the HRR curve highlight the complexity of fire development in the multi-room and multi-window test setup that was used. The fire was started in Zone 1 (bedroom) which had the same fuel load as Test PRF-04, but the arrangement of furnishings was different: the first-ignited-item (a queen size bed assembly) was on the east side of the room in PRF-08 (Figure 33 in Part 1 of the Report [1]). Although the average FLED for the entire space was 617 MJ/m^2, it is important to note that the two zones had vastly different FLEDs: 919 MJ/m^2 in Zone 1 and 388 MJ/m^2 in Zone 2.

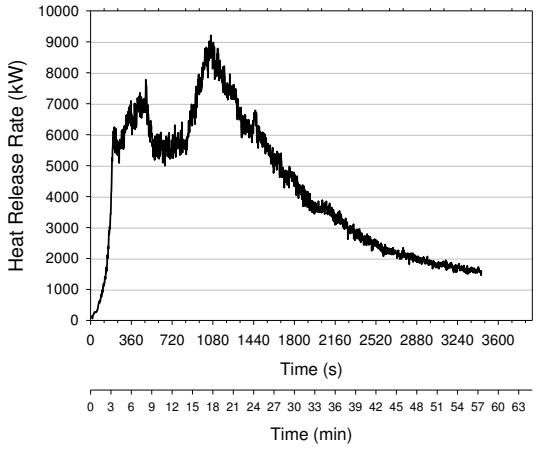

Figure 93. HRR vs. time for Test PRF-08.

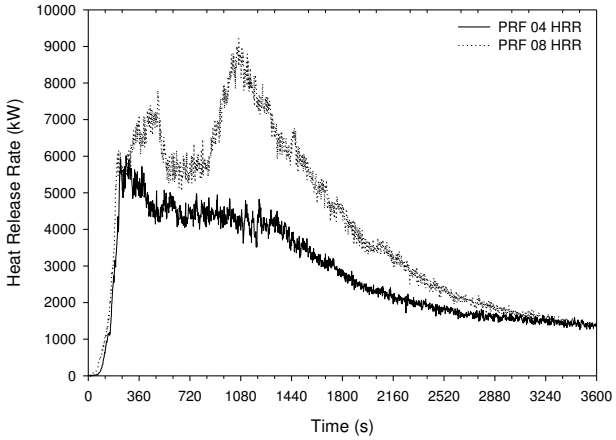

Figure 94. Comparison HRR vs. time results for Tests PRF-04 and -08.

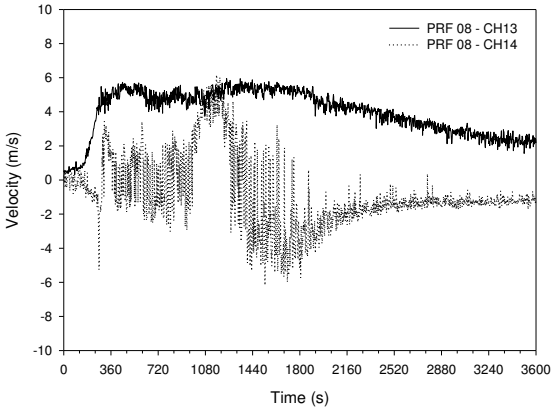

Figure 95. Zone 1 window 1 velocity profiles at 1.13 m (CH13) and 0.38 m (CH14) above sill for Test PRF-08.

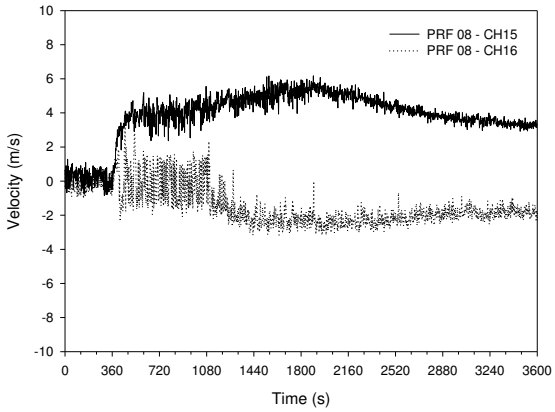

Figure 96. Zone 2 window 2 velocity profiles at 0.9 m (CH15) and 0.3 m (CH16) above sill for Test PRF-08.

The results of Test PRF-08 will be compared with PRF-04 to evaluate the effect of increased ventilation, fuel load and compartment dimension (since the partition wall between zones 1 and 2 was expected to be destroyed during the fire). Figure 94 shows that, despite the differences in fuel load arrangement, the fire growth periods for Tests PRF-08 and -04 were identical for the first 240 s. The difference in HRR profiles and multiple peaks in Test PRF-08 can be explained as follows:

1. At 270 s, the fire began burning through the door between Zone 1 and Zone 2 (living room). The effect was an increasing rate of air supply to the fire in the bedroom (due to the flow induced by buoyancy in the fire room) and hence the continued increase in HRR to values above 6,000 kW and significant departure from single-room (PRF-04) behaviour, which is validated by extra ventilation through the rapidly deteriorating door. An analysis of graphs of velocities profiles (Figures 95 and 96) in the windows in zones 1 and 2 supports this observation.

2. At 390 s, the door was completely consumed and maximum ventilation from both windows was available to Zone 1. Observations and temperature data confirmed that flashover had not yet occurred in Zone 2. Therefore, the first peak of 7,818 kW at 496 s was due to the sudden availability of full ventilation as well as the combustion of pyrolysis products generated from Zone 1 areas near the doorway. The drop in HRR to values of around 5,700 kW marks the transition of Zone 1 to Stage R4, while Zone 2 was still in the post-flashover Stage R3. At 1,070 s, a second HRR peak occurs likely due the combined effect of the burning of the fuel load in Zone 2 and destruction of the partition wall between Zones 1 and 2. Figure 95 shows a sudden increase of air inflow through the measurement location in the window in Zone 1). Due to the complexity of fire behaviour in this scenario, it is difficult to determine where the dominant combustion zone was located without recourse to temperature and other data. There is a continuous decay in HRR after the second peak until the end of the test when the values and rate of decay approaches the single-room profile.

The predicted value of the ventilation controlled HRRv (6,840 kW for $F_v = 4.56$) does not show good agreement with measured values in the post-flashover phase as was the case for tests with a single window in configurations B1 and B2. Although there is a relatively steady period between 480 s and 980 s, the measured average value of around 5,500 kW is much lower than the theoretical value of 6,840 kW.

Figures 97 and 98 show the temperature profiles at 2.4 m height from the four TC trees in Zone 1 and three TC trees in Zone 2, respectively. In Zone 1, temperature trends and levels are similar to previous results for tests in configuration B1, e.g. PRF-04. However, in Zone 1, the effect of the door and zonal burning behaviour caused by air flow to the dominant combustion region (Zone 1), the large difference in FLEDs (and composition of combustibles) in the two zones, as well as the destruction of the door and partition wall factor into the shape of the temperature profiles in Zone 2. Zone 1 experiences higher initial temperatures with a peak of about 1,200°C at 800s (on CH45), whereas a peak temperature of about 1,160°C is reached in Zone 2 at about 1,780 s. The results are reflected in the heat flux profiles recorded at the east and west wall locations at a 1.9 m height (Figure 99): temperatures in Zone 2 were below 1,000°C for most of the duration of the post-flashover phase, as shown in Figure 100. Therefore, the temperature conditions were more severe in Zone 1.

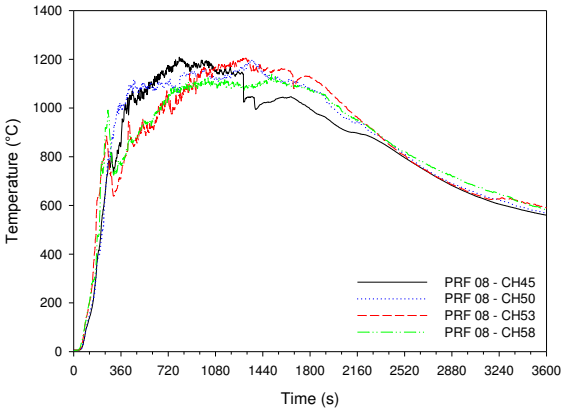

Figure 97. Temperatures at 2.4 m from four TC trees in Zone 1 (SW-CH50; SE-CH58; NW-CH45; NE-CH53).

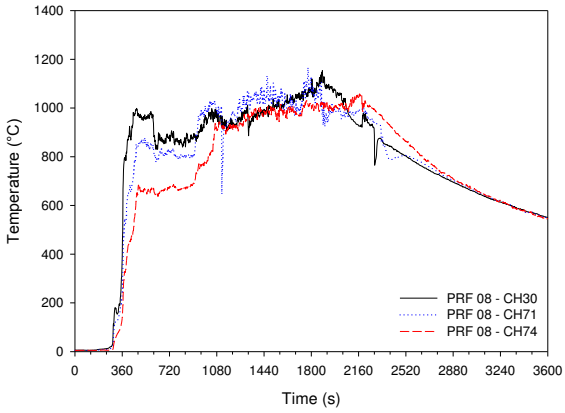

Figure 98. Temperatures at 2.4 m from three TC trees in Zone 2 (South-CH30; Centre-CH71; North-CH74).

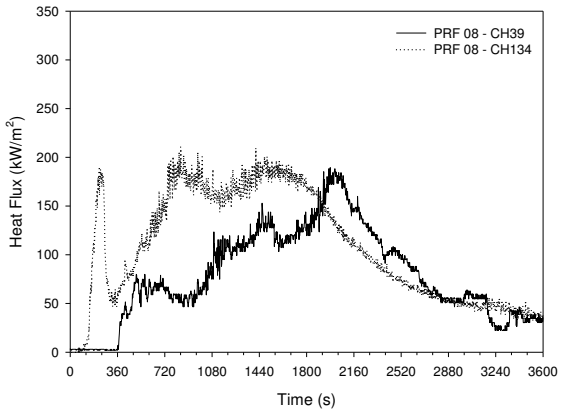

Figure 99. Heat flux at east wall (CH134, Zone 1) and west wall (CH39, Zone 2) in Test PRF-08).

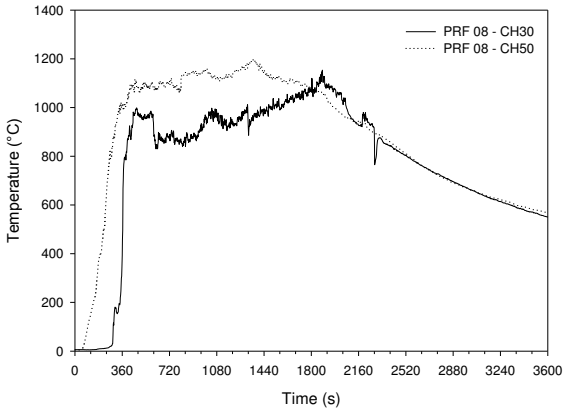

Figure 100. Temperature profile at 2.4 m in Zone 1 (CH30) and Zone 2 (CH50) in Test PRF-08.

The results of this research suggest that the distribution of fuel load (particularly the thermoplastic materials) has an effect on the zonal burning behaviour and determines which area will experience the most severe temperature conditions. In this case, the fact that Zone 1 had a considerably larger FLED than Zone 2 (919 MJ/m^2 vs. 388 MJ/m^2) is an important factor. For large rooms (area greater than 16 m^2) the temperature distribution is increasingly non-uniform.

Table 33 lists the estimated duration of various fire stages for Test PRF-08 and compares the results to Test PRF-04. The results show that the steady Stage R4 is of considerably longer duration in Zone 1 compared to Zone 2 (23.9 min vs. 4.8 min, respectively). The duration of Stage R4 in Zone 1 is also longer in PRF-08 than it is in PRF-04 (23.9 min vs. 15.7 min). A comparison of PRF-08 and PRF-04 temperature profiles from the SW tree at 2.4 m (Figure 101) confirms that higher temperatures (around 1,100°C) lasted for a longer period in PRF-08. As well, PRF-08

(Zone 1) clearly had higher mean maximum temperatures in the SW zone (1,118°C in PRF-08 vs. 1,080°C in PRF-04), as shown in Table 34. However, comparison of heat flux measurements at the ceiling and east wall locations (Figure 102) suggests that the radiation intensity in both tests was comparable. This is further supported by fire performance results for test wall sections TWS-01 and -02 (Table 35). Given that PRF-08 and -04 had the same bedroom fuel load, the results suggest that there was additional injection (or suction) of fuel into Zone 1 in PRF-08, which could have only come from Zone 2. In addition, it is possible that the actual HRR in Zone 1 was higher than it was in PRF-04 due to increased ventilation in PRF-08. It is difficult to make a conclusive statement since there was no means of breaking up the global HRR (measured using the calorimeter) into the three different components: 1) external HRR; 2) Zone 1 HRR, and; 3) Zone 2 HRR. It is postulated (with the support of temperature data) that Zone 1 HRR is much greater than Zone 2 HRR and hence the higher temperatures and prolonged duration of Stage R4 in Zone 2.

Table 33. Duration of stages of fire development for Tests PRF-08 and -04.

Zone	Peak HRR (kW)	t_{HRRv} (min)	Δt_{R2} (min)	Δt_{R3} (min)	Δt_{R4} (min)	Δt_{R5} (min)
PRF-08 Zone 1	-	-	3.7	2.3	23.9	31.1
PRF-08 Zone 2	-	-	7.3	19.7	4.8	29.2
PRF-04	6,014 (4.0) †	3.1	2.4	4.3	15.7	38.6

† time to peak HRR; t_{HRRv} – time to reach HRRv; Δt_{RX} – duration of fire development Stage RX, Where X= 2 to 5;

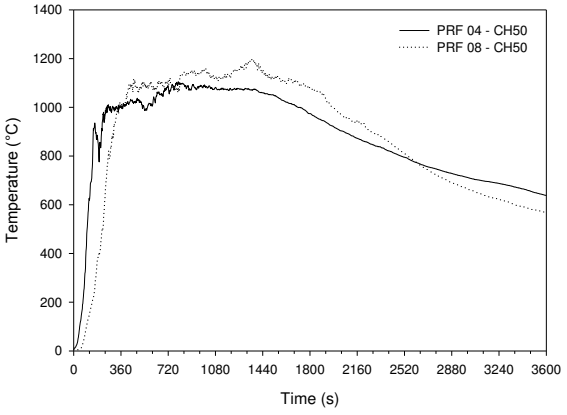

Figure 101. PRF-08 and PRF-04 temperature profiles measured at the SW tree at 2.4 m.

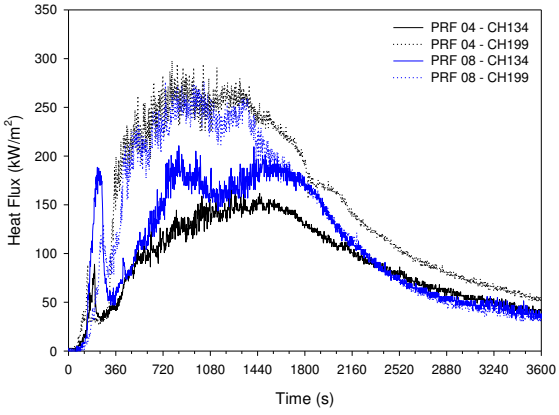

Figure 102. Heat flux at ceiling center (CH199) and east wall (CH134) in Tests PRF-04 and -08.

Table 34. Temperatures at 2.4 m height in section of the room during Stage R4 in Tests PRF-08 and -04.

Test ID	Peak HRR (kW)		Temperature values in zone NW (°C)	NE (°C)	SW (°C)	SE (°C)	Duration of Stage R4 (min)
PRF-08 Zone 1	9,230	Min-Max	942 – 1,209	769 – 1,209	1,003–1,197	787-1,138	23.9
		Mean	1,094	1,083	1,118	1,053	
		SD †	69	109	35	80	
PRF-08 Zone 2	9,230		**South**	**Center**	North	-	4.8
		Min-Max	1,018-1,154	924-1,167	957-1,032		
		Mean	1,069	1,023	999		
		SD	29	51	17		
PRF-04	6,014	Min-Max	921-1,264	621-1,188	770-1,125	776-1,158	15.7
		Mean	1,129	959	1,080	947	
		SD	53	57	57	72	

† SD – Standard deviation

Table 35. Fire performance results for TWSs in Tests PRF-04 and 08.

Test ID	Duration (min)	Peak HRR (kW)	TWS Time to Temperature Rise of 180°C TWS-01 (RGWB) (min)	TWS-02 (XGWB) (min)	TWS-03 (RGWB) (min)	TW-04 (XGWB) (min)
PRF-04	61	6,014	24	53	19	28
PRF-08	61	9,150	28	49	None	None

RGWB: Regular gypsum board (12.7 mm thick); XGWB: Type X gypsum board (15.8 mm thick)
None: Test section was not installed.

4.3.5.1 Summary

The fire behaviour exhibited in Test PRF-08 had complex fire dynamics with strong zonal burning characteristics. For the purpose of fire characterization, the bedroom area stands out as the area with the most severe temperature conditions. Other important conclusions and observations are:

1. High post-flashover temperatures (mean values of about 1,100°C) were concentrated in the bedroom area, likely due to the higher FLED.
2. The measured maximum instantaneous temperatures were around 1,200°C and occurred in a region near the window in Zone 1.
3. The impact of the fire on the test wall sections was comparable to that in Test PRF-04. The results suggest that the intensity of the fires in these two tests was equivalent, although Test PRF-08 had a considerably higher peak HRR. Therefore, although the overall fuel load

in PRF-08 was greater than that in PRF-04, the fire was most severe in the bedroom (Zone 1), which had the highest FLED.

4.3.6 Main Floor (Configuration B6)

Tests PRF-10 and -14 were conducted to study fire behaviour in one large compartment of approximately 42 m^2, which simulated a main floor in a multi-family dwelling. The two tests were designed to have the same fuel load (quantity, layout and composition) and differed only in the location of the first-ignited-item; a loveseat in the living area was the first-ignited item in PRF-10 whereas the fire started with a simulated stove-top ignition source in PRF-14, as shown in Figure 103. Figure 104 shows the layout of the instrumentation (mostly TC trees) and Figure 105 shows the division of the fire room in four combustion zones, for convenience of discussing the results since it is known beforehand (based on knowledge developed thus far) that the fires exhibited zonal burning behaviour. As indicated, division of the area into four zones is simply for convenience and was not arrived at using any analysis of the temperature field. In reality, there is likely to be more than four zones with irregularly shaped areas, but the TC temperature grid was not fine enough to enable a detailed study of the temperature field.

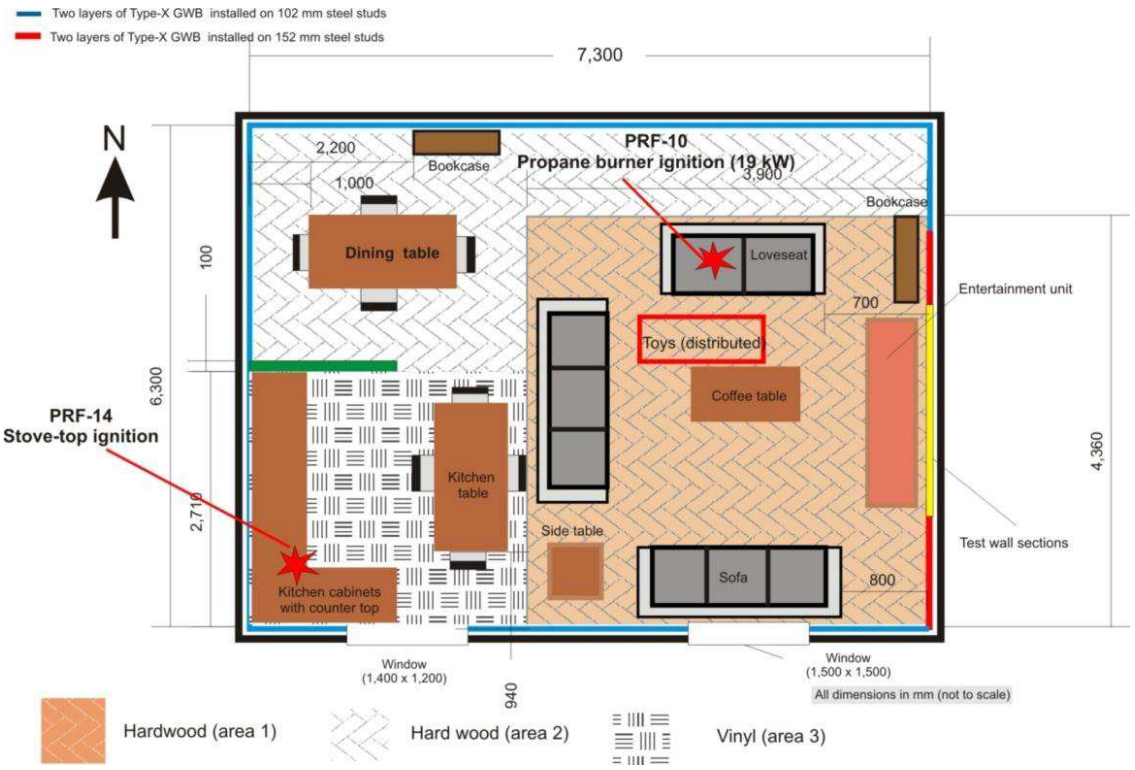

Figure 103. Fuel load layout and ignition locations in Tests PRF-10 and -14.

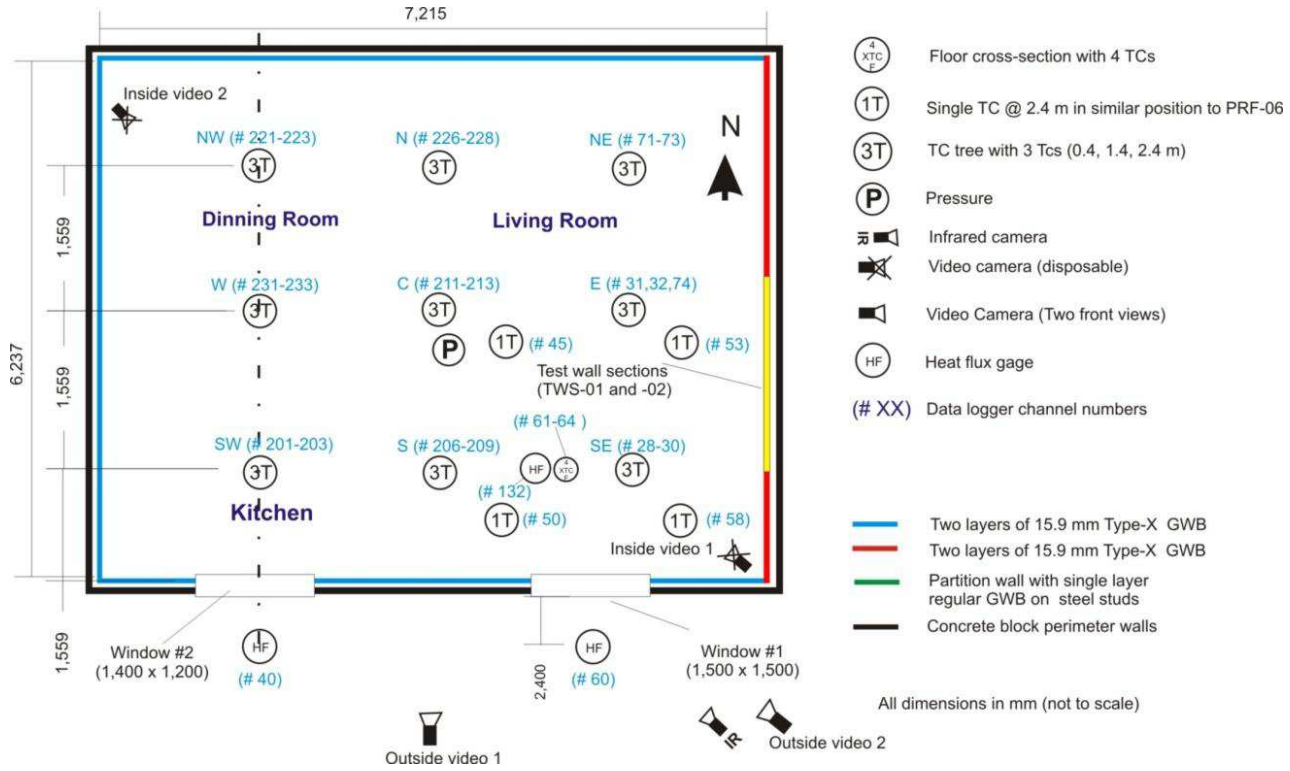

Figure 104. Layout of instrumentation in Tests PRF-10 and -14.

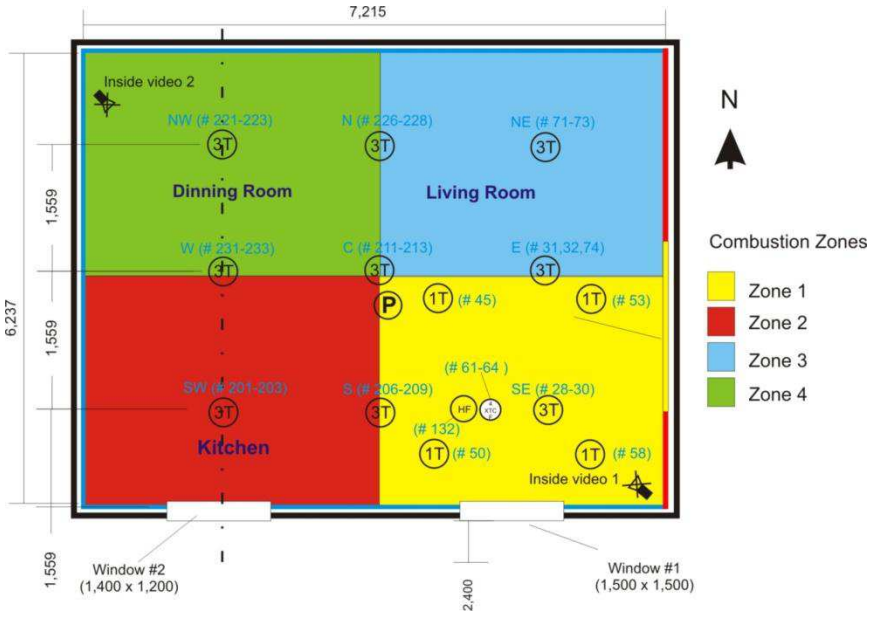

Figure 105. Division of the fire room in Tests PRF-10 and -14 into combustion zones.

Figure 106 shows the HRR vs. time graphs for Tests PRF-10 and -14. The fire developed rapidly in Test PRF-10 since the first-ignited-item was a loveseat. In Test PRF-14, fire development was slow because the first-ignited-item was a wooden kitchen cabinet and wood furniture does not ignite as

readily as upholstered furniture. Both tests reached similar peak HRR values and were terminated early (at different times) since the fire burnt through the ceiling.

As mentioned earlier, Tests PRF-10 and -14 exhibited multiple flashovers as defined in Section 4.2.2.1 “Observations of Key Features of Fire Behaviour”. In Test PRF-10, the first instance of flashover was localized in the living room area (Zones 1 and 3) at about 3 min, as shown in Figure 5. Flashover in the kitchen area (Zone 2) was observed to occur at about 13 min, as shown in Figure 6. Until flashover occurred in Zone 2, there was a virtual partition between the east (Zones 1 and 3) and west (Zones 2 and 4) side of the compartment. Figure 107 shows the temperatures at 2.4 m in the southern section of the fire compartment (Zones 1 and 2) and it can be seen that peak temperatures in Zone 1 were around 1,100°C within 300 s and stayed around that level for about 2,100 s, whereas the hot layer temperatures in Zone 2 were increasing slowly and did not reach 1,000°C until 1,300 s. Temperature data in both tests show signs of corruption at various times during the fully-developed phase. Therefore, the temperature spikes and zero readings recorded after 1,800 s in Figure 107 are considered to be spurious outputs that were likely caused by false hot-junctions created by electrical shorting of TC wires at locations where the protective sheath had melted.

According to the temperature data, the temperature at 1.4 m on the SW TC tree in Zone 2 was around 800°C when flashover was observed. Since the temperature at that location had exceeded 600°C, it is likely that flashover conditions were met, but there was a lack of oxygen to support combustion since most of the air coming through the windows was being drawn to active combustion Zones 1 and 2.

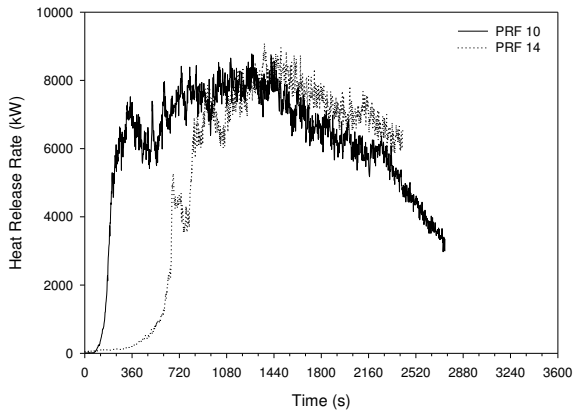

Figure 106. HRR vs. time for Tests PRF-10 and -14.

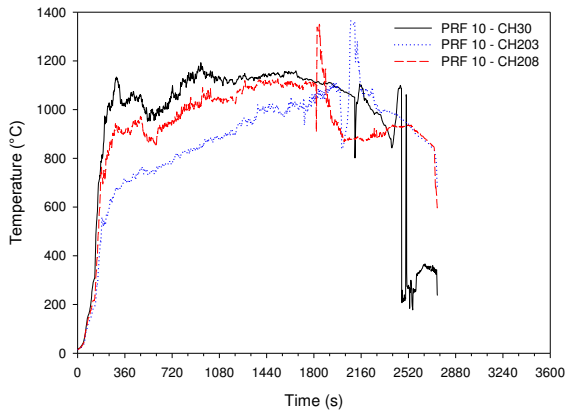

Figure 107. Temperatures in the southern regions in Test PRF-10 (SW-CH203; S-CH208; SE-CH30).

Figure 108 shows the temperature measured by the TC located at 2.4 m height at the center of each zone in Test PRF-10. The results show that there was a wider temperature variation throughout the space compared to Test PRF-06 (Figure 109).

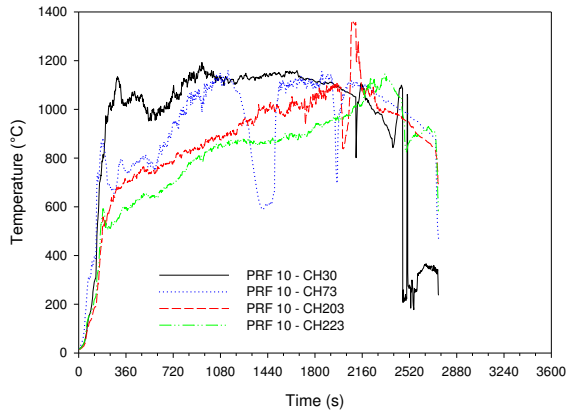

Figure 108. Temperatures at 2.4 m at the center of each zone in Test PRF-10 (Zone 1 – CH30; Zone 2 – 203; Zone 3 – CH73; Zone 4 – CH223).

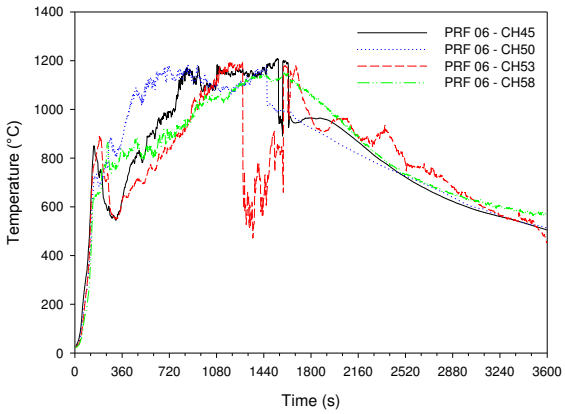

Figure 109. Temperatures at 2.4 m at the center of each zone in Test PRF-06 (NE – CH53; NW – 45; SE – CH58; SW – CH50).

Figure 110 shows the temperature profiles in the south zones in Test PRF-14. While the results are consistent with the HRR profile (i.e., delayed fire development), a new phenomenon is revealed: shortly after the second flashover occurred in Zones 1 and 3, a cross-over point occurs at about 817 s (13.6 m), at which time the temperature in Zone 1 (CH30) rises above the temperature in Zone 2 (CH203). It is interesting that the temperature in Zone 2 simultaneously drops to a lower value of about 750°C while that in Zone 1 rises to 1,000°C. As discussed in Section 4.2.2.3, “Visual Assessment of Fire Development”, it was observed that although the fire originated in Zone 2, the dominant combustion region became Zones 1 and 3 after these areas experienced flashover. This

is likely due the differences in pyrolysis rates between the thermoplastic and wood-based fuels: Zones 1 and 3 with largely thermoplastic combustibles (upholstered sofas) ultimately commanded consumption of available oxygen over Zones 2 and 4, which had largely wood combustibles. Further experimental investigation of the circumstances leading to this phenomenon, e.g. influence of ventilation settings and other variables, was beyond the scope of the research.

Figure 111 shows the temperatures measured by the TC located at a 2.4 m height at the center of each zone in Test PRF-14. As was the case with Test PRF-10, temperatures are lower in the northern Zones (3 and 4). The longest and earliest duration of high temperature was recorded in Zone 1. However, the temperature data in Zone 1 (CH30) was corrupted (Figure 112) after about 1,300 s due to failure of thermocouples (likely caused by short-circuiting problems, as discussed earlier). This is confirmed by conducting an inverse temperature calculation using the heat flux measured at 1.9 m height at the east wall and plotting it together with the data from the TC on CH30. The result is shown in Figure 113: the measured (CH30) and inverse temperatures are in excellent agreement until the TC failed. Therefore, it is concluded that temperatures in Zone 1 remained around 1,100°C until the test was terminated.

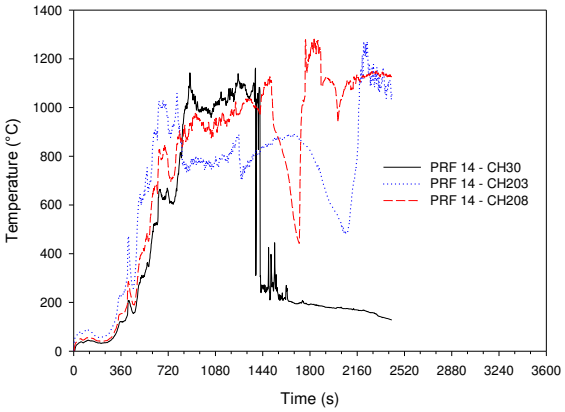

Figure 110. Temperatures in the southern regions in Test PRF-14 (SW-CH203; S-CH208; SE-CH30).

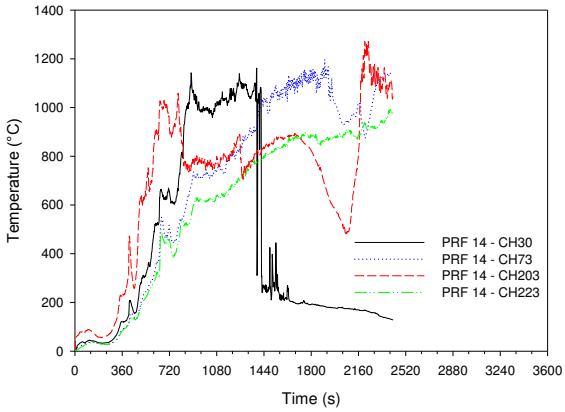

Figure 111. Temperatures at 2.4 m at the center of each zone in Test PRF-14 (Zone 1 – CH30; Zone 2 – 203; Zone 3 – CH73; Zone 4 – CH223).

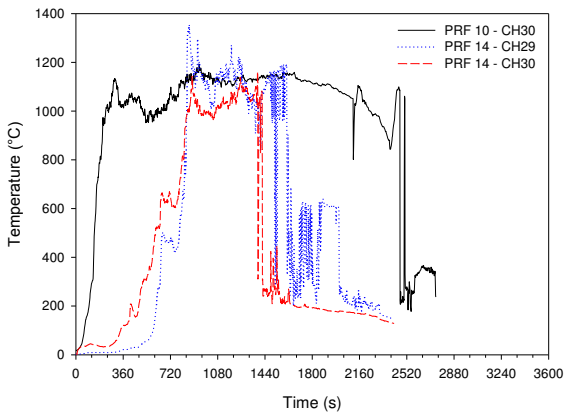

Figure 112. Temperatures in the SE section in Tests PRF-10 and 14 (CH29 – 1.4 m height; CH30 – 2.4 m height).

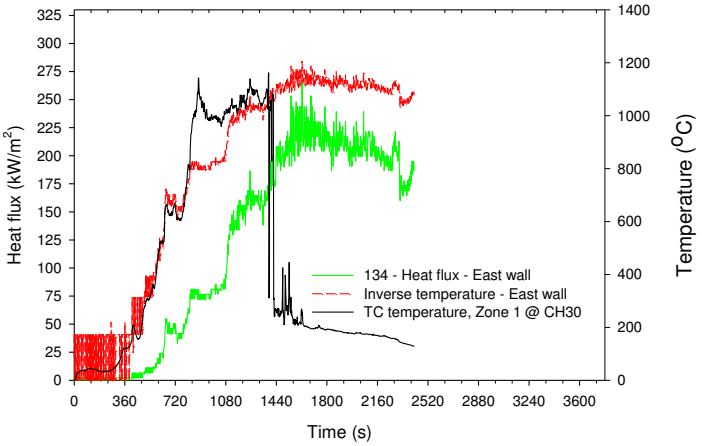

Figure 113. Graph of heat flux at east wall (1.9 m) and inverse temperature in Test PRF-14.

Table 36 shows the results of the fire performance of TWS-01 and -02 in Tests PRF-10 and -14. The results are compared with those from Test PRF-06 since the fuel load characteristics in the living room areas were similar. The fire performance of TWS-01 in Test PRF-14 was longer than that in PRF-10 by 9 min, which is proportional to the fire growth delay in PRF-14. The results show that the fire performance of TWS-01 in Test PRF-10 was comparable to that in Test PRF-06. This suggests that the increased room size, ventilation and fuel in Test PRF-10 did not result in more severe fire conditions during the first 30 minutes of the test vs. the smaller room in Test PRF-06. However, the duration of Stage R4 was considerably longer in PRF-10 than in PRF-06 (20.9 min vs. 12.8 min), as shown in Table 36, which suggests that temperatures above 1,000°C lasted for a longer period than in PRF-06. In Tests PRF-10 and -14, TWS-02 did not reach insulation failure during the duration of the tests. Both tests were terminated early (as shown in Table 38) due to failure of the ceiling assembly. Whether ceiling failure in PRF-10 and -14 suggests more severe ceiling exposure than in PRF-06, it is difficult to draw comparisons since there were differences in the construction of the ceiling. Tests PRF-10 and -14 had additional joints on the ceiling, which were not present in PRF-06. However, the results (Figures 114 and 115) show that PRF-10 had a longer fully-developed phase than PRF-06 and this could have contributed to the pre-mature failure of the ceiling assembly.

Table 38 lists the temperatures measured at 2.4 m in the living room area in all three tests. Peak temperatures in the SW location were comparable. There is a greater variation in maximum temperatures recorded in the four sections in Tests PRF-10 and -14 than there is in Test PRF-06.

Table 36. Fire performance results for TWSs in Tests PRF-10, -14 and -06.

Test ID	Duration (min)	Peak HRR (kW)	TWS Time to Temperature Rise of 180°C			
			TWS-01 (RGWB) (min)	TWS-02 (XGWB) (min)	TWS-03 (RGWB) (min)	TW-04 (XGWB) (min)
PRF-10	45	8,776	30	NULL	None	None
PRF-14	40	9,090	39	NULL	None	None
PRF-06	61	5,133	28	49	None	None

RGWB: Regular gypsum board (12.7 mm thick); XGWB: Type X gypsum board (15.8 mm thick)
None: Test section was not installed; NULL: ATSTM E119/ULC-S101 failure criteria were not reached.

Table 37. Duration of stages of fire development for Tests PRF-10, -14 and -06.

Zone	Peak HRR (kW)	t_{HRRv} (min)	Δt_{R2} (min)	Δt_{R3} (min)	Δt_{R4} (min)	Δt_{R5} (min)
PRF-10 Zone 1	8,776	4.8	2.6	9.6	20.9	-
PRF-10 Zone 2	8,776	4.8	5.6	26.7	7.6	-
PRF-14 Zone 1	9,090	14.3	13.5	1.5	-	-
PRF-14 Zone 2	9,090	14.3	10.0	26.3	4.1	-
PRF-06	5,133 (4.3) †	3.2	2.3	5.1	12.8	39.8

† time to peak HRR; t_{HRRv} – time to reach HRRv; Δt_{RX} – duration of fire development Stage RX, where X = 2 to 5.

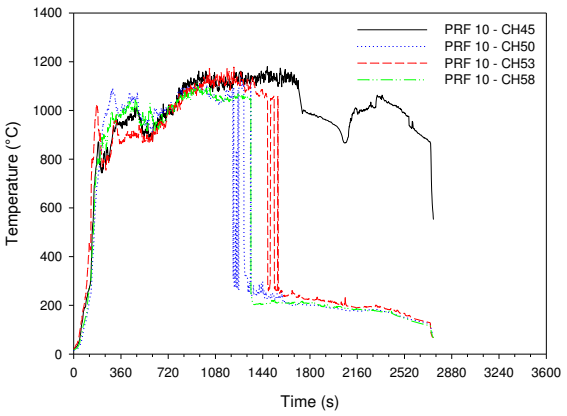

Figure 114. Temperatures at 2.4 m height in Test PRF-10.

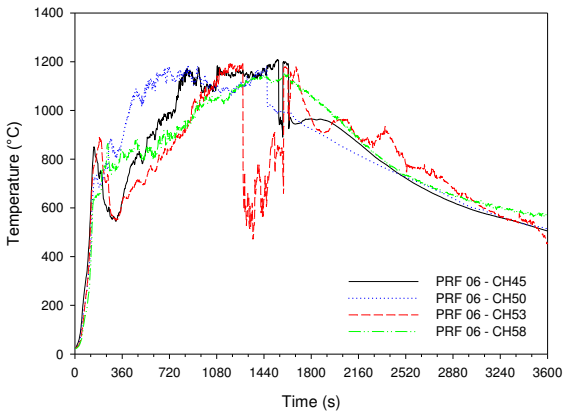

Figure 115. Temperatures at 2.4 m height in Test PRF-06.

Table 38. Temperatures at 2.4 m height in sections of the room during Stage R4 in Tests PRF-10, -14 and -06.

Test ID	Peak HRR (kW)		Temperature values in zone 1-SE (°C)	2-SW (°C)	3-NE (°C)	4-NW (°C)	Duration of Stage R4 (min)
PRF-10	9,230	Min-Max	1,080-1,243	795-1,110	593-1,162	704-970	20.9
		Mean	1,163	954	1,004	863	
		SD †	48	85	165	58	
PRF-14	9,230	Min-Max	959-1,155	706-890	709-921	596-782	7.6
		Mean	1,036	786	787	668	
		SD	40	35	68	54	
PRF-06	5,133	Min-Max	743-1,202	663-1,307	953-1,224	860-1,064	12.8
		Mean	1,037	966	1,119	971	
		SD	137	199	40	46	

†SD – Standard deviation

Table 39 lists the peak values of the heat flux measured at various locations. The graphs of the heat flux profiles for Tests PRF-10 and -14 are given in Figures C-258 and C-332, in Part 1 of the Report [1], respectively. The graphs for PRF-06 are given in Figures C-166 and C-167 in Part 1 of the report.

Table 39. Peak radiation flux at various locations in Tests PRF-10, -14 and -06.

Test ID	Floor	Peak heat flux at various surfaces (kW/m^2) West wall	East wall	Ceiling center	North wall	Outside 1 @ 2.4 m	Outside 2@ 2.4 m
PRF-10	236	X	188	270	159	47	39
PRF-14	224	X	266	X	234	41	43
PRF-06	276	239	197	266	255	37	X

Outside 1: Facing living room window; Outside 2: Facing kitchen window; X – No data

4.4 External Burning and Heat Radiation

Table 40 summarizes the results of heat flux measurements that were taken at two locations outside the test room. The heat flux gages (in tests with a single room) were installed at distances of 2.4 m and 4.8 m from Window #1, at an elevation such that the perpendicular lines drawn from the centers of the window and heat flux gages were aligned. In tests with two windows, such as PRF-08, -10 and -14, the heat flux gage that was normally installed at the 4.8 m location was moved to a location that was 2.4 m away from Window #2. The graphs of heat flux graphs vs. time were typically bell-shaped profiles that are skewed to the right, as shown in Figure 116 for Tests PRF-02, -04, -05 and -06.

Table 40. Results of heat flux measurements outside the test rooms.

Test ID	2.4 m from window				4.8 m from window		
	Window ID and Fv	Q''_{max} (kW/m^2)	t1 (min)	t2 (min)	Q''_{max} (kW/m^2	t1 (min)	t2 (min)
PRF-02	V2 (1.84) †	27 (31) ††	4.5	51	7 (31) ††	NULL	NULL
PRF-03	V1 (2.76)	44 (15)	3	NULL†††	12(24)	24	24
PRF-04	V1 (2.76)	41 (16)	3	41	9 (-)[4]	NULL	NULL
PRF-05	V2 (1.84)	33 (13)	5	42	NULL	NULL	NULL
PRF-06	V1 (1.84)	37 (13)	3	27	9 (7)	NULL	NULL
PRF-07	V5 (2.76)	32 (7)	3	34	9 (-)[4]	NULL	NULL
PRF-09	V3 (1.00)	16 (17)	14	56	<5	NULL	NULL
PRF-12	V1(1.84)	37 (18)	4	32	NULL	NULL	NULL
PRF-13	V1(1.84)	26 (11)	5	31	NULL	NULL	NULL
	2.4 m from Windows 1				**2.4 m from Window 2**		
PRF-08	V4 (4.56)	42 (19)	4	25	16 (23)	13	32
PRF-10	V4 (4.56)	47 (21)	4	44	NULL	NULL	NULL
PRF-14	V4 (4.56)	43 (26)	13	NULL	41 (29)	10	NULL

† Ventilation factor; †† Time (s) when the peak value occurred;

t1: Time when heat flux exceeded the critical value of 12 kW/m^2; t2: time when heat flux fell below 12 kW/m^2;

NULL: Data not available due to instrumentation malfunction or other omission; (-): Data were too noisy

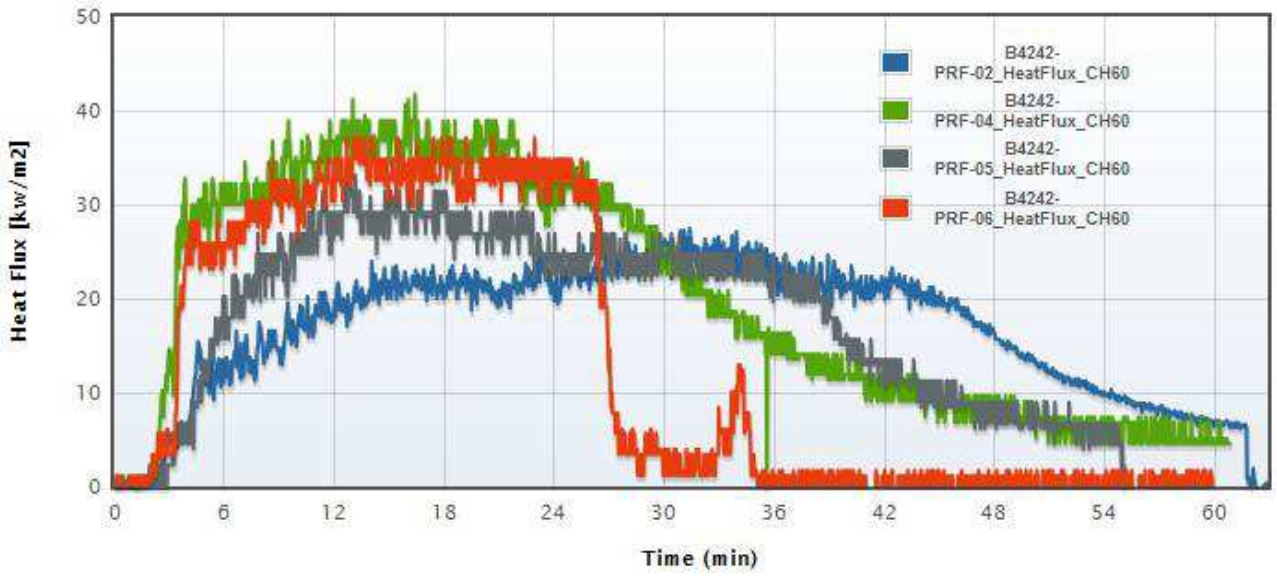

Figure 116. External heat flux measurements at 2.4 m from Window #1 for Tests PRF-02, -04, -05 and -06.

In all of the tests, the heat flux measured at 2.4 m from the window(s) exceeded 12 kW/m^2, which is the threshold for piloted ignition of wood-based materials [6]. At 4.8 m, the heat flux in all but one single-room test did not reach 12 kW/m^2. The results show that the peak heat flux at the 2.4 m location depended on the window size with the highest value of 44 kW/m^2 being recorded with Window V1 (the largest window size), while the lowest peak value of 16 kW/m^2 was recorded with Window V3 (the smallest window).

In all of the fires, there was a considerable amount of external burning and there was significant flame extension out of the windows as shown in Figures 117 and 118. The maximum lateral flame extension distance, from the window, was estimated to be approximately 1.5 m.

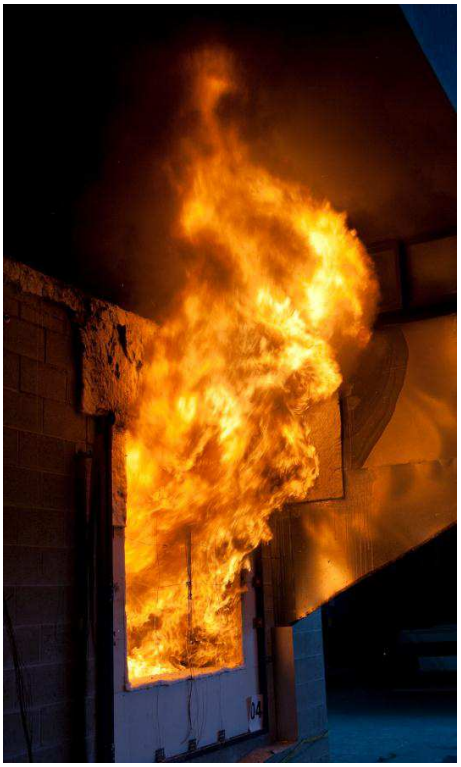

Figure 117. Extent of external burning: flames issuing out of the window during the post-flashover stage in Test PRF-04.

Figure 118. Extent of external burning: flames issuing out of the windows during the post-flashover stage in Test PRF-14.

4.5 Tenability

4.5.1 Room of Fire Origin

The concentrations of O_2, CO and CO_2 were only measured in the room of fire origin in two of the tests, PRF-01 and PRF-02. The measurements were discontinued in subsequent tests since the results from PRF-01 and -02 showed that there was limited value in the measurements because the gas analyzers reached saturation levels shortly after flashover, as shown in Figures 119 and

120 (PRF-01 and -02, respectively). Considering exposure to O_2 vitiation alone, it is reported unconsciousness can occur rapidly in people when the concentration of O_2 falls below 10% [41]. Times to flashover in PRF-01 and PRF-02 were 156 s and 152 s, respectively, based on an average hot layer temperature of 600°C. As discussed earlier, the fire rooms rapidly filled with smoke and there was no visibility in the room at the time of flashover. Therefore, under the ignition scenario used in this research, the period during which the room is tenable is very small and the flashover signals the end of any chance of survival for people.

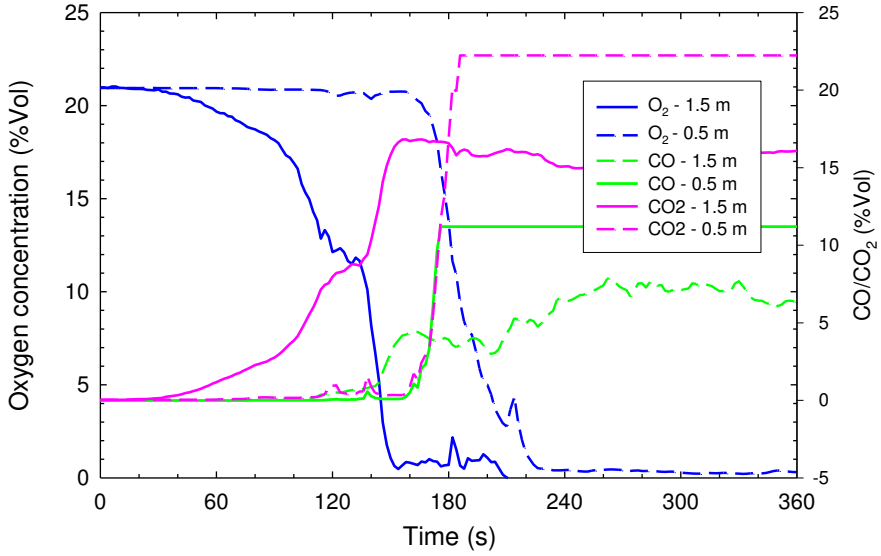

Figure 119. Test PRF-01: Results of O_2, CO and CO_2 in the North East quadrant.

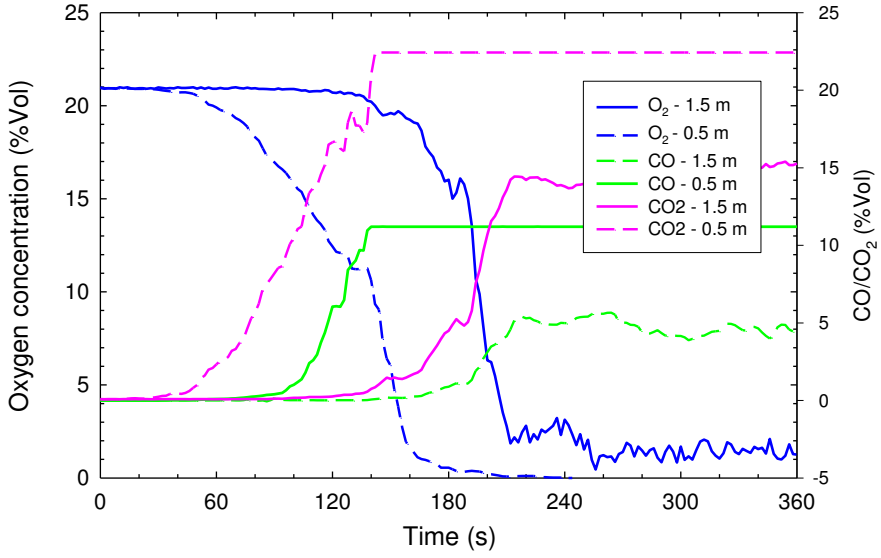

Figure 120. Test PRF-02: Results of O_2, CO and CO_2 in the North East quadrant.

4.5.2 Adjacent Spaces

The impact of the flow of fire effluent into an adjacent room was investigated in Test PRF-07. Figure 121 shows the layout of the instrumentation: The test used a fuel load configuration that was identical to Test PRF-05, but the doorway at the back of the room (North West corner) was left open so that the fire effluent could flow into the adjacent room. Windows #1 and #2 were the sources of ventilation. Measurements of the concentration of O_2, CO and CO_2, and smoke obscuration were taken at the indicated locations in the adjacent room.

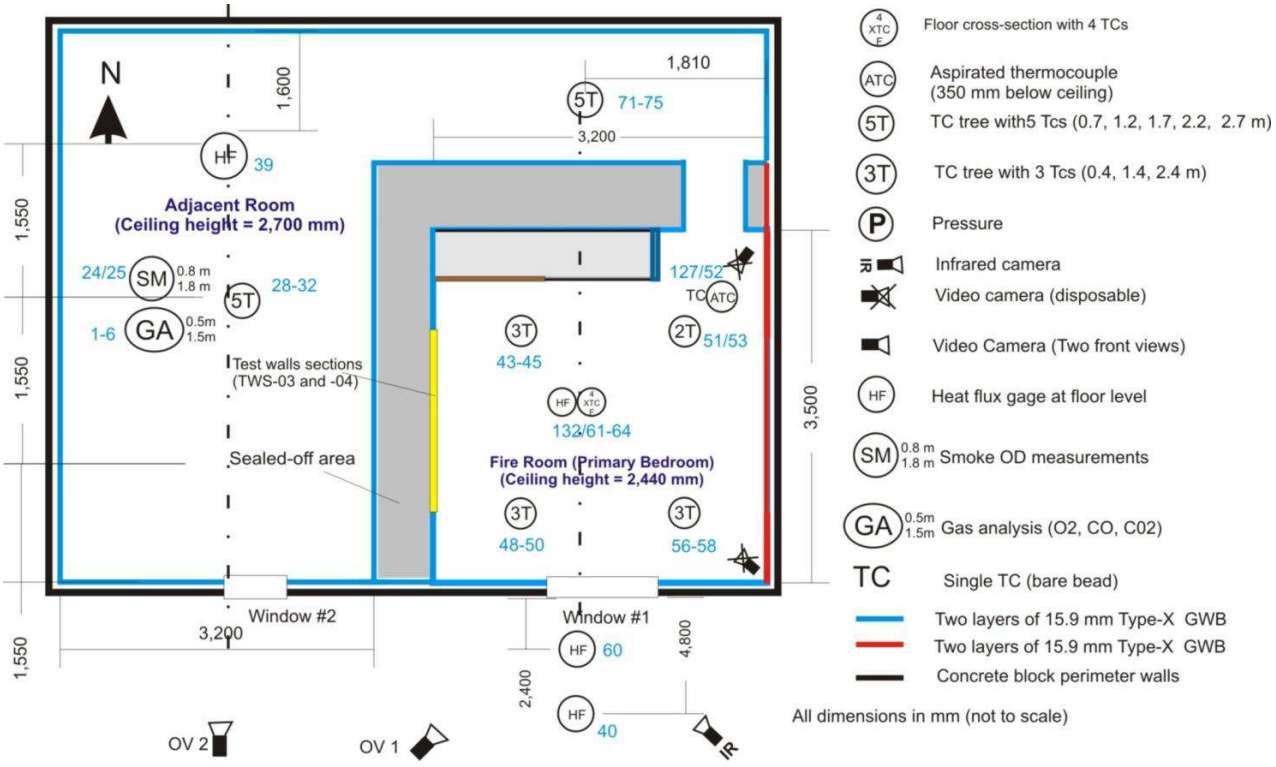

Figure 121. Test PRF-07 - Instrumentation floor plan showing location of TC trees.

Figure 122 shows the results of O_2, CO and CO_2 measurements in the adjacent room and Figure 123 shows the results of smoke obscuration measurements. A OD/m value of 2.0 m^{-1} is considered to be a value at which most people cannot see beyond 0.5 m [41] and hence would have difficulty finding their way to an exit. This OD/m threshold was exceeded at 240 s (at 0.8 m above the floor) and 200 s (at 1.8 m above the floor). Figure 124 shows the temperature profiles near the smoke meter and smoke sampling locations. Using a fractional effective dose (FED) value of 1 as the point of incapacitation [41], the results for each incapacitation parameter (calculated using the procedure outlined by Su et. al. [41]) are given in Figure 125 and show that the environment became untenable, shortly after flashover had occurred, from 200 s (based on CO and CO_2) to 330 s (based

on low O_2). Figure 125 also shows the tenability analysis based on CO and convected heat, considered individually.

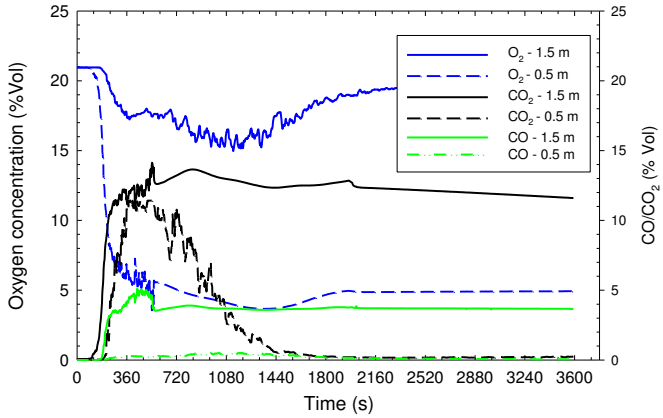

Figure 122. Test PRF-01: Test PRF-07: Results of O_2, CO and CO_2 measurements in the adjacent space.

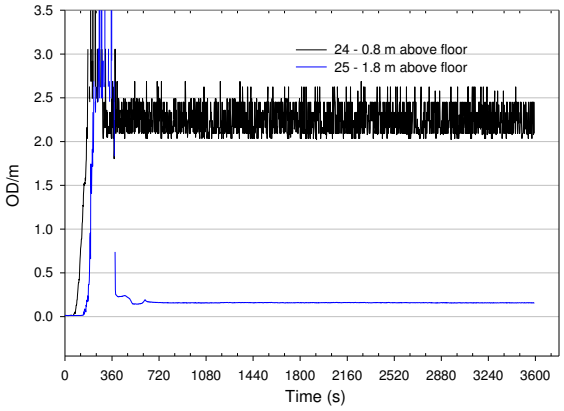

Figure 123. Test PRF-07: Results of smoke obscuration measurements in the adjacent space.

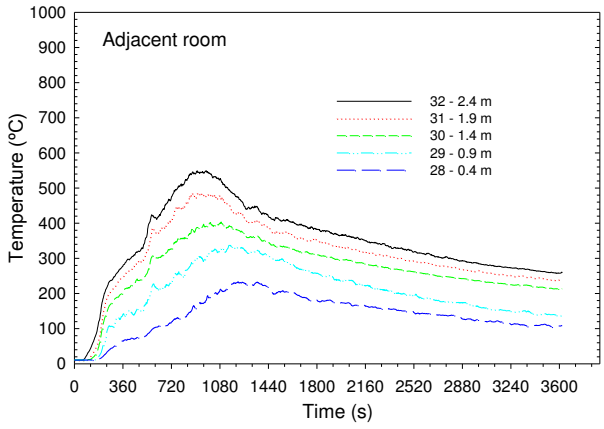

Figure 124. Test PRF-07: Temperature profiles in the adjacent space.

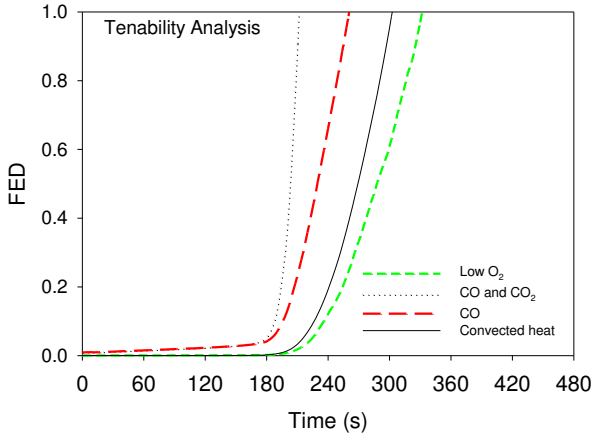

Figure 125. Test PRF-07: Results of tenability analysis in the adjacent space.

4.6 Overall Conclusions on Room Fire Behaviour

The tests provided a wealth of information on the characteristics of room fires. The results clearly show that fire development and severity varies within a residential building due to differences in fuel load characteristics, ventilation and geometric dimensions of various living spaces within a dwelling. Each of the six base configurations studied resulted in a unique fire, but there were discernible trends in fire development, room HRR and temperature characteristics that can be used to form analytical conclusions. While the conclusions from this research are valid for the test configurations studied, extrapolating from the test data to predict the outcome of fires in a range of real-world

residential dwellings requires analytical approaches that recognize and account for deviations from test parameters, such as mode of ignition, fuel load quantity and composition, ventilation and thermal boundary conditions.

For the purpose of this work, fire temperature is perhaps the most important property since it constitutes the thermal impact that ultimately causes failure of structural assemblies and fire spread to adjacent areas. Life safety of building occupants is, of course, of paramount concern during the pre-flashover period of room fires. However, for the rapidly developing flashover fires studied in this research, the test rooms became untenable within a few minutes of ignition.

4.6.1 Fire Growth

Figure 126 compares the HRR vs. time graphs for all of the representative tests with t-squared fire growth curves. This research has chosen to compare the fire growth rate of the tested fires with t-squared fires due to the fact that they have a long history of use within the field of fire safety engineering and are convenient for performing quick calculations where it is justified to do so. All of the tests, in which the first-ignited-item was a PCF, had fire growth rates that were consistent with the ultra-fast or fast t-square fire growth.

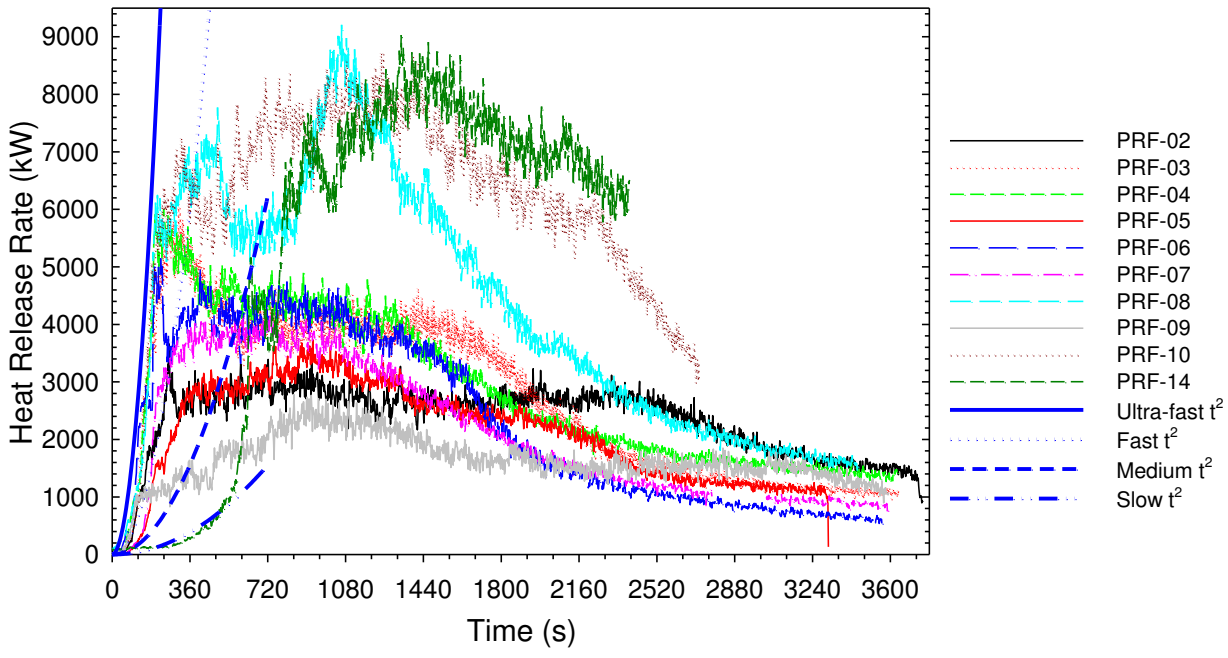

Figure 126. Comparison of fire growth rates between PRF tests and t^2 fires.

The fire growth rate in Test PRF-14, where a SCF (kitchen cabinet) was the first-ignited-item, initially aligns with a slow t-squared fire growth for the first 540 s, but transitions to an ultra-fast

t-squared fire growth near the time of flashover in Zone 2 (kitchen area). Therefore, it is concluded that:

1. An ultra-fast t-squared fire growth is a credible conservative representation of the HRR vs. time profile up to the ventilation limit for the residential bedroom and living room configurations (in all tests except for PRF-14) studied in this research, in which a non-fire retarded PCF was the first-ignited-item using a flaming ignition source.
2. A slow t-square fire represented the initial pre-flashover HRR vs. time profile in Test PRF-14 where the first-ignited-item was a SCF. However, the fire growth transitioned to an ultra-fast t-squared fire growth as the fire approached flashover in the area of origin.

4.6.2 Time to Flashover

In 12 of the tests (excluding Test PRF-11, which had an active sprinkler installed), where the first-ignited-item was a PCF (either a bed assembly or a sofa), the fires developed rapidly and flashover (full room involvement) was observed to occur within 168 s on average (with a standard deviation of 30 s). The results are summarized in Figure 127.

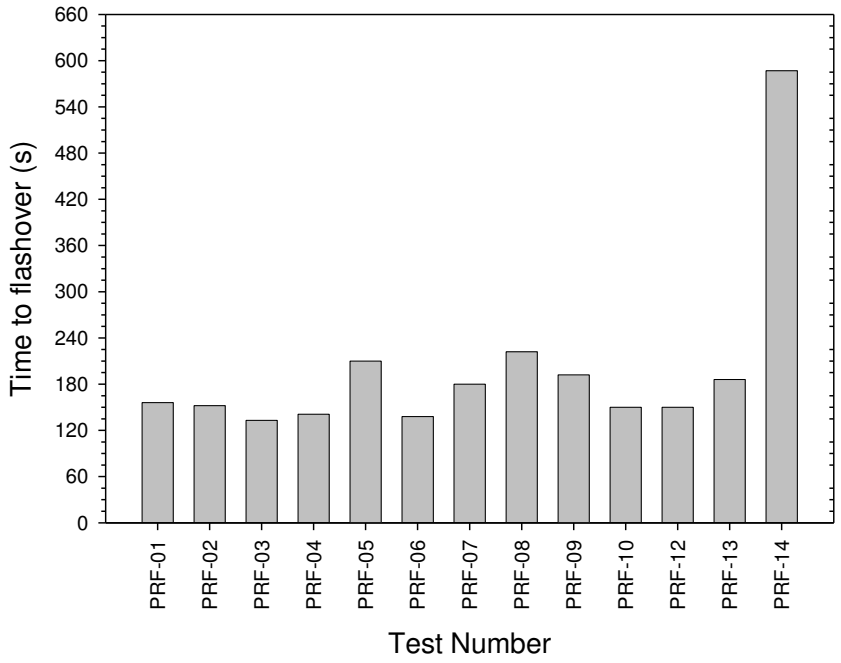

Figure 127. Time to flashover for all of the tests.

In one test, PRF-14, where the first-ignited-item was a kitchen cabinet that was ignited by a simulated stove-top ignition source (an oval roaster containing two litres of cooking oil), the first instance of flashover occurred at 587 s after ignition.

4.6.3 Multiple Flashovers:

One important finding was that large spaces (main floor configuration in Tests PRF-10 and -14) experienced multiple flashovers, i.e. flashover did not occur instantaneously across the entire space. A partial flashover first occurred in the zone where the first-ignited-item was located with other zones following suit after a few minutes delay. It is believed that a complex combination of factors relating to fluid flow dynamics and uneven oxygen distribution created by the buoyant fire plume in the zone of fire origin was responsible for the observed behaviour; specifically that other zones lacked sufficient oxygen to ignite the pyrolysis products even though temperatures and heat flux levels were conductive for flashover. Further analysis and investigation of this phenomenon would have required additional gas analysis instrumentation, which was beyond the scope of this research.

4.6.4 Post-Flashover to Fully-Developed Phases

While HRR is the primary cause of temperature rise, the results show that there are considerable differences in HRR profiles (as shown in Figure 126), and peak values vary widely for post-flashover fires since the HRR is a strong function of ventilation, among other variables such as fuel load composition. For instance, peak HRR values (for post-flashover fires) obtained in this test series (excluding Test PRF-11) varied from 2,793 kW to 9,230 kW (mean of 5,847 kW and standard deviation of 2,122 kW), whereas the instantaneous peak temperatures only varied from about 1,090°C to 1,272°C (mean of 1,090°C and standard deviation of 48°C). Figure 128 shows the graph of the average room temperature measured at 2.4 m height vs. time for the entire test series. The results show that, regardless of test variables (such as, ventilation, fuel load, ignition method and room size), the mean maximum temperatures fall within a narrow range of between 1,050°C to 1,200°C. However, test variables, particularly ventilation, first-ignited-item and composition of the fuel load have a significant effect on the time of attainment of the peak temperatures, as can be seen in Figure 129. While the instantaneous maximum temperature value alone has little significance because it does not convey information about its time of attainment and duration, both of which are important aspects of quantifying fire severity, the results confirm the existence of a practical thermodynamic mean maximum temperature, for tests conducted of in this study, of approximately 1200°C regardless of test variables and can be seen from Figure 128. The mean maximum temperature (during the post-flashover phase) in rooms of considerably different configurations and construction materials to those considered in this work may differ from the values found in this work.

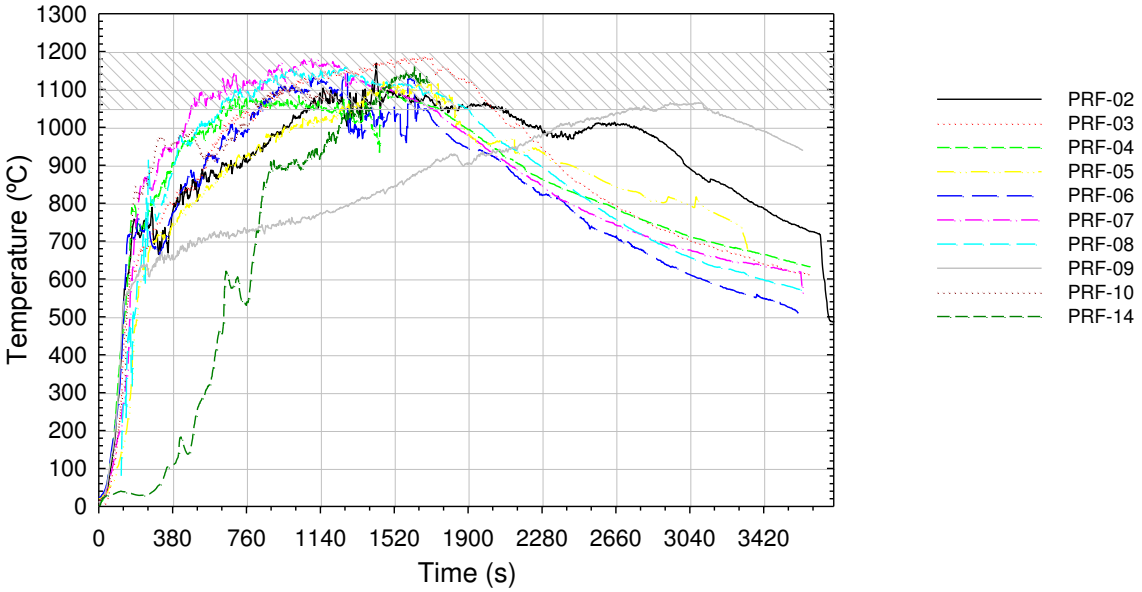

Figure 128. Mean temperature (at a height of 2.4 m) vs. time for representative tests.

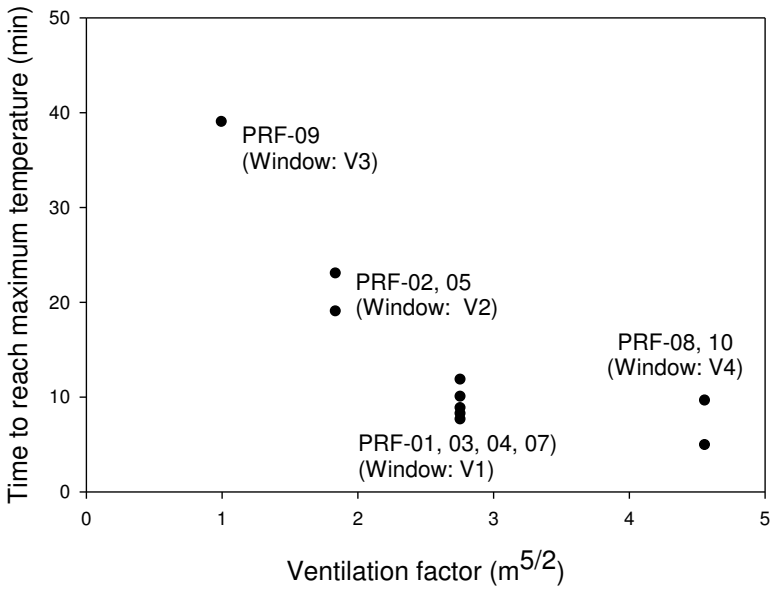

Figure 129. Effect of ventilation on the time to reach the maximum fire temperature.

One of the most significant finding was that the post-flashover period of the fires consisted of two distinct phases, the unsteady phase (Stage R3) and the steady phase (Stage R4), as shown in Figure 4, each having unique temperature and HRR characteristics.

- Unsteady phase:
  - Occurred immediately after flashover.
  - Characterized by room temperatures between 600 - 1,000°C, under-ventilated (oxygen-deficient) room combustion, significant external heat release with the peak

HRR exceeding the ventilation-controlled value by a large margin depending on the fuel load and ventilation characteristics.

- For a given fuel load density, its duration generally increased with decreasing the window size.
- For a given FLED, a long duration (due to low ventilation), results in a less severe impact of the fire on room boundaries since initial post-flashover temperatures will be lower.

- Steady phase:
  - Period of the fire during which the optimum combustion efficiency is reached and there are lower excess pyrolysis gases and less oxygen deficiency.
  - Maximum fire temperatures occur in this period.

4.6.5 External Combustion

It was observed that there was considerable external combustion in many of the tests. The analysis of the results presented earlier, showed that there was considerable external combustion shortly after flashover had occurred. The amount of external combustion was estimated to be up to about 15% and varied depending on the test setup, as shown in Figure 130. The estimated value was based on the assumption that the maximum heat release supported by the ventilation opening occurred inside the room. However, it is possible that the room heat release fell short of the ventilation-limited value due to poor combustion efficiency in Stage R3. This implies that the external heat release was possibly greater than 15%.

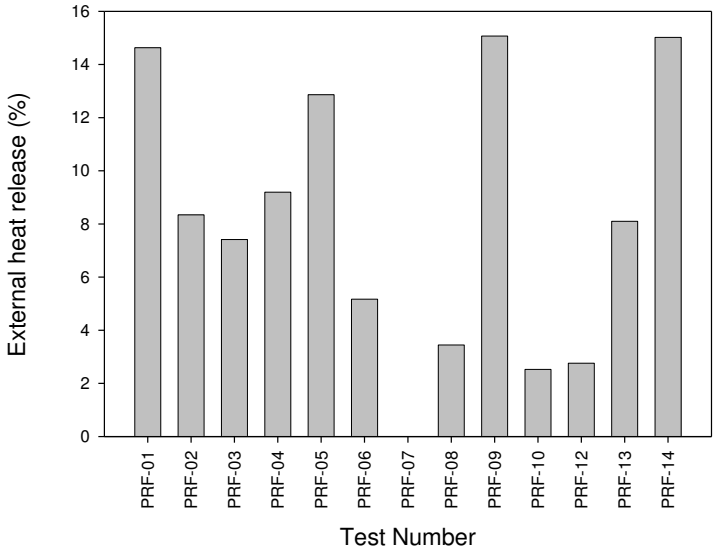

Figure 130. Percentage of external heat release.

It was noticed that external combustion was a characteristic feature of fires involving real furnishings and is mostly attributed to excess pyrolysis products that are liberated by fuel loads containing thermo plastic materials. This resulted in the peak HRR occurring in Stage R3 for tests with a single window. However, for tests with two windows (e.g. PRF-08, -10 and -14) more complex fire behaviour was obtained with the HRR profiles showing two distinct peaks due to zonal combustion behaviour in large spaces.

4.6.6 Decay Phase

Figure 126 shows the decay characteristics of the tests. The HRR at the end of the 1 hour test duration ranged from about 600 kW to 1,500 kW depending on the test configuration. It was observed that, at some point during the fully-developed phase, most of the furnishings in the tests collapsed into heaps. It is believed that the reduction of the surface area due to collapse of furnishings and fall-out of GWB from the ceiling likely initiated the decay phase. All of the wood furnishings used in the tests, such as drawer chests, were made of engineered wood products, such as fibre board and particle board, and were observed to collapse into heaps during the tests with individual furnishings that were conducted in Phase 1 of the project [2]. Photographs taken towards the end of the tests, given in Appendix E of Part 1 of the report [1], show the extent of GWB fall out and collapse of the furnishings.

Although temperatures were declining during the decay phase, the importance of this phase is highlighted by the fact that the temperature on the unexposed side of the test wall sections (TWS -02 and -03) reached 200°C during this period.

4.6.7 Zonal Burning Behaviour

The fire environment became increasingly non-uniform with increasing room dimensions. The results show that the well-stirred-reactor model is not a valid approximation of the temperature environment in the tests conducted in this research. Temperatures in the room were higher in zones that were near the windows.

5 Realistic Design Fires

This section addresses the first objective of the project, which was to produce a set of realistic design fires for multi-suite dwellings from the experimental data. In this research, the term “base configuration” is used to describe the different rooms and spaces that were tested. The tests conducted were grouped into six base configurations. The details of each test and qualitative description of fire development that is presented in Sections 3 and 4 essentially characterize the test fire scenarios. That is, adequate information is provided about the ignition scenarios, fuel load density and arrangements, room configurations (including window openings) and the fire

development. The basic scenario used in all but one of the tests was that of a fast developing fire initiated by either an item of upholstered seating furniture or a bed assembly. The one test with a different ignition scenario utilized an oil pan placed on a hot plate to simulate a stove top fire.

In Section 4, a detailed analysis of the room temperatures that were measured in each test was presented. It was noted that there were greater temperature variations in Stage R3 than in Stage R4. Therefore it was suggested that the mean temperature was more appropriate for use in Stage R4 where temperatures in the upper half of the room were more uniform (smaller standard deviation).

Representative design fires will be presented for five of the six base configurations (excluding B3, used in Test PRF-09) in terms of the temporal variation of HRR and room temperatures. The five base configurations essentially cover the full range of residential rooms and spaces that were studied in this project. Since this project was concerned with quantifying relatively severe fires (characterized by prolonged mean maximum temperatures that are in range of approximately 1,050 to 1,200°C) during the fully-developed phase of a room fire, only those base configurations that meet these temperature conditions are considered here. The less severe fire obtained in Test PRF-09 (with smaller window) may not be a suitable fire scenario for assessing the structural impact of fire, although it may be used in other types of fire safety problems that involve limited ventilation. It is emphasized that this project was concerned with characterizing fire behaviour and developing the understanding of how variables such as ventilation and fuel load density and composition impact fully-developed fire conditions, which was accomplished in Section 4. The graphs of HRR and temperature vs. time that can be used as design fires for the five base configurations are given in Figures A-1 to A-16 in Appendix A. Due to the noise in the HRR data, the HRR vs. time graphs that are provided in Appendix A include data that has been smoothed using a running median method to make the data suitable for input into calculation methods, for example. Based on the analysis of the results, the following statements are made regarding the HRR and temperature results:

1. **HRR vs. Time:** For tests conducted with a single window, the peak HRR in the room will be considered to be governed by the size of the windows and it is assumed that measured values that are above the ventilation limit represent external combustion. Tests in larger rooms with multiple windows (such as, tests PRF-08, PRF-10 and PRF-14) had more complex HRR vs. time graphs and therefore care needs to be exercised in using the results due to the pattern of zonal burning behaviour that was identified in this research.
2. **Temperature vs. Time:** Two temperatures vs. time graphs will be provided for each base configuration: an average and a maximum profile. While average values may be suitable for representing some thermodynamic properties in certain engineering problems, this project

was concerned with addressing conservative fire scenarios, in which prolonged high temperatures (in the range of approximately 1,050°C to 1,200°C) occur, and hence the reason for using the 95th percentile fuel load density values and large windows in respective scenarios. Therefore, for consistency, this research suggests that the zone with the most severe temperature (high temperature zone) history should serve as the temperature vs. time profile for the design fire for the entire room. The test results showed that room boundaries in the high temperature zone were destroyed earlier than elsewhere in the room. Therefore, in a room with a fire resistant door, as was the case in the tests, the high temperature zone governs the potential spread of fire to adjacent spaces due to failure of the wall or ceiling boundaries. However, in reality, most rooms of fire origin (such as bedrooms and living rooms) typically have combustible (non-fire resistant) doors, which would likely be breached by the fire earlier than wall or ceilings boundaries lined with either regular or Type X gypsum board, as was observed in one test (PRF-08) conducted in this work, where the door was destroyed in approximately 360 s. The following notations and definitions will be used in the graphs:

a. T_{R_AVG}: Average upper layer temperature in the room that is obtained by taking the average of TCs in all four quadrants of the room that were located at elevations of 1.4 m and 2.4 m above floor (considered to be the hot layer).
b. T_{R_max}: Average upper layer temperature in the quadrant of the room where maximum temperatures were measured that is obtained by taking the average of the TCs located at elevations of 1.4 m and 2.4 m above floor.

A summary of design fires graphs for HRR and temperature, which are provided in Appendix A, is given in Table 41.

Table 41. HRR and Temperature Design Fire Graphs Derived from Test Data.

No.	Base configuration	Tests	HRR vs. Time	Temperature vs. Time
B1	Primary bedroom	PRF-01, -02, -03, -04	Figures A-1 and A-3	Figures A-2 and A-4
B2	Secondary bedroom #1	PRF-05, -07	Figures A-5 and A-7	Figures A-6 and A-8
B4	Living room	PRF-06, -11, -12, -13	Figure A-9	Figure A-10
B5	Secondary suite	PRF-08	Figure A-11	Figure A-12
B6	Main floor (living/dining/kitchen)	PRF-10, -14	Figures A-13 and A-15	Figures A-14 and A-16

5.1 Correlation of Results

5.1.1 Growth Phase (Stage R2)

For both HRR and temperature, the growth phase, Stage R2, correlates well with a power law (t-squared) function given by Equation (5.1), which contains only one parameter:

$$Y = \frac{1}{\lambda} t^2 \tag{5.1}$$

where

- Y is the dependant variable (either HRR or temperature).
- t is time (s).
- λ is a correlation coefficient, obtained through regression analysis.

For HRR, Stage R3 was characterized by HRR values that significantly exceeded the ventilation limit due to external burning, as discussed earlier. In Stage R4, for tests conducted with a single window, the average HRR was found to be in good agreement with the theoretical HRRv values given in Table 3.

5.1.2 Fully-Developed Phase (Stage R3)

Figures 131 to 135 show that the temperature rise in Stage R3 of the fully-developed phase can be approximated by a linear correlation for all but one of the tests considered here. The exception is Test PRF-03, where the data are not amenable to correlation. The graphs in Figures 131 to 135 illustrate the difficulty of correlating the data in Stage R3, especially during the early part of Stage R3, which has wide temperature fluctuations in some tests. Table 42 gives the results of the linear regression analysis. The correlation is given by:

$$T = yo + at^2 \tag{5.1}$$

where

- T: is temperature (^{o}C).
- t: is time (s).
- a: is the gradient of the line (^{o}C / s).

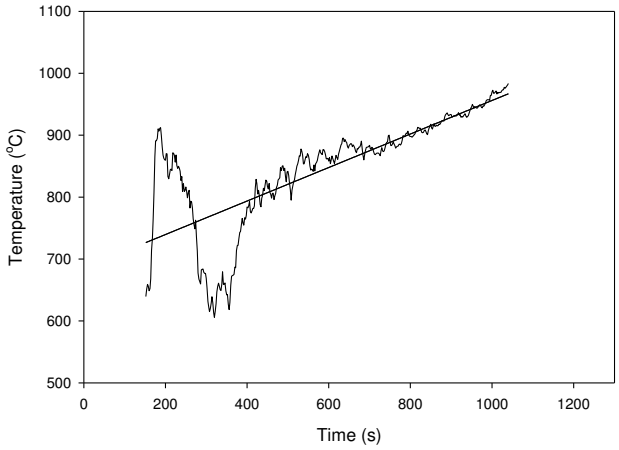

Figure 131. Linear curve fit for the mean maximum temperature rise in Stage R3 for Test PRF-02.

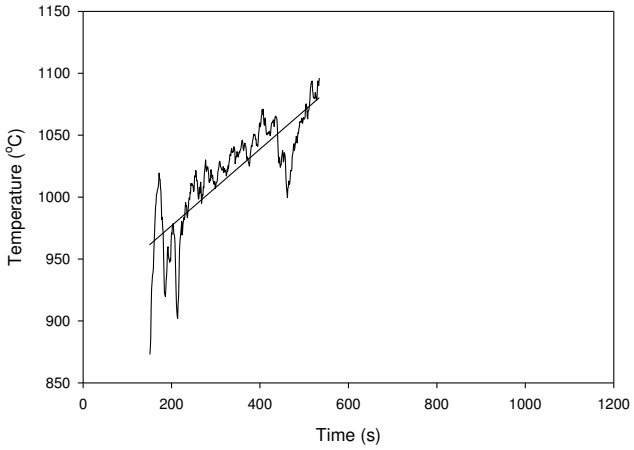

Figure 132. Linear curve fit for the mean maximum temperature rise in Stage R3 for Test PRF-03.

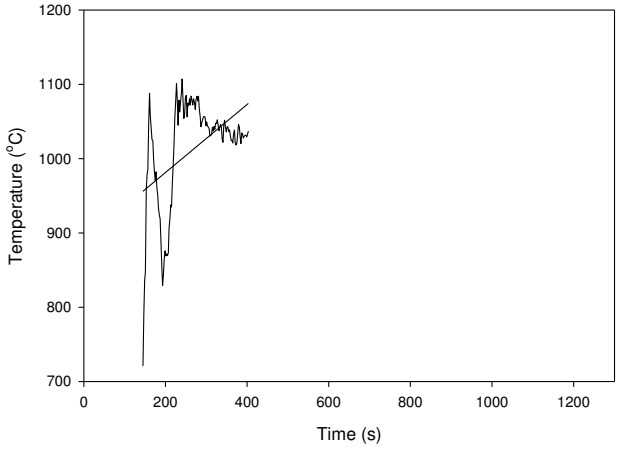

Figure 133. Linear curve fit for the mean maximum temperature rise in Stage R3 for Test PRF-04.

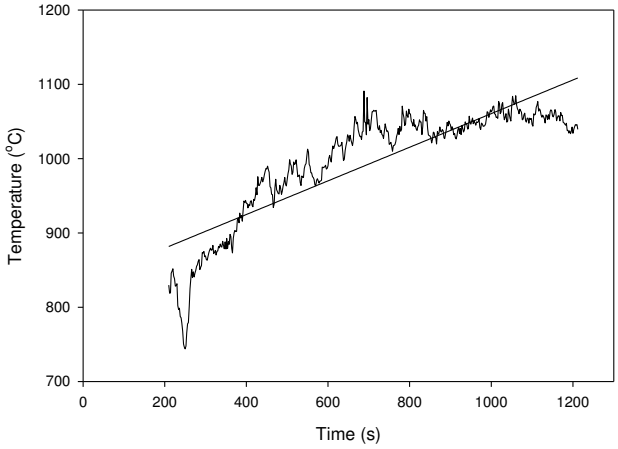

Figure 134. Linear curve fit for the mean maximum temperature rise in Stage R3 for Test PRF-05.

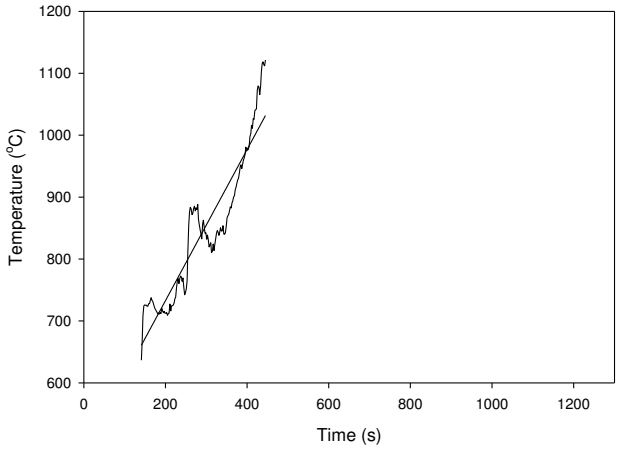

Figure 135. Linear curve fit for the mean maximum temperature rise in Stage R3 for Test PRF-06.

Table 42. Linear regression results for Stage R3.

Test ID	yo (°C)	a	R†	R3 duration (s)	
				Δt_{R2}	Δt_{R3}
PRF-02	685.5	0.27	0.77	150	1,026
PRF-03	915	0.31	0.77	132	402
PRF-04	889.7	0.45	0.48	144	258
PRF-05	834.3	0.46	0.86	210	1,044
PRF-06	488.6	1.22	0.93	138	306

† R: Correlation coefficient; Δt_{R2} – time from ignition to the start of Stage R3; Δt_{R3} – Duration of Stage R3.

5.1.3 Fully-Developed Phase (Stage R4)

The mean hot layer temperature (either for a single zone or for the entire room) can be taken to be a single value since the standard deviation in Stage R4 is relatively small, as shown in Table 43. For example, for Test PRF-03, the mean maximum temperature during the 17.5 min duration of Stage R4 can be taken as either 1,203°C (a conservation high value obtained in the SW zone) or 1,120°C (average value for all four zones).

Table 43. Temperatures at 1.4 m height (measured by a single TC) in each of the four zones of the room during Stage R4 for Tests PRF-02, -03, -04, -05 and -06.

Test ID	Duration of Stage R4 (min)		Temperature values in zone NW (°C)	NE (°C)	SW (°C)	SE (°C)	Room mean[††] (°C)
PRF-02	20.3	Min-Max	1,005-1,096	984-1,181	979-1,067	985-1,105	
		Mean	1,056	1,060	1,030	1,036	1,046
		SD [†]	18	39	79	19	39
PRF-03	17.5	Min-Max	801-1,299	764-1,304	1,120-1,240	873-1,230	
		Mean	1,125	1,032	1,203	1,118	1,120
		SD[††]	126	35	25	77	66
PRF-04	15.7	Min-Max	921-1,264	621-1,188	770-1,125	776-1,158	
		Mean	1,129	959	1,080	947	1,029
		SD	53	57	57	72	60
PRF-05	16.0	Min-Max	1,064-1,204	891-1,114	992-1,130	1,035-1,179	
		Mean	1,140	1,053	1,090	1,085	1,092
		SD	36	39	22	28	31
PRF-06	12.8	Min-Max	743-1,202	663-1,307	953-1,224	860-1,064	
		Mean	1037	966	1,119	971	1,032
		SD	137	199	40	46	98

[†] SD – Standard deviation; [††] Room mean: average for all four zones.

5.1.4 Decay Phase (Stage R5)

The nonlinear decay phase for most of the tests can be modelled by using suitable polynomials (such as multi-parameter exponential decay or hyperbolic functions) and regression analysis to derive coefficients. However, it is difficult to find a simple correlation (similar to the power law used for the growth phase) since the values of the HRR and time at which the decay phase begun were different for all of the tests. The possibility of using polynomial regression to model the decay phase for HRR and temperature is demonstrated for Tests PRF-02, 03, 04 and 06. In order to fit the data to a two-parameter hyperbolic function, which is given by Equation (7.2), the data for the decay phase were normalized by shifting the origin of the decay graph to the onset of the decay phase, i.e. time is taken to be zero at the start of decay and the HRR and temperature ordinates are defined as differences (HRR or temperature drops).

Regression type: Two-parameter hyperbolic decay function

$$Y = XHT + \frac{at}{b+t} \tag{5.2}$$

where:

- *a* and *b* are correlation coefficients (constants) obtained from regression analysis;
- *Y* is the dependant variable (either HRR drop or temperature drop);
- *t* is time (s);
- *XHT* is the value of either temperature or HRR at the start of the decay phase;

Tables 44 and 45 give the coefficients for Equations (5.1) and (5.2) that were obtained using regression analysis. The T_{R_max} temperature profiles were used in all cases. Figures 136 and 137 show examples of decay phase curve fits for HRR and temperature, respectively, for Test PRF-04.

Since the value of HRRv and fuel load characteristics (density and composition) influence the shape of the decay profile (coefficients a and b), the coefficients of the decay correlations given in Tables 44 and 45 are specific to the indicated tests and any application to other fire scenarios needs to be rationalized, which is beyond the scope of this research.

Table 44. Parameters for use in the HRR correlation for the growth and decay phases in Tests PRF-02, 03, 04, 05 and 06.

Test ID	Growth	XHT	Δt_{R2-4}	Δt_{R5}	Decay	
	α	(kW)	(min)	(min)	a	b
PRF-02	37.9	2,828	39.9	23.5	-3,774	2,219
PRF-03	28.8	4,217	26.4	36.6	-3,504	706
PRF-04	28.6	4,006	22.4	38.6	-4,361	1,674
PRF-05	55.2	2018	36.9	19.1	-1,703	52
PRF-06	9.84	3,936	20.2	39.8	-5,210	1,081

Δt_{R2-4} – Time to decay (min); Δt_{R5} – Duration of decay phase (min)

Table 45. Parameters for use in the temperature correlation for the growth and decay phases in Tests PRF-02, 03, 04, 05 and 06.

Test ID	XHT	Growth	Decay	
	(°C)	α	a	b
PRF-02†	976	37.9	N/A	N/A
PRF-03	1,183	28.8	-1,983	9,336
PRF-04	1,088	28.6	-1,366	4,350
PRF-05	1,008	55.2	N/A	N/A
PRF-06	1,115	9.84	-4,773	409

N/A: Missing data since test was terminated early into the decay phase;

† PRF-02 had a complex decay phase, the latter part of which was predominantly linear

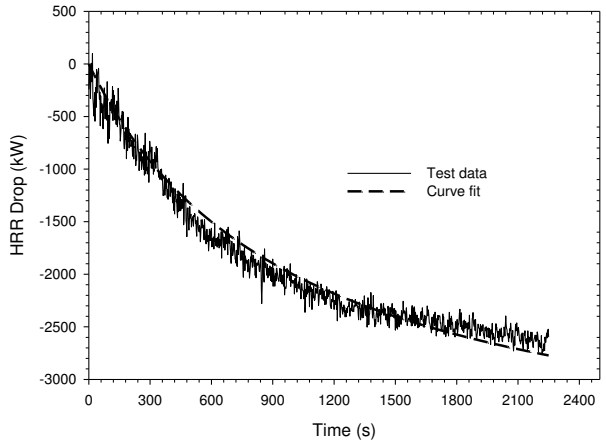

Figure 136. Curve fit for the HRR decay in Test PRF-04.

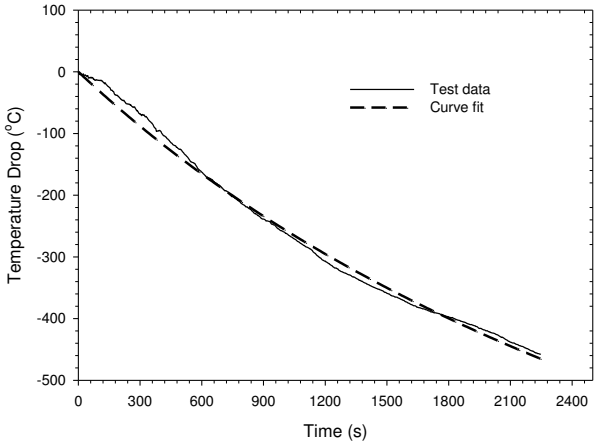

Figure 137. Curve fit for temperature (T_{R_max}) decay in Test PRF-04.

6 Analytical Results

The test results have shown that fires in which a PCF was the first-ignited-item, with a strong ignition source, developed rapidly and flashover occurred within 300 s of ignition. For situations where the pre-flashover period is the region of interest, this research has shown that the HRR profile can be modelled as t-squared fires up to the ventilation limit. The average room (hot layer) temperatures during the pre-flashover period can be calculated using an existing correlation that was developed by Quintiere et al. [17], which given by Equation:

$$\Delta T_g = 480\left(\frac{\dot{Q}}{\sqrt{g}\ c_p\rho_\infty T_\infty A_o\sqrt{H_o}}\right)^{2/3}\left(\frac{h_k A_T}{\sqrt{g}\ c_p\rho_\infty T_\infty A_o\sqrt{H_o}}\right)^{-1/3} \quad (6.1)$$

where ΔT_g is the temperature rise above the initial ambient temperature of the room.

For a given HRR ($\dot{Q}$), room dimensions and ventilation conditions, the value of ΔT_g calculated using Equation (6.1) is sensitive to the thermal physical properties and thickness of the wall lining materials. The applicability of Equation (6.1) was evaluated by using data from test PRF-03. The results are given in Table 46. The thermal properties of the wall lining material (Type X gypsum board) used in the calculations were: thermal conductivity of 0.25 w/m.K, density of 770 kg/m^3 and specific heat capacity of 1.1 kJ/kg.K [42]. The results show that the pre-flashover temperatures calculated using Equation (6.1) were within 10% of the measured values.

Table 46. Comparison of measured and calculated pre-flashover temperatures for test PRF-03.

Time(s)	HRR (kW)	T_{expt} (^oC)	T_{cal} (^oC)	$T_{cal} - T_{expt}$ (K)	% error
60	137	80	88	8	10
90	429	196	202	6	3
120	1362	446	454	8	2
132	1983	607	592	-15	-3

T_{cal} – Calculated temperature; T_{expt} – Measured temperature;

In between flashover and the onset of the decay phase, the magnitude of the global HRR (room HRR plus external HRR) can exceed the theoretical ventilation-controlled value by a significant margin during Stage R3 and approaches the ventilation-controlled value during Stage R4. The experimental results show that the extent of external HRR depends on fuel load composition (plastics vs. wood content) and ventilation, but the exact relationship has not been modelled in this research project.

6.1 Evaluation of Existing Methods

The results of mean maximum post-flashover temperatures (mean for all four zones) measured in the tests are compared with calculations for temperature and fire duration using the following four existing methods, which were given in Section 2, are compared with test results (for Tests PRF-02 to PRF-10):

1. Correlation by Law (Equation (2.12))
2. Correlation by Ma et al. (Equation (2.19))
3. Correlation by Tanaka (Equations (2.22) and (2.23))
4. Eurocode method (Equation (2.26))

Two of the above methods calculate a single peak temperature for the entire duration of the post-flashover period, while the other two methods (Tanaka and Eurocode) calculate the temperature vs. time profile. The results given in Figure 138 show that none of the methods are in good agreement with the measured temperatures: the Eurocode method over predicts the temperatures, Law's method is only in good agreement with about 50% of the test data while the rest of the methods considerably under predict the measured temperatures.

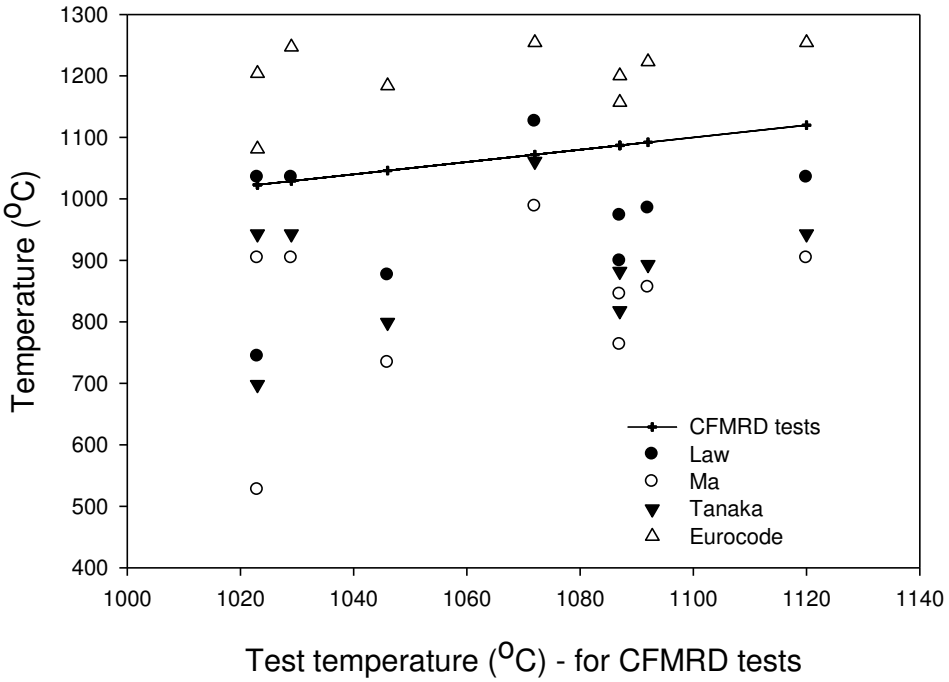

Figure 138. Peak temperature calculations from existing methods compared with test results.

As for the duration of the post-flashover period (time-to-decay), Figure 139 shows that all four methods over-predict the onset of the decay phase by a large margin. Over-predicting duration of the post-flashover phase maybe considered appropriate for design purposes since it results in a conservative solution. The reason for the poor prediction of the CFMRD test results is likely because existing methods were developed using data from fire tests in which the fuel loads largely consisted of cellulose-based materials, such as wood-cribs. Wood-based fuels produce less excess pyrolysis gases under oxygen-deficient conditions (i.e. the burning rate is slower), which promotes a longer burning duration. Thermal plastic materials, by contrast, undergo intense pyrolysis even under oxygen-deficient conditions, when they are exposed to sufficiently high thermal radiation. The excess fuel gases are simply transported outside the room where combustion is completed, resulting in a considerably greater flame extension out of the window opening, higher measured HRR than the theoretical ventilation-limited value and short post-flashover duration.

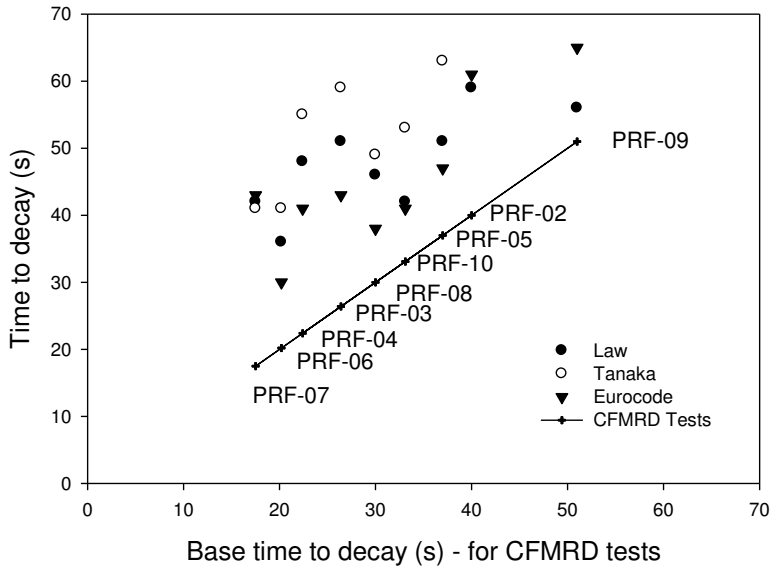

Figure 139. Calculations of time-to-decay from existing methods compared with test results.

In the tests conducted in this research, there are two possible reasons for shorter duration of the post-flashover phase:

1) It was observed that fuel loads (real furnishings) lost their geometric integrity during the post-flashover phase as they collapsed into heaps, which was likely accompanied by a drastic reduction in the available surface area and, consequently, burning rate; this likely contributed to the early onset of the decay phase, and;
2) There was a significant (estimated to be up to 15%, as shown in Figure 130) amount of heat release that occurred outside the fire room, especially during Stage R3, during which stage the measured HRR exceeded the ventilation-controlled HRR value. Therefore, existing methods that assume no external heat release are expected to predict longer post-flashover fire durations. It is noteworthy that such an assumption is a conservative scenario given the multiplicity of fuel load, ventilation and geometric parameters in the population of real dwellings.

Further analysis of the results of temperature calculations using the Eurocode method, shows that although it predicted the peak temperature values very well, the shape of the curves and, particularly, the time-to-peak and rate of fire decay do not agree with the test data obtained in this research, as shown in Figure 140, for Tests PRF-03, -05 and -09.

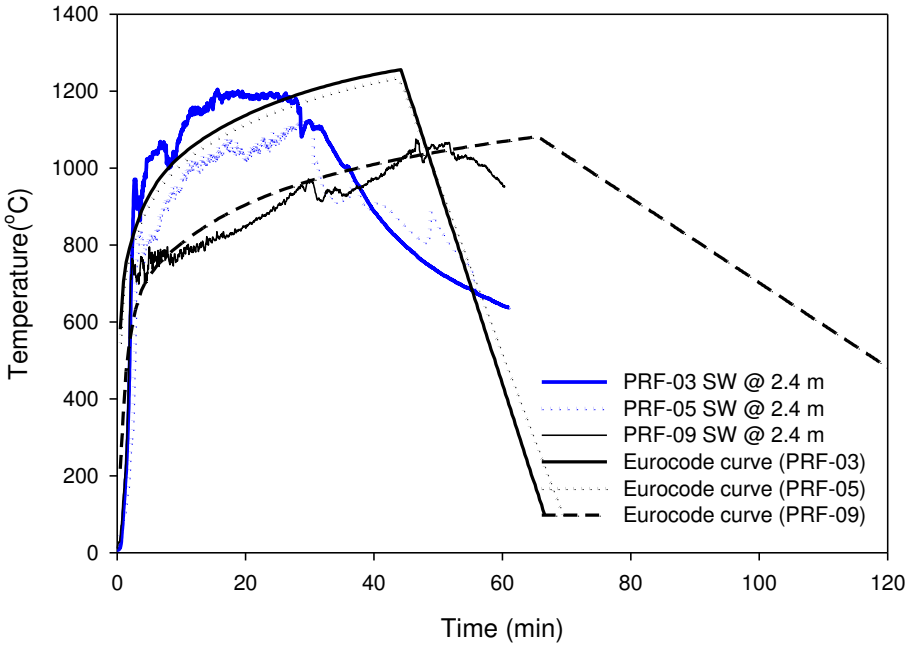

Figure 140. Comparison of temperature profiles from the Eurocode method and CFMRD tests.

6.2 The CFMRD Calculation Method

Given that one of the main objectives of this research was to study fully-developed fires and develop a method for calculating design fires, this research concludes the following as the basis for developing a calculation method:

1. The growth phase of residential room fires can be modeled using existing t-squared fires up to the ventilation limit.
2. The experimentally measured HRR vs. time profile during the fully-developed stage is not appropriate for use in calculating the fire temperature in the room because it includes a significant proportion of external heat release that has essentially no effect on room temperature in a heat balance approach. However, the external heat release is considered to be a manifestation of a fuel-rich room combustion atmosphere, which is associated with poor combustion efficiency. This gives rise to the unsteady fully-developed phase, Stage R3, during which the HRR exceeds the ventilation limit, but the room temperatures were typically below 1,000°C due to a combination of poor combustion efficiency and heat losses to the boundaries. Therefore, the hot layer temperature during the fully-developed period cannot be represented by a single value. There are two possible ways of handling the fully-developed phase:
    a. Conservative scenario: assume that the maximum temperature is achieved when the ventilation limit is reached, and lasts for the duration of the fully-developed phase, or;

b. Realistically model the fully-developed phase (Stages R3 and R4). Modelling of Stage R3 will be considered in this research.

3. The correlation for calculating the ventilation-controlled HRR predicts the measured average HRR in Stage R4 with good accuracy for rooms having a single window. For rooms with multiple windows, it was difficult to assess accuracy due to the complexity of the HRR profiles.

The results of this research shows that, regardless of the parameters, all the tests conducted achieved a mean maximum temperature that was within 1,150°C ± 100°C. However, the main difference between the tests is the time taken to reach Stage R4 and its duration. This is attributed to various parameters such as ventilation and fuel load configuration. Therefore, the crux of the post-flashover problem is the prediction of the duration of Stage R3 and the mean maximum temperature (and its duration) in Stage R4.

6.2.1 Duration of the Fully-Developed Phase

The duration of the fully-developed phase (R3+R4) is known to be dependent on fuel load (type and quantity) and its burning rate (largely determined by ventilation). The time-to-decay is obtained by adding the time from ignition to flashover (growth period) to the duration of the fully-developed phase. Here the focus is on the duration of the fully-developed phase because the growth period depends on the ignition scenario, as was observed, e.g. in Test PRF-14.

Analysis of the results shows that there is no strong correlation between the duration of the fully-developed phase and either of the two parameters (inverse opening factor and total HR), as shown in Figures 141 and 142. However, there is a correlation between the duration of fully-developed phase and the ratio of total HR to HRRv as shown in Figure 143, where longer durations of the full-developed stage are related to higher ratios of HR to HRRv. This translates into a correlation between the % of HR released during the fully-developed phase and size of the window (inverse opening factor), as shown in Figure 144.

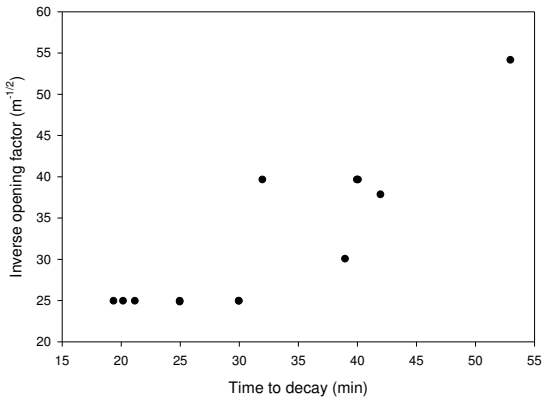

Figure 141. Graph of inverse opening factor vs. time-to-decay for PRF tests.

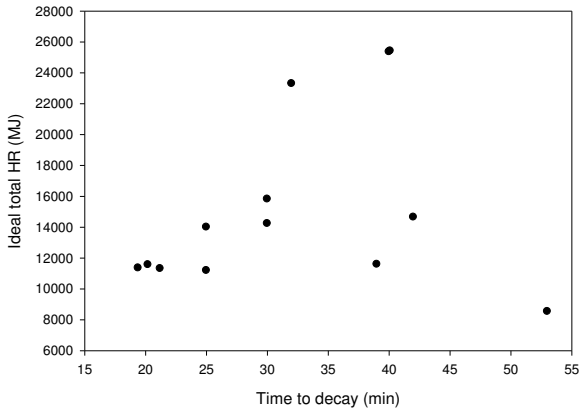

Figure 142. Graph of ideal total HR vs. time-to-decay for PRF tests.

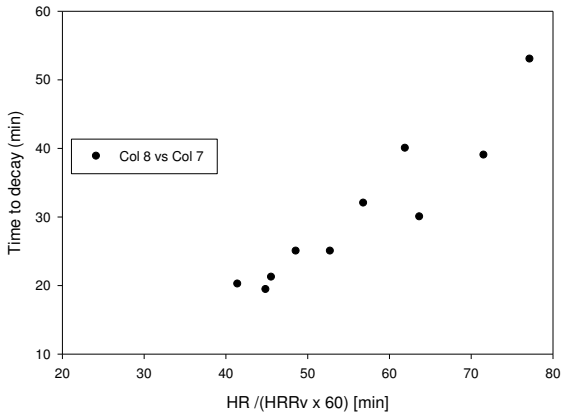

Figure 143. Correlation of time to decay.

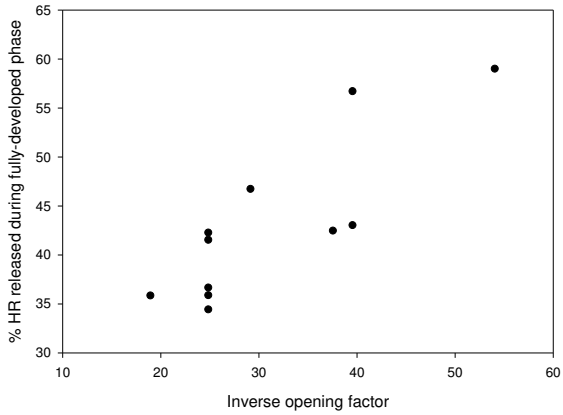

Figure 144. % HR released during fully-developed phase vs. inverse opening factor.

Figure 145 is a bar chart showing the estimated duration of the fully-developed phase and percentage of fuel load consumed for eleven of the tests; on average approximately 43% of the fuel load was consumed during the fully-developed phase with a standard deviation of 7%. The maximum amount of fuel load consumed during the fully-developed period was 58%, which was obtained in Test PRF-10. In the literature, it is commonly assumed that 60% of the fuel load is consumed during the fully-developed period, which is close to the upper limit of 58% obtained in this research. The amount of fuel load consumed during the growth phase (in this research) was found to be an average of 3% (with a standard deviation of 1.5%). Therefore, it is very small compared to the energy released during the fully-developed phase. In view of the results from this research, the literature assumption of 60% represents the upper limit (or conservative scenario, i.e. longer duration of the fully-developed phase).

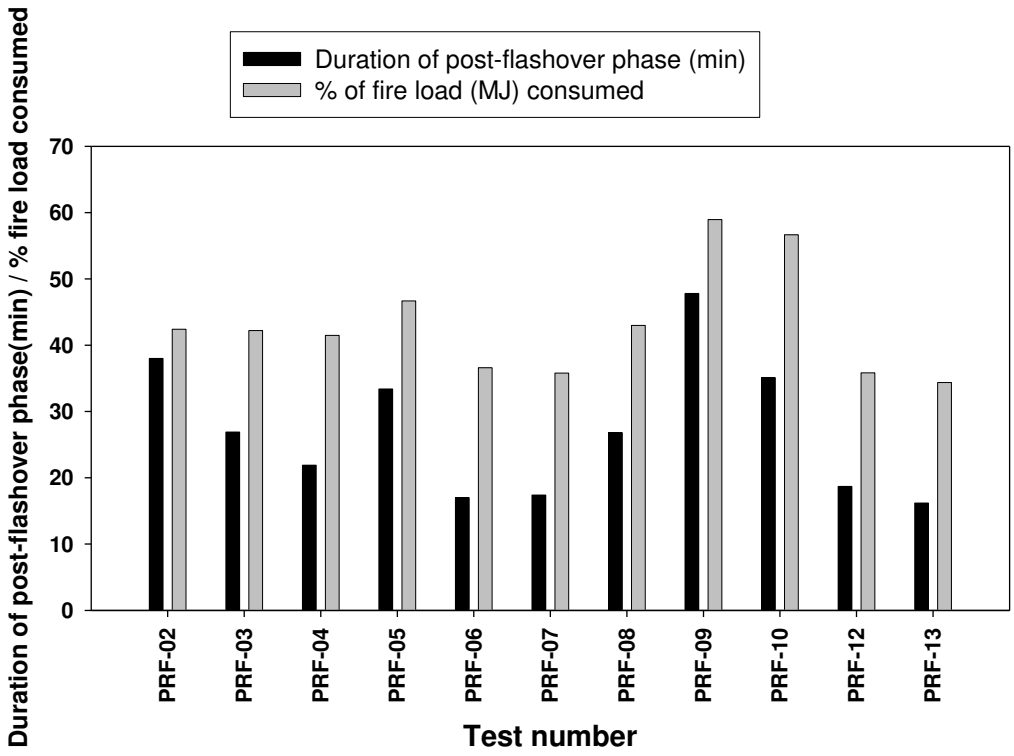

Figure 145. Bar chart showing the duration of the post-flashover phase and % fuel load consumed for eleven of the tests.

Figure 146 shows the results of predicting the duration of the fully-developed phase using the average and maximum values (43% and 58%, respectively) obtained from the tests. Using the average value under-predicts the duration of the fully-developed phase in four of the tests, whereas the maximum value over-predicts by as much as 60% in one case. Therefore, the approach taken to predict the duration of the fully-developed phase depends on the objectives of the task at hand. If the conservative scenario is of primary interest, then the 60% assumption is reasonable. Otherwise, for the test data developed in this research, a linear correlation of the data in Figure 144 can be used to predict the fraction of energy (X1) released during the fully-developed phase with an uncertainty of ± 14%. The correlation is:

$$X1 = 22.10 + 0.67 IF_O \tag{6.2}$$

where IF_O is the inverse of the opening factor, which is given by Equation (2.2).

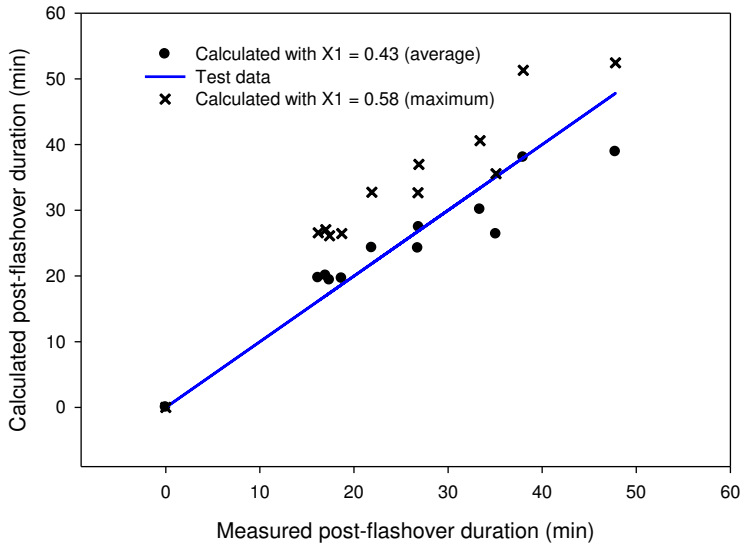

Figure 146. Comparison of the full-developed period calculated using X1 = 0.43 and X2 = 0.58.

Therefore, the following equation is recommended for calculating the duration of the fully-developed phase. The factor "X1" can either be taken as 0.6 (based on the 60% assumption) for a Conservative scenario or estimated from Equation (6.3).

$$t_{FD} = \frac{FL \,.X1}{90.FV} \tag{6.3}$$

where:

t_{FD} = Duration of the fully-developed phase (min)

FL = total fuel load (MJ)

X1 = Fraction of FL consumed at decay (during the fully-developed phase)

FV = Ventilation factor

It is noted that Equation (6.3) is a commonly used expression (that was derived from the understanding that the fire duration is proportional to total energy released by the fire (FL) during the fully-developed phase divided by the rate of burning. Therefore, the contribution of this work is the correlation of the expression to the experimental data that has produced specific values for variable X1. An ISO International Standard [43] suggests that a value of X1 = 0.8 can be used to determine the onset of the decay phase, however it was clearly noted that this value was a rough estimate and that further research was needed to accurately determine the onset of decay – this research, as contribution to that end, supports a value of X1 = 0.6 to be a conservative estimate.

6.2.2 Duration of Stage R3

The duration of Stage R3 determines the time of attainment of the maximum mean post-flashover temperature, i.e. this temperature occurs at the end of Stage R3. Analysis of the results, for the tests conducted in this research, shows that the duration of Stage R3 depends on the ventilation factor (window size), composition of the fuel load and its exposed surface area. During Stage R3, the temperature rise (after flashover) can be assumed to be linear. The focus here is on the fire conditions in the zones near the window that experience optimal combustion efficiency and hence the most severe temperature conditions. Other zones that were located deeper inside the room were seen to experience vastly different (less severe) temperature conditions as described earlier.

Figure 147 shows that the duration of Stage R3 generally increased with decreasing window size. Modelling Stage R3 is complicated by the fact that the room HRR and combustion efficiency are unknown and cannot be measured accurately in fire tests [20]. Babrauskas [18] developed a method for calculating temperatures in post-flashover fires, which included the effect of combustion efficiency and burning rate stoichiometry. It was stated that the method could potentially calculate temperatures in Stage R3 (transient stage), but it is noted that the parameters required in Babrauskas' method to account for combustion efficiency and stoichiometry (fuel-to-air mixture ratios) at every stage of the post-flashover fire are difficult to obtain in most design situations [19, 20].

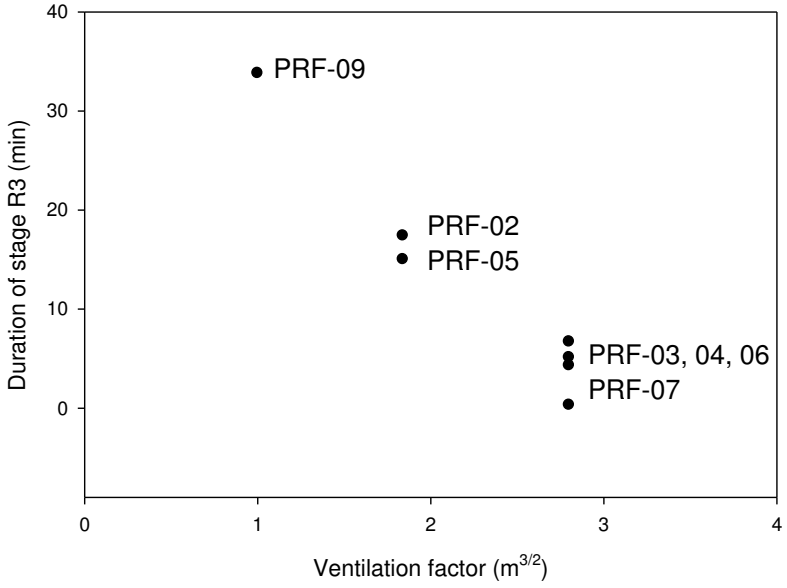

Figure 147. Duration of Stage R3 vs. ventilation factor for tests with a single window.

In modelling the duration of Stage R3, t_{R3}, it is assumed that:

1) There is sufficient fuel load to give rise to a fully-developed fire, which was true for all of the tests in this research;
2) The room boundaries are constructed with gypsum board in the same manner as in the tests, and;
3) The floor area of the room is between 11.2 m^2 and 16 m^2.

Consider that t_{R3} is a function of the following variables:

$$t_{R3} = fn(A_s, F_V, HRR_{pa}) \tag{6.4}$$

where:

A_s (m^2) = Exposed surface area of the fuel load

F_V = Ventilation factor

HRR_{pa} (kW/m^2) = Average peak HRR per m^2 for the fuel load based on Cone calorimeter test data (conducted at a heat flux exposure of 50 kW/m^2)

The weighted HRR_{pa} differs from an arithmetic mean in that the contribution of individual components of the fuel load is based on their respectively quantities, for example, if the fuel load consists of two materials A and B in the proportions X% and Y% by mass, the weighted HRR_{pa} is equal to: $(HRR_{pa}.X)_A + (HRR_{pa}.Y)_B$. The rationale behind this approach is that, after flashover, exposed surfaces of the fuel load release fuel volatiles at pyrolysis rates that are consistent with burning characteristics of constituent materials, e.g. thermoplastics materials have higher pyrolysis rates than wood; this is taken account of in the weighted HRR_{pa}. Based on existing cone calorimeter data, thermoplastics and wood materials have peak HRR_{pa} values of about 400 kW/m^2 and 200 kW/m^2, respectively, and weighted HRR_{pa} values for the tests conducted in this research were typically lower than 300 kW/m^2 since the fuel loads had a significantly greater mass percentage of wood products. Therefore, with this approach, the duration of Stage R3 is expected to increase with thermoplastics content (as well as fuel surface area). The heat content of the fuel load (FL) is not included in the relationship because it is assumed that the surface area is the controlling variable in Stage R3, whereas the FL has an impact on the duration Stage R4.

In Stage R3, there is an excess supply of fuel volatiles immediately after flashover, which gives rise to poor combustion efficiency and increased amount of external combustion. Poor combustion efficiency is thought to be the main cause of the low temperatures in Stage R3 and a certain amount of the fuel load and/or excess fuel needs to be expended (controlled by ventilation) before the combustion efficiency can be high enough to yield high temperatures. Therefore, despite the longer duration of the post-flashover phase at reduced ventilation (e.g. PRF-02 vs. PRF-04 and PRF-05 vs. PRF-09), the severity of the resulting fire is less than that for a comparable fuel load burned at higher ventilation settings precisely due to the longer duration of Stage R3 at lower

ventilation settings. In this model, it is assumed that the ventilation factor has an effect on the time it takes to consume excess fuel or a certain proportion of the fuel load until excess fuel is minimized. It is also acknowledged that thermal properties (and surface area) of the room boundaries play a role during Stage R3. However, it is assumed that the effect of wall lining materials will be automatically factored into any derived method since it was not a variable in the tests.

Figure 148 shows the graph of t_{R3} vs. $\frac{A_s.HRR_{pa}}{1500.F_V}$. Therefore, t_{R3} can be estimated from the following quadratic correlation of results for tests with a single window:

$$t_{R3} = yo + ax + bx^2 \tag{6.5}$$

where:

yo = 34.52

a = -34.39

b = 9.54

$$x = \frac{A_s.HRR_{pa}}{1500.F_V}$$

With the following limits (within experimental bounds):

- *1.0 ≤ FV ≤ 2.8*
- *5,000 (kW) ≤ A_s.HRR_{pa} ≤ 9,500 (kW)*
- t_{R3} = 0 when $\frac{A_s.HRR_{pa}}{1500.F_V} \leq 1.5$ (for very large ventilation openings)

Equation (6.5) predicts results within ± 25% as shown in Figure 149 and Table 47. Considering that the measurement of t_{R3} is also subject to error, given the complexity of room fire behaviour, the correlation provides a reasonable estimate and the error margin may not be significant for short t_{R3} durations. The error margins are widened by a few outliers (PRF-02, -05 and -07); perhaps further analysis of the test results can enhance the accuracy of the estimates. However, given the complexity of the tests, the correlation of t_{R3} to $\frac{A_s.HRR_{pa}}{1500.F_V}$ promises a viable simple calculation method for predicting the time to reach the peak temperature. Given the broadness of this study, perhaps further research focusing on fewer parameters is required to enhance calculation methods.

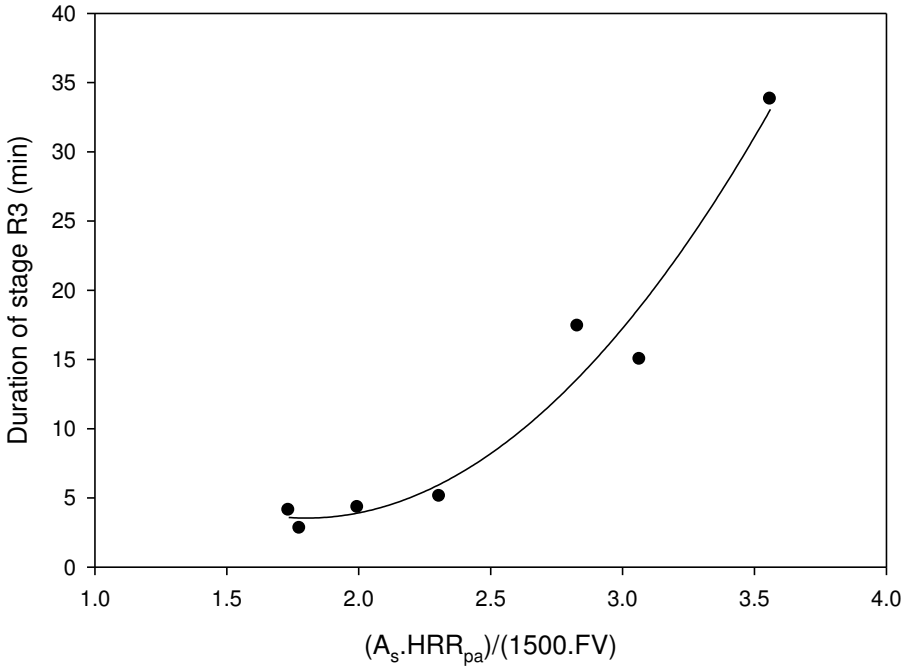

Figure 148. Variation of t_{R3} with $\frac{A_s.HRR_{pa}}{1500.F_V}$

Table 47. Correlation parameters and results for t_{R3}.

Test No.	F_V ($m^{5/2}$)	As (m^2)	HRRpa (kW/m^2)	As.HRRpa (kW)	t_{R3} (min)	Calculated t_{R3} (min)	t_{R3} error (%)
PRF-02	1.84	33	254.6	8,460	15.0	18.7	+25%
PRF-03	2.8	33	214.6	7,170	4.1	3.6	-13%
PRF-04	2.8	33	250.0	8,242	4.3	3.9	-10%
PRF-05	1.84	31	255.1	7,811	17.4	13.6	-22%
PRF-06	2.8	40	236.5	9,532	5.1	5.9	+17%
PRF-07	2.8	32	231.0	7,344	2.8	3.5	+26%
PRF-09	1.0	24	226.0	5,341	33.8	33.0	-2%

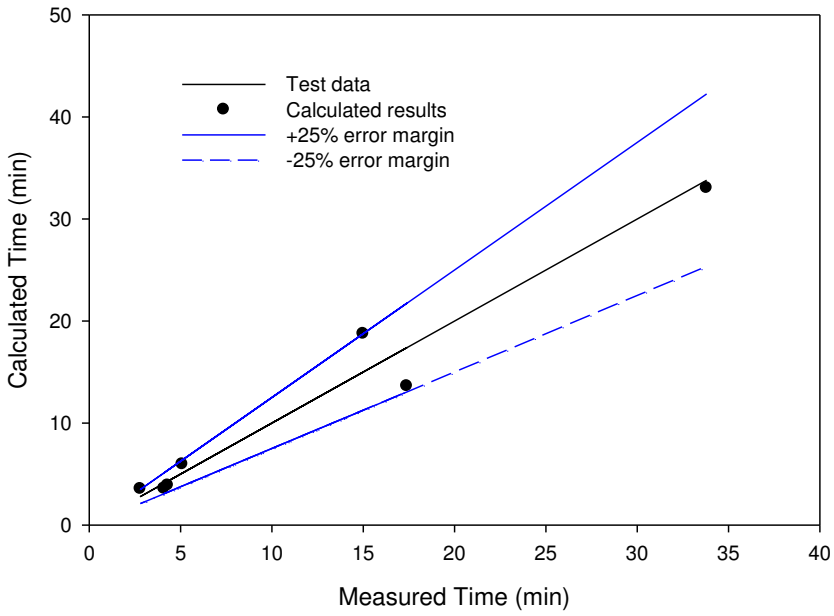

Figure 149. Comparison of calculated and measured duration of Stage R3.

6.2.3 Maximum temperature in Stage R4

The mean maximum temperature in Stage R4 and the duration of R4 are a key measure of fire severity. Analysis of the results (Figure 128) shows that, regardless of test variables (such as, ventilation, fuel load, ignition method and room size), the mean maximum temperatures fall within a narrow range of between 1,150°C +/- 100°C. The test results show that the temperatures during Stage R4 do not remain steady, but rather fluctuate around a mean value.

Temperatures in the zones near the window were higher than those towards the back of the room where there was a limited supply of oxygen. This suggests that the room environment is not well-mixed and combustion efficiency varies with location. The problem is compounded by the uncertainty and corruption of the TC data experienced during the tests. While there is evidence that ventilation had an effect on the value of the peak temperature, the difference between the lowest ventilated test (PRF-09) and highest ventilated tests (e.g. PRF-03, -04 and 10) is around 100 - 150°C, which is considerable difference from a thermal radiation standpoint. Therefore, based on the results from this research, the most significant effect of ventilation was on the time to reach Stage R4 (mean maximum temperature), magnitude of the mean maximum temperature and its duration.

Using a heat balance analysis for stage R4, the following typical equation is derived (neglecting the heat required to heat the gases and combustibles, which is assumed to be small), which can be solved for the fire temperature:'

$$HRR_{Room} = Q_{Conv} + Q_{Rad} + Q_{wall} \tag{6.6}$$

where:

HRR_{Room} = portion of HRR released inside the room (not equal to the measured total HRR)

Q_{Conv} = convective heat losses through openings = $\dot{m}_g C_p (T_g - T_\infty)$

Q_{Rad} = radiation heat losses through the openings = $\sigma A_o (T_g^4 - T_\infty^4)$

Q_{wall} = wall heat losses = $\varepsilon \sigma F A_{wall} (T_g^4 - T_{wall}^4) + h_g A_{wall} (T_g - T_{wall})$

where:

$\dot{m}_g$ - mass flow rate of hot gases out of the room;

C_p - specific heat capacity of hot gases;

T_g - temperature of hot gases (fire temperature);

T_∞ - temperature of ambient air;

T_{wall} - wall surface temperature; h_g - convective heat transfer coefficient;

F - radiation view factor;

ε - emissivity of fire gases;

σ - Radiation (Stefan-Boltzmann) constant.

The HRR in the room is given as:

$$HRR_{Room} = HRRv.\eta \tag{6.7}$$

where:

η = Combustion efficiency.

$HRRv = 1500.FV$ (Ventilation-controlled peak HRR)

The wall heat losses are estimated from (based on correlating test data):

$$Q_{wall} = HRR_{room}\left[1.4 - \theta_2)\right] \tag{6.8}$$

where:

θ_2 = Wall loss parameter developed by Babrauskas[18] given by:

$$\theta_2 = 1.0 - 0.94 \exp\left[-54 \left(\frac{A_o \sqrt{H_o}}{A_T} \right)^{2/3} \left(\frac{L}{k} \right)^{1/3} \right] \quad (6.9)$$

where:

L = wall thickness (m)

k = thermal conductivity of the wall linings (W/m-k)

Therefore, the equation that needs to be solved for the unknown fire temperature, T_g, using a numerical procedure, such as Newton's method for root solving (which converges in about three to four iterations), is:

$$\sigma \varepsilon A_o (T_g^4 - T_\infty^4) + \dot{m}_g c_p (T_g - T_\infty) - HRR_{room} (\theta_2 - 0.4) = 0 \quad (6.10)$$

The mass flow rate of the hot gases out of the room is calculated from the HRRv. In this research, the emissivity of the fire gases and combustion efficiency in Stage R4 were assumed to be 0.98 and 95% (0.95), respectively. The results of mean maximum temperature calculations for 12 of the tests in this research are shown in Table 48. The uncertainty of the predicted results for all but two tests is within + 10% (i.e. the method over predicts), as shown in Figure 150. The poor prediction of temperatures in tests PRF-12 and -14 is likely due to uncertainties in the measured temperatures since the mean values of 1,066°C (in PRF-12) and 1,036°C (in PRF-14) appear low when compared with similar tests (PRF-06 and PRF-10).

Table 48. Comparison of measured and calculated temperatures.

Test No.	FV ($m^{5/2}$)	Measured† T_{max} (°C)	Calculated T_{max} (°C)	% Error	T_∞ (°C)
PRF-02	1.84	1,060	1,151	8.5	6.6
PRF-03	2.8	1,202	1,202	0.0	-15.0
PRF-04	2.8	1,129	1,208	7.0	-1.0
PRF-05	1.84	1,140	1,184	4.0	19.1
PRF-06	2.8	1,119	1,218	9.0	20.0
PRF-07	2.8	1,142	1,205	5.5	12.5
PRF-08	4.56	1,118	1,168	4.5	-14.0
PRF-09	1.0	1,039	1,069	3.0	-6.0
PRF-10	4.56	1,163	1,183	8	20.0
PRF-12	2.8	1,066	1,220	14.4	24.0
PRF-14	4.56	1,036	1,172	13.1	-3.0

† Mean maximum temperature in the zone with the highest temperatures

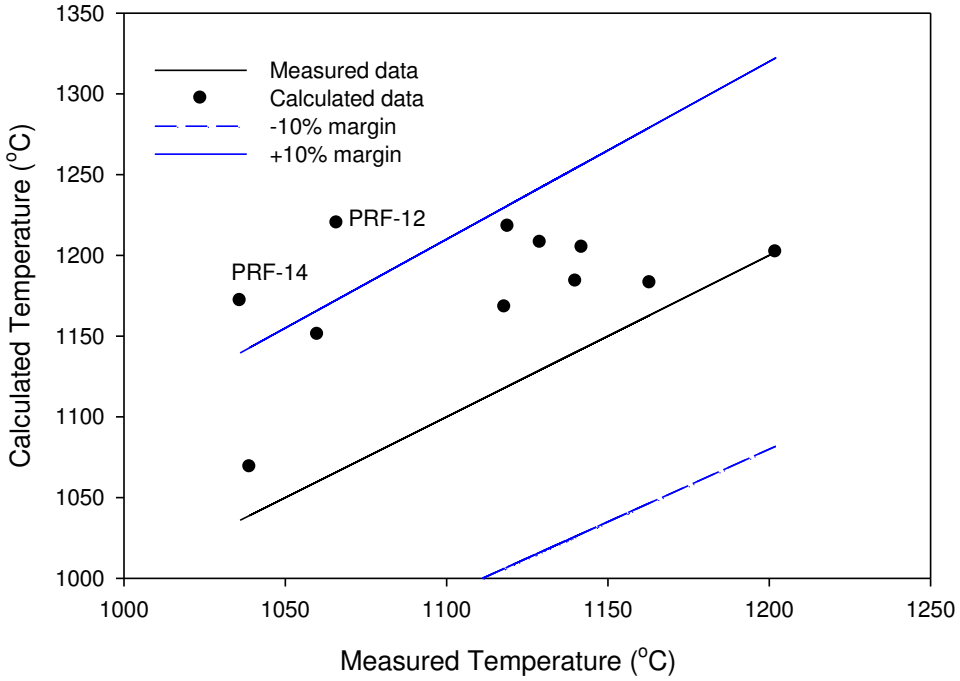

Figure 150. Comparison of the calculated and measured mean maximum temperatures.

The sensitivity of Equation (6.10) to changes in the ventilation factor and floor area (room size) is shown in Figures 151 and 152, respectively. In Figure 151, the calculations were carried out for a room with dimensions 4,200 mm x 3,800 mm x 2,440 mm (used in Tests PRF-02, -03, -04 and -06) with an ambient temperature of 15°C. The results show that the rate of change of peak temperature decreases with increasing ventilation factors above a value of 2, peaking at about 1,250°C for ventilation factors of about 5. There is no further temperature rise with increasing ventilation factors (due to the thermodynamic temperature limit). Although the HRR would be significantly greater, its only effect would be to reduce the duration of the fully-developed phase; there is no data from the tests conducted in this research to determine whether the fire temperatures during the fully-developed phase begin to decline beyond a certain threshold ventilation factor as is suggested in some published literature. Figure 152 shows the effect of fixing the window size at 1,500 mm x 1,500 mm (ventilation factor of 2.8 and HRRv of about 4,100 kW) and increasing the size of the room. The result is that the peak temperature continuously drops with the increasing room size due to the increasing wall heat losses.

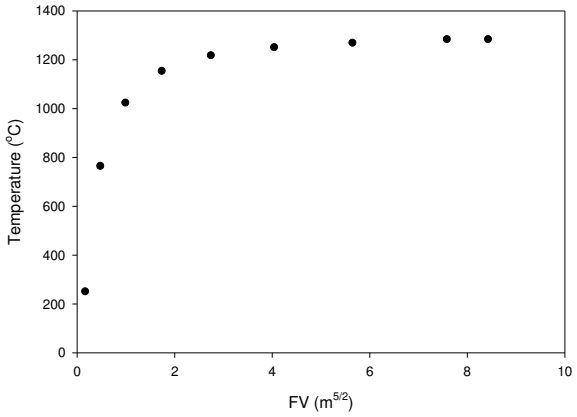

Figure 151. Effect of window size on peak temperature for a fixed room size.

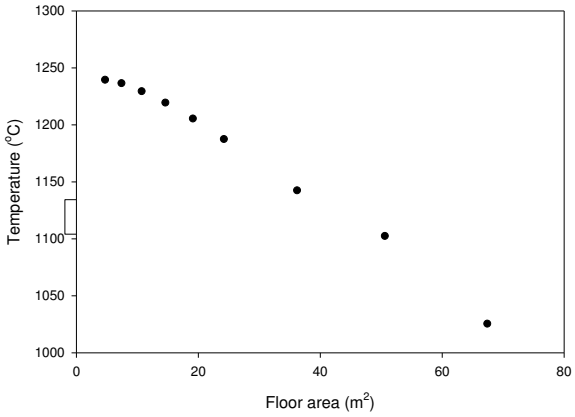

Figure 152. Effect of floor area (room size) on peak temperature for fixed window size.

6.3 Comparison with Published Test Data

The methods developed for calculating t_{R3} and mean maximum temperature are compared with data for a post-flashover test that was conducted at the Underwriters Laboratories (UL) [44] to evaluate the accuracy of the results. The objective of the UL tests was to study the impact of room fire behaviour on Firefighter ventilation tactics. In common with this research, one of the motivations for the UL study was the perceived change in the residential fire environment over the past several decades due to the increased presence of synthetic materials in residential furnishings, as well as changes in fuel loads, home sizes and prevalence of open floor plans. Of interest to the CFMRD research was a test conducted in a simulated living room that was referred to as a “modern room”. The test setup is shown in Figure153. The test details are as given in Table 49.

Table 49. Details of the UL living room test.

Parameter	**Details**
Room size	3.66 m x 3.66 m x 2.44 m (area of 13.4 m^2)
Ventilation opening	2.44 m wide x 2.13 m high (HRRv = 11,377 kW)
Construction type	Lightweight wood frame with 12.7 mm thick gypsum board walls and ceiling
Main fuel load (No mass provided)	Floor finish: carpet with padding Sectional sofa (microfiber ticking with PUF filling) Engineered wood coffee table, end table, television stand, 37 inch flat panel television, a number of plastic toys and paper products, other furnishings as shown in Figure 153
Ignition method	Flaming ignition source: lit candle placed on the side of the sofa
Test duration	The fire was extinguished after sustaining the post-flashover period for a short period of time.

In the UL test, flashover occurred at 3.5 minutes after ignition. The peak temperature was reported to be 1,300°C - the temperature profiles are shown in Figure 154.

Figure 153. UL living room test setup (2 minutes after ignition) [44].

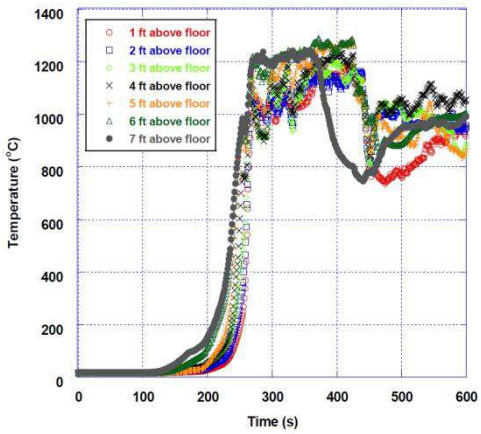

Figure 154. UL living room test measured temperatures [44].

6.3.1 Comparison with calculated results using the CFMRD method

Comparing results with Test PRF-06 (Living room), flashover in PRF-06 occurred at 2.3 minutes vs. 3.5 min in the UL. The slightly longer time to flashover is because the UL test had a longer incipient phase since a weaker ignition source was used (compared to the 19 kW propane source used in PRF-06) as well as the large ventilation opening. Focusing on the fully-developed period:

1. **Stage R3:** Assuming a similar fuel surface area to PRF-06 (since no information was provided in the UL tests), the ratio $\frac{A_s.HRR_{pa}}{1500.FV} = 0.83$, which is much less than 1.5.

   Therefore t_{R3} in the UL test equals zero since the extremely large opening supplied sufficient oxygen (HRRv of 11,377 kW vs. 4,133 kW in PRF-03).
2. **Stage R4 - Peak temperature:** The estimated peak temperature using the CFMRD method is 1,277°C (compared with 1,300°C measured result) occurring upon attainment of the HRRv.
3. **Duration of the fully-developed phase:** Cannot be reliably calculated since the total mass of fuel was not reported in the UL tests. However, assuming a similar FLED to PRF-06, which is likely an over estimate, results in a fully-developed phase of 217 s (vs. approximately 150 s in the UL test, based on Figure 154).

The predictions using the proposed methods yield good results for this one example, which suggests that the calculation methodology has correctly modelled the key parameters. However, one outside example is not sufficient to fully validate the methods although it highlights the application of the knowledge developed in this research.

7 Conclusion

This research has developed information to quantify fuel loads, combustion characteristics of typical residential furnishings and ultimately fires in multi-suite residential dwellings as per the objectives of the project. The research has also provided a set of representative HRR and temperature vs. time design fire graphs that can be used to model fires in various rooms and spaces in multi-suite residential dwellings. Beginning with fuel load surveys and fire experiments to establish the combustion characteristics of typical residential furnishings, the research culminated in the execution of 14 full-scale post-flashover room tests, which were analyzed in this report to develop new knowledge and enhance the current understanding of room fires, and to develop methods of calculating fire severity parameters, such as the post-flashover temperature profile and duration. In 12 of the tests where the first-ignited-item was a primary combustible furnishing item, such as a bed assembly or an upholstered two-seat sofa, that was ignited with a strong ignition source, the fires developed rapidly and flashover occurred within 168 s on average (with a standard deviation of 30s). In one test, PRF-14, where the first-ignited-item was a kitchen cabinet that was ignited with a simulated stove-top ignition source (an oval roaster containing two litres of cooking oil), the first instance of flashover occurred at 587 s after ignition. The peak HRR values (for the fires) obtained in this test series (excluding Test PRF-11) varied from 2,793 kW to 9,230 kW, whereas the mean maximum temperatures during the fully-developed phase (stage R4) only varied from about 1,036°C to 1,203°C.

This report provided a detailed analysis of all of the fire tests and developed a new understanding of the characteristics of room fires involving modern furnishings and established a number of conclusions regarding the effect of parameters such as: ventilation, composition of the fuel load, fuel load density, room size, ignition scenario (flammability of first-ignited item). The research addressed a range of issues concerning fire development in residential dwellings and provided an in-depth scientific analysis that, it is hoped, can enable readers to tailor the results of this research to meet various objectives taking into account the limitations that were necessary for tests of this magnitude to be successfully conducted under controlled laboratory conditions.

The following are the main conclusions:

1. Tests in primary bedroom configurations resulted in the shortest duration to the test wall sections reaching 200°C on unexposed surface since they contained the largest fuel loads and floor area.
2. The ceiling generally experienced a significantly greater thermal exposure compared to the walls due to direct flame impingement (likely causing higher convective heat transfer coefficients) and temperature stratification due to buoyancy (higher temperatures in the top half of the room).

3. The temperature conditions in the real fires considered in this research were more severe—during the first 30 min—than in standard ASTM E119 and CAN/ULC S101 test furnaces. The fires studied here had relatively short fully-developed phases and were well into the decay phase by the time 60 min had elapsed. A simulated test wall section (TWS-04) with a 1 hr fire resistance rating in a standard fire test achieved a lowest fire performance time of 28 minutes in Test PRF-04, whereas the fire performance of a test section simulating an interior non-fire-rated partition wall (TWS-03) was 19 minutes.
4. The research identified a post-flashover phase of the fire (Stage R3), which had a significant effect on initial room temperatures and, consequently, the destructive impact of a room fire. The peak HRR occurred during Stage R3 and significantly exceeded the ventilation-controlled value by as much as 45% in one case. Stage R3 is thought to be largely caused by inefficient combustion resulting from the excessive amount of fuel volatiles generated after flashover and is an inevitable consequence of the composition of fuel loads in a modern dwellings as determined in this research.
5. There were two patterns of flashover, single flashover and multiple flashovers, depending on the size of the fire room. Small- to medium-sized rooms (floor area of not more than 16.0 m^2, with a single window) experienced a single flashover, whereas large rooms (e.g. main floor with an area greater than 16 m^2 with more than one window) experience multiple flashovers as defined in this research.
6. The non-uniformity in the combustion environment increased with room size, which was identified as a zonal burning phenomenon associated with combustion of real fuel loads in a room with windows located at the front of the room. Fire severity varied as such: areas near the windows experienced higher temperature conditions than those that were further away.
7. A larger window size caused more severe temperature conditions than a smaller window size based on the impact of the fires on test wall sections. This research demonstrates that the main reason for this outcome was that the time to reach the mean maximum temperature increased with reducing ventilation, which resulted in a short steady fully-developed phase (Stage R4).
8. A number of existing correlations were evaluated against the test data and the results were as follows:
    a. t-squared fire growth approximation: The growth phase of residential room fires can be modelled using existing t-squared fires up to the ventilation limit;
    b. Correlations for flashover: Babrauskas' correlation gave the best overall predictions;
    c. Correlation for calculating the ventilation-controlled HRR (Equation (2.6)): Predicts the measured average HRR in Stage R4 with good accuracy for a room with a single

window. For rooms with multiple windows, it was difficult to assess accuracy due to the complexity of the HRR profiles.

d. Correlations for post-flashover temperatures: All of the four existing methods that were gave poor predictions of the measured mean maximum temperatures. However, one method (Law's correlation) gave good predictions for 50% of the test data. None of the methods was able to predict the temperature vs. time profiles of the tests.
e. Correlations for post-flashover fire duration: All existing correlations significantly over-predicted the duration of the post flashover phase since many of the methods do not take account of external combustion and collapse of furnishings, which this research indicates contributes to the shorter post-flashover durations in the tests.

9. Regardless of the parameters, all the tests conducted reached a mean maximum temperature that was within 1,150°C ± 100°C. However, the main difference between the tests, due to various parameters such as ventilation and fuel load configuration, is the time taken to reach the peak temperature (Stage R4) and its duration.
10. The experimentally measured HRR vs. time profile during the fully-developed stage is not appropriate for use in calculating the fire temperature in the room because it includes a significant proportion of external heat release that has essentially no effect on room temperature in a heat balance approach. However, the measured HRR profile provides a good measure of the extent of external combustion and the potential danger to external targets.
11. Methods were proposed for calculating the following:
    a. Equation (6.3): The duration of the post-flashover phase (onset of decay);
    b. Equation(6.5): The time to reach the mean maximum temperature taking into consideration the effect of ventilation, fuel composition and exposed surface, and;
    c. Equation (6.10): The peak temperature in the post-flashover Stage R4, assuming the room was a single well-mixed zone, which is a conservative scenario.

7.1 Realistic Design Fires for Multi-Suite Dwellings

A set of HRR and temperature vs. time design fire curves that were based on measurements (smoothed) from the experiments conducted in this research is given in Appendix A. In extrapolating the experimental results from this project to other scenarios that differ from the experimental configurations, it is important to consider that the fire tests only included movable fuel loads (contents), floor finish materials and limited structural fuel loads, namely the sub-floor constructed with OSB. Therefore, other combustible structural fuel loads, such as wood floor joists, wall studs, roof trusses, doors, door and window frames and decorative trims were not included.

Given that fires conducted in this project have shown that fire-exposed single layers of either Type X or regular gypsum board can be destroyed as early as 20 to 30 minutes from ignition, by the rapidly developing fires, it is envisaged that the duration of the post-flashover phase, and consequently high temperatures, will be extended due to the additional fuel contributed by combustible structural elements and combustibles in any adjacent spaces to which the fire spreads. These additional fuel loads should be included into the total fuel load used to define residential design fires. The results of this research suggests there is not a single design fire that can be applied to a whole dwelling but rather a set of design fires for various rooms in the dwelling unit. The impact of thermal properties of room boundaries was not evaluated, therefore the results specifically relate to rooms lined with gypsum board.

While the fire tests were carefully designed to be realistic, it is recognized that in real buildings there is an infinite number of variations and permutations of all of the key parameters that affect fire development, which can lead to deviations from the experimental results found in this research. Therefore, rather than to prescribe design fires derived under experimental conditions, which involved some limitations in order to successfully conduct the fire tests in a laboratory environment, this research has developed substantial scientific knowledge on fuel loads, combustion behaviour of individual furnishings and fully-furnished room fires, and proposed calculation approaches that can assist potential users to address various fire safety design and evaluation objectives. Based on the analysis of the results presented in this report, it is recommended that the first step in the selection of a design fire should be a determination of the objectives and consideration of parameters of the problem at hand because fire severity depends on the type of room, its dimensions, type of first ignited item (whether PCF or SCF) and other parameters that may have not been considered in this research. The results of this research provide valuable knowledge about the effect of key parameters such as window size and first ignited items on the outcome of the fire.

While the main objective of the research was to study high intensity fires that have the potential to pose a danger to adjacent suites, the test results revealed that there was a significant variation in fire severity within a single room due to the complexity of fire dynamics as discussed in this report, which makes it difficult to describe the fires using average values of key fire properties, such as temperature. Therefore, the issue of prescribing or selecting a design fire requires additional contextual details in order to select the appropriate combination of governing parameters, such as fuel load density and composition, room size, ventilation settings and ignition scenario. The results from this research provide valuable insight into the interaction of governing parameters and their impact on the outcome of the fire. Therefore, in this regard, every test conducted in this research provides a valid set of fire characteristics for the types of residential rooms that were tested, as

given in Section 4. A comprehensive collection of graphs of all of the key measured fire properties for the fires are provided in Part 1 of this report [1].

8 Acknowledgments

The authors are very grateful to all the staff at the NRC-IRC Construction, Fire Research who contributed in various ways to the accomplishment of this work. Deserving special mention are the following staff:

- Russ Thomas, Director of the Fire Research, during the course of the project: Chaired the consortium meetings.
- *Bruce Taber*: Facilitated scheduling of the tests and provided numerous valuable technical advices;
- *Joseph Su*: Attended and chaired some meetings, and assisted with tenability calculations.
- *Sasa Muradori, Josip Cingel and Mike Ryan*: Assisted with setting up and conducting the fire tests;
- *Pier-Simon Lafrance*: Constructed and instrumented the test wall sections;
- *George Crampton*: Provide numerous valuable technical advices, designed the load cell arrangement used in Test PRF-13 and assisted with smoke obscuration measurements.

9 References

1. Bwalya, A.C., Gibbs, E., Lougheed, G. and Kashef, A. 2012. "Characterization of Fires in Multi-Suite Residential Dwellings Project, Part 1: A Compilation of Post-Flashover Room Fire Test Data", Institute for Research in Construction, National Research Council Canada, Client Report, Ottawa, Canada.
2. Bwalya, A.C., Lougheed, G., and Kashef, A. 2010. "Characterization of Fires in Multi-Suite Residential Dwellings: Phase 1 - Room Fire Experiments with Individual Furnishings", *Institute for Research in Construction, National Research Council Canada*, *Research Report*, IRC-RR-302, Ottawa, Canada.
3. Buchanan, A.H. 2001. *Structural Design for Fire Safety*, Wiley, New York.
4. Karlsson, Bjorn and Quintiere, James G. 2000. *Enclosure Fire Dynamics*, CRC Press, USA.
5. Cox, G. (ed), 1995. *Combustion Fundamentals of Fire*, Academic Press, London, UK.
6. Drysdale, D. 1998. *An Introduction to Fire Dynamics*, John Wiley and Sons, USA.
7. ISO/TR 13387-2:1999(E): Fire Safety Engineering - Part 2: Design Fire Scenarios and Design Fires", International Organization for Standardization, Geneva, Switzerland.
8. Bwalya, A.C. 2008. "An Overview of Design Fires for Building Compartments", Fire Technology, Vol. 44, pp.167-184.

9. Meacham, Brian J. 1997. "Assessment of the Technological Requirements for the Realization of Performance-Based Fire Safety Design in the United States - Phase I: Fundamental Requirements", Second International Conference on Fire Research and Engineering (ICFRE2), August 3-8, Gaithersburg, USA, pp. 212-225.
10. National Fire Protection Association, 2000. "NFPA 92B: Smoke Management Systems in Malls, Atria, and Large Areas", Quincy, MA, USA.
11. Society of Fire Protection Engineers, 2002. "The SFPE Handbook of Fire Protection Engineering", Society of Fire Protection Engineers (SFPE) NFPA International, 3rd Edition, Quincy, MA, USA.
12. Poulsen, Annemarie, Bwalya, Alex, and Jomaas, Grunde. 2012. "Evaluation of the Onset of Flashover in Room Fire Experiments", Fire Technology, Online First.
13. Zdanowski, M., Teodorczyk, A., and Wojcicki, S. 1986. "A Simple Mathematical Model of Flashover in Compartment Fires", Fire and Materials, Vol. 10, p.145-150 .
14. Harmathy, T.Z. 1972. "A New Look at Compartment Fires, Parts I and II", National Research Council of Canada, Research Report 566, Ottawa, Canada.
15. Babrauskas, V. 1980. "Estimating Room Flashover Potential ", Fire Technology, Vol.16, No.2, p.94-103.
16. Thomas, P.H. 1981. "Testing Products and Materials for their Contribution to Flashover in Rooms", Fire and Materials, Vol.5, p.103-111.
17. McCaffrey, B.J., Quintiere, J.G., and Harkleroad, M.F. 1981. "Estimating Room Temperatures and the Likelihood of Flashover Using Fire Test Data Correlations", Fire Technology, Vol.17, No.2, pp. 98-119.
18. Babrauskas, V. 1981. "A Closed Form Approximation for Post-Flashover Compartment Fire Temperatures", Fire Safety Journal, Vol. 4, pp. 63-73.
19. Hurley, M.J. 2005. "Evaluation of Models of Fully-developed Post-Flashover Compartment Fires", Journal of Fire Protection Engineering, Vol.15, pp. 174 - 197.
20. Yii, Jennifer. 2002. "Modelling the Effects of Fuel Types and Ventilation Openings on Post-Flashover Compartment Fires ", University of Canterbury Research Report, Ph.D. Thesis, 2003/1, New Zealand.
21. Rein, G., Torero, J., Jahn, W., Stern-Gottfried, J., Ryder, N., Desanghere, S., Lazaro, M., Mowrer, F., Coles, A., Joyeux, D., Alvear, D., Capote, J., Jowsey, A., Abecassis-Empis, C., and Reszka, P. 2009. "Round-Robin Study of a Priori Modelling Predictions of the Dalmarnock Fire Test One ", Fire Safety Journal, Vol. 44, p. 590-602.
22. Stern-Gottfried, J., Rein, G., Bisby, L. and Torero, J. 2010. "Experimental Review of the Homogeneous Temperature Assumption in Post-Flashover Compartment Fires", Fire Safety Journal, Vol. 45, p. 249-261.

23. Ma, Zhongcheng and Makelainen, Pentti. 2000. "Parametric Temperature-Time Curves of Medium Compartment Fires for Structural Design", Fire Safety Journal, Vol. 34, p. 361-375.
24. Tanaka, T., Sato, M., and Wakamatsu, T. 1997. Simple Formula for Ventilation Controlled Fire Temperatures. U.S./Japan Government Cooperative Program on Natural Resources (UJNR). Fire Research and Safety. 13th Joint Panel Meeting. Volume 1. March 13-20, 1996, Gaithersburg, MD, Beall, K. A., Editor(s), Vol. 1, pp. 341-356 (June).
25. Kawagoe, Kunio and Sekine, Takashi. 1964. "Estimation of Fire Temperature-Time Curve in Rooms", Building Research Institute Occasional Report No. 17, Japan.
26. European Committee for Standardization. 1995. "EUROCODE 1: Basis of Design and Actions on Structures. Part 2-2: Actions on Structures Exposed to Fire", ENV 1991-2-2: 1995E.
27. Magnusson, S.E. and Thelandersson, S. 1970. "Temperature-Time Curves for the Complete Process of Fire Development - A Theoretical Study of Wood Fuels in Enclosed Spaces", Acta Polytechnica Scandinavica, Stockholm, Sweden.
28. Bwalya, A.C., Lougheed, G., Kashef, A. and Saber, H. 2008. "Survey Results of Combustible Contents and Floor Areas in Canadian Multi-Family Dwellings", *Institute for Research in Construction, National Research Council Canada*, *Research Report*, IRC-RR-253, November, Ottawa, Canada.
29. ASTM Standard E1537, 2012. "Standard Test Method for Fire Testing of Upholstered Furniture", ASTM International, West Conshohocken, PA, USA, DOI: 10.1520/E1537-12, www.astm.org.
30. Soderbom, J., Van Hees, P., and Meirsschaert, P. 1996. "Influence of Ignition Sources on Heat Release Rate in the Furniture Calorimeter", Fire and Materials, Vol.20, No., p.61-67.
31. Babrauskas, Vytenis and Peacock, Richard D. 1992. "Heat Release Rate: The Single Most Important Variable in Fire Hazard", Fire Safety Journal, Vol.18, No., p.255-272.
32. Nyman, Jonathan. 2002. "Equivalent Fire Resistance Ratings of Construction Elements Exposed to Realistic Fires", University of Canterbury, M.Sc. Thesis, New Zealand.
33. ASTM Standard E119. 2012a. “Standard Test Method for Fire Tests of Building Construction and Materials”, ASTM International, West Conshohocken, PA, USA, 2012, **DOI:** 10.1520/E0119-12A, www.astm.org.
34. CAN/ULC-S101-07. “Standard Methods of Fire Endurance Tests of Building Construction and Materials”, Canadian General Standards Board, Ottawa, Ontario, Canada, 4th Ed., 2007.

35. Bwalya, A.C. 2005. "Fire Resistance Tests of Non-Insulated Walls with Parallel and Perpendicular Orientation of Gypsum Board", Institute for Research in Construction, National Research Council Canada, Research Report, IRC-RR-188, 27, Ottawa, Ontario, Canada.
36. Blevins, Linda G. and Pitts, William M. 1999. "Modeling of Bare and Aspirated Thermocouples in Compartment Fires ", Fire Safety Journal, Vol. 33, No. 4, November, p. 239-259.
37. Pitts, W.M., Braun, E., Peacock, R.D., Mitler, H.E., Johnsson, E.L., Reneke, P.A., and Blevins, L.G. 2002. Temperature Uncertainties for Bare-Bead and Aspirated Thermocouple Measurements in Fire Environments. Thermal Measurements: The Foundation of Fire Standards. ASTM STP 1427, L. A. Gritzo and N. J. Alvares, Eds., ASTM International, West Conshohocken, PA, USA.
38. Kim, Sung Chan and Hamins, Anthony. 2008. "On the Temperature Measurement Bias and Time Response of an Aspirated Thermocouple in Fire Environment", Journal of Fire Sciences, Vol. 26, No. 6, p. 509.
39. Bwalya A.C., Lougheed, G., Kashef, A. and Saber, H. 2010. "Survey Results of Combustible Contents and Floor Areas in Canadian Multi-Family Dwellings", Fire Technology, Vol. 46, No. 1, p. 1-20.
40. Su, J.Z., Bénichou N., Bwalya, A.C., Lougheed, G.D., Taber, B.C., Leroux, P., Kashef, A. and Thomas, J. R. 2009. Fire Performance of Houses. Phase I. Study of Unprotected Floor Assemblies in Basement Fire Scenarios. Part 2 - Results of Tests UF-03 and UF-09 (Wood I-Joists A), Research Report, NRC Institute for Research in Construction, RR-247 , Ottawa, Canada.
41. Park, S., Manzello, S.L., Bentz, D.P. and Mizukami, T. 2008. Determining Thermal Properties of Gypsum Board at Elevated Temperatures, Fire and Materials, Vol. 34, pp. 237-250.
42. ISO/TS 16733:2006. 2006. "Fire Safety Engineering - Selection of Design Fire Scenarios and Design Fires ", International Organization for Standardization, Geneva, Switzerland.
43. Kerber, S. 2010. "Impact of Ventilation on Fire Behaviour in Legacy and Contemporary Residential Construction", Underwriters Laboratories, USA.

Appendix A: HRR and Temperature vs. Time Design Fire Curves

A.1 Base Configuration B1 – Primary Bedroom

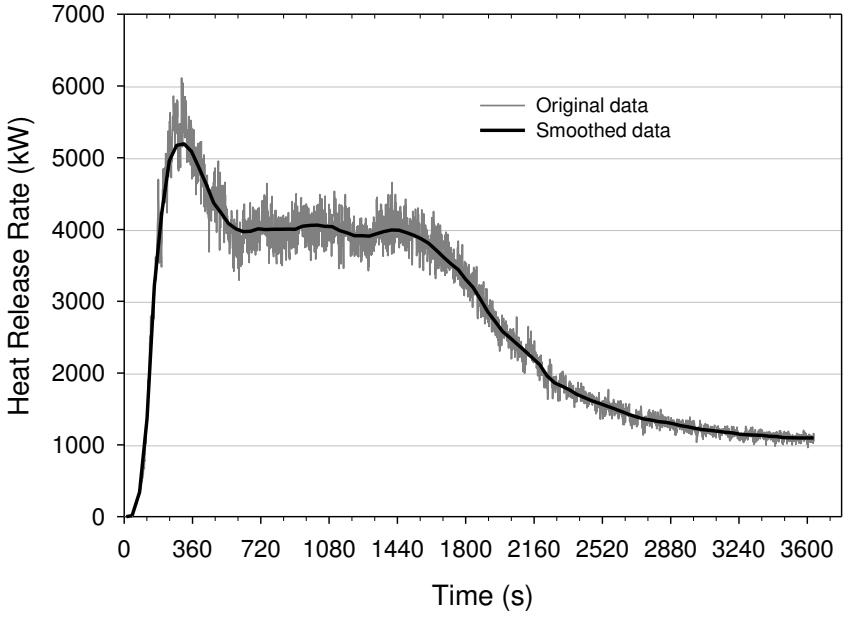

Figure A - 1. HRR vs. time graph for Test PRF-03.

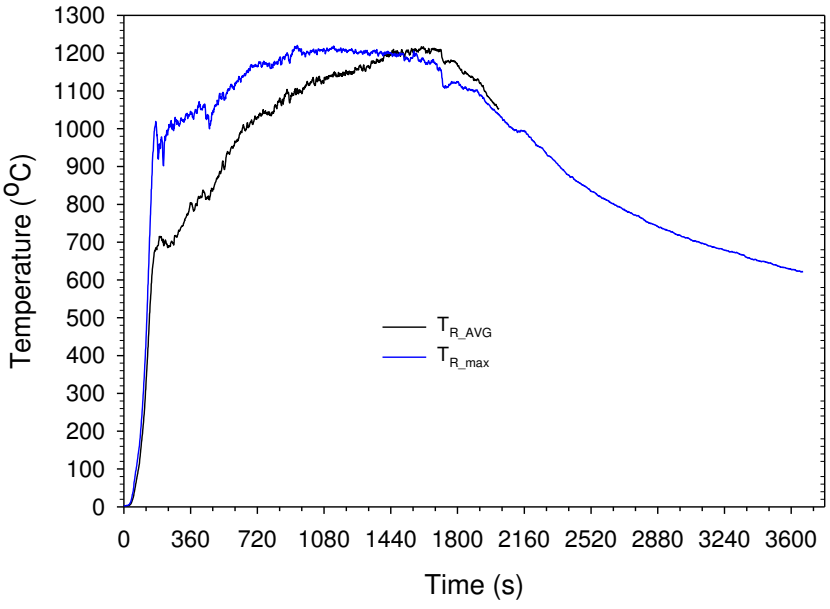

Figure A - 2. Room average (T_{R_AVG}) and maximum (T_{R_max}) temperature profiles for Test PRF-03. (*Note: The T_{R_AVG} curve has a shorter duration than the T_{R_max} curve due to corruption of thermocouple data towards the end of the test*).

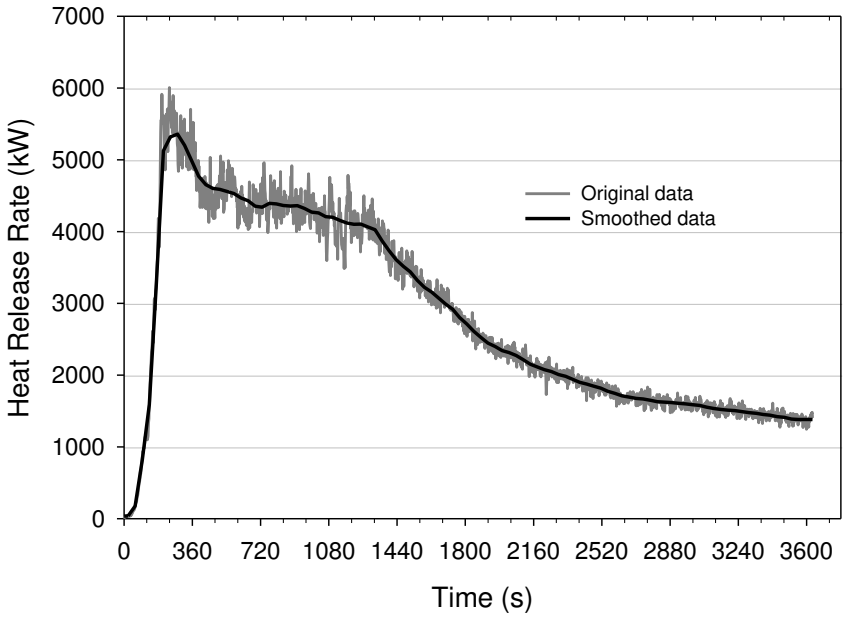

Figure A - 3. HRR vs. time graph for Test PRF-04.

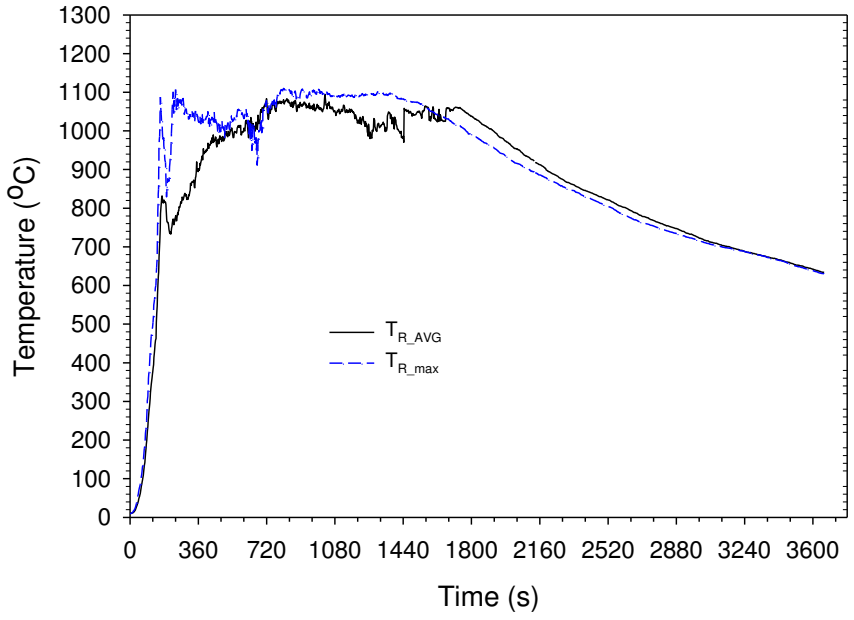

Figure A - 4. Room average (T_{R_AVG}) and maximum (T_{R_max}) temperature profiles for Test PRF-04.

A.2 Base Configuration B2 – Secondary Bedroom with Window # V2

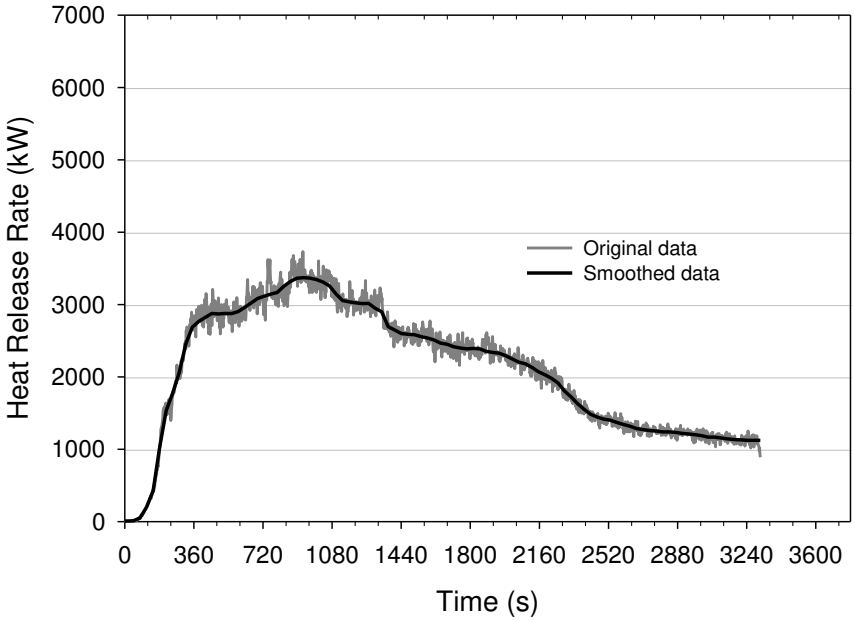

Figure A - 5. HRR vs. time graph for Test PRF-05.

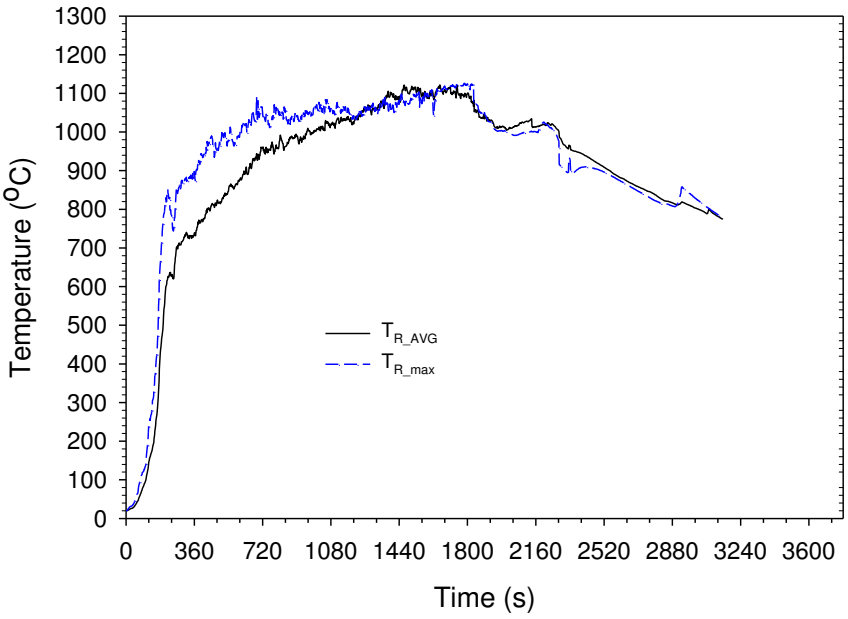

Figure A - 6. Room average (TR_AVG) and maximum (TR_max) temperature profiles for Test PRF-05.

A.4 Base Configuration B2 – Secondary Bedroom #2 with Window # V5

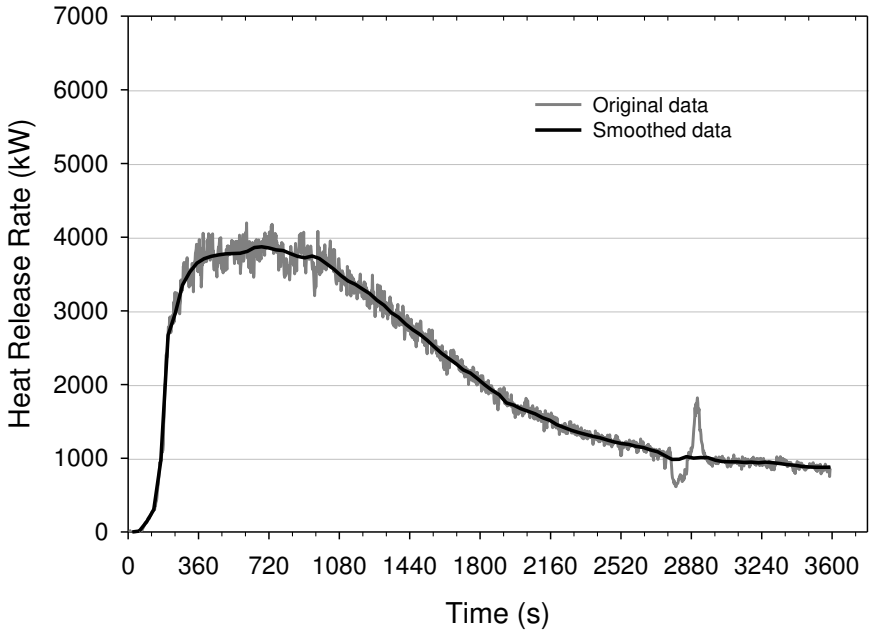

Figure A - 7. HRR vs. time graph for Test PRF-07.

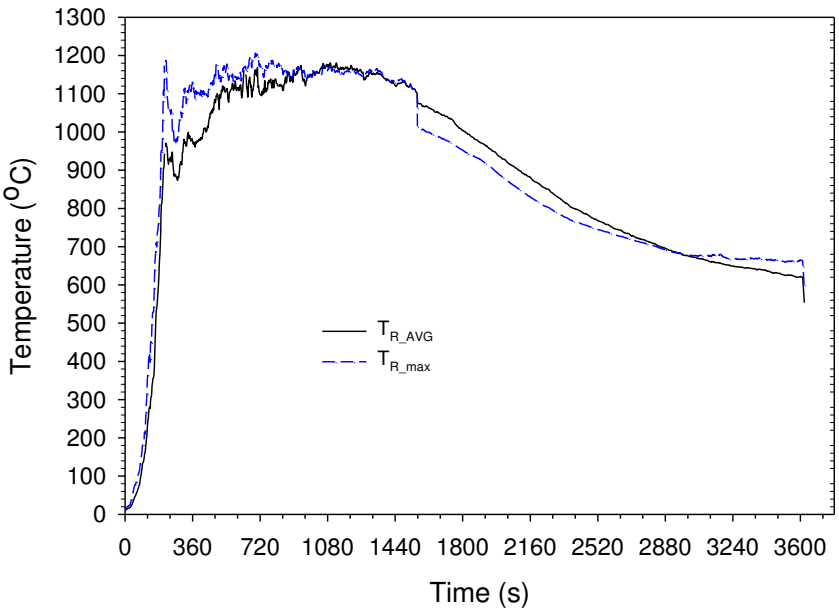

Figure A - 8. Room average (TR_AVG) and maximum (TR_max) temperature profiles for Test PRF-07.

A.3 Base Configuration B4 – Living Room

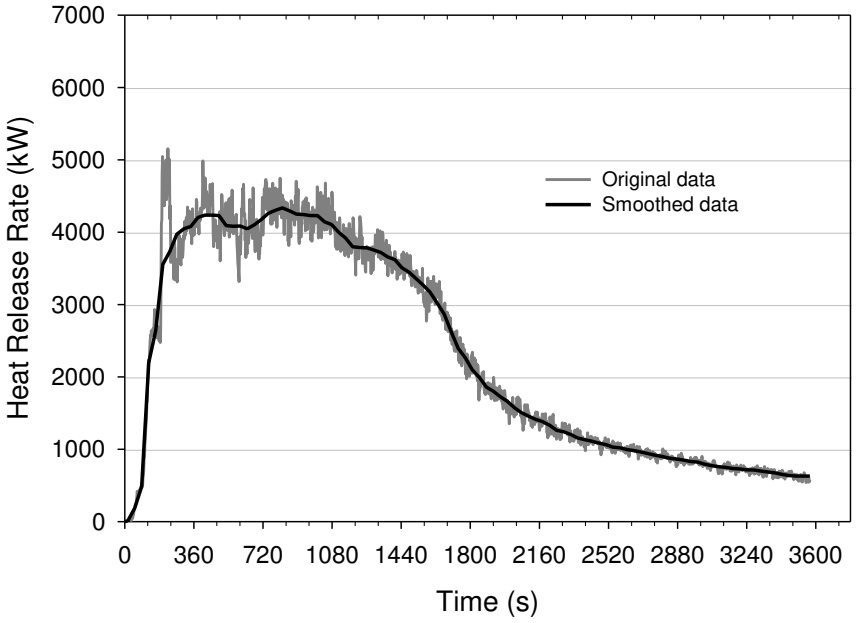

Figure A - 9. HRR vs. time graph for Test PRF-06.

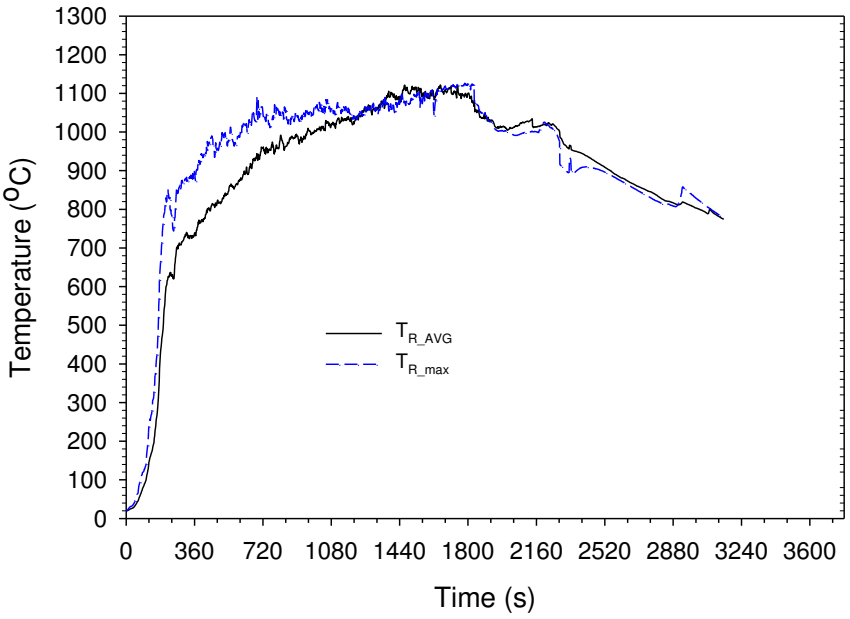

Figure A - 10. Room average (TR_AVG) and maximum (TR_max) temperature profiles for Test PRF-06.

A.6 Base Configuration B5 – Secondary Suite

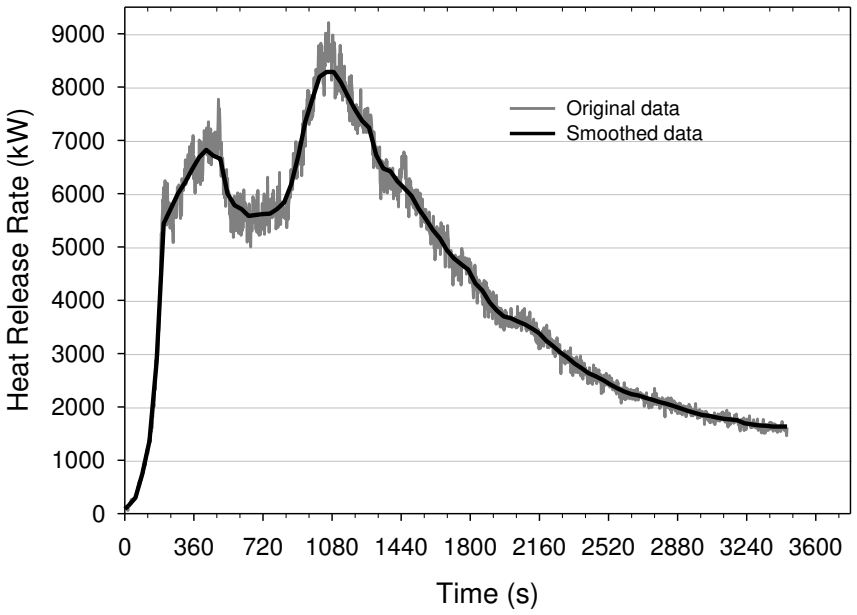

Figure A - 11. HRR vs. time graph for Test PRF-08.

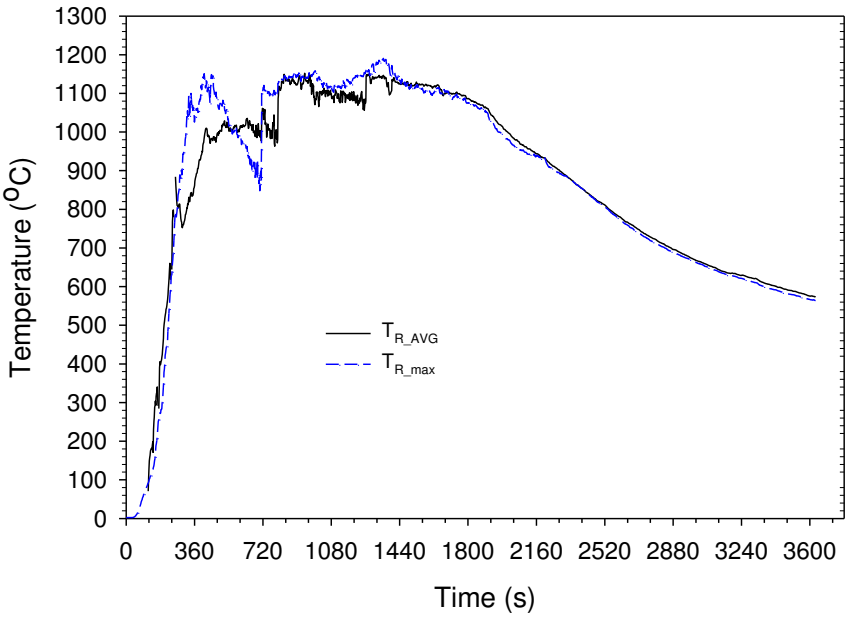

Figure A - 12. Bedroom room average (TR_AVG) and maximum (TR_max) temperature profiles for Test PRF-08.

A.7 Base Configuration B6 – Main Floor

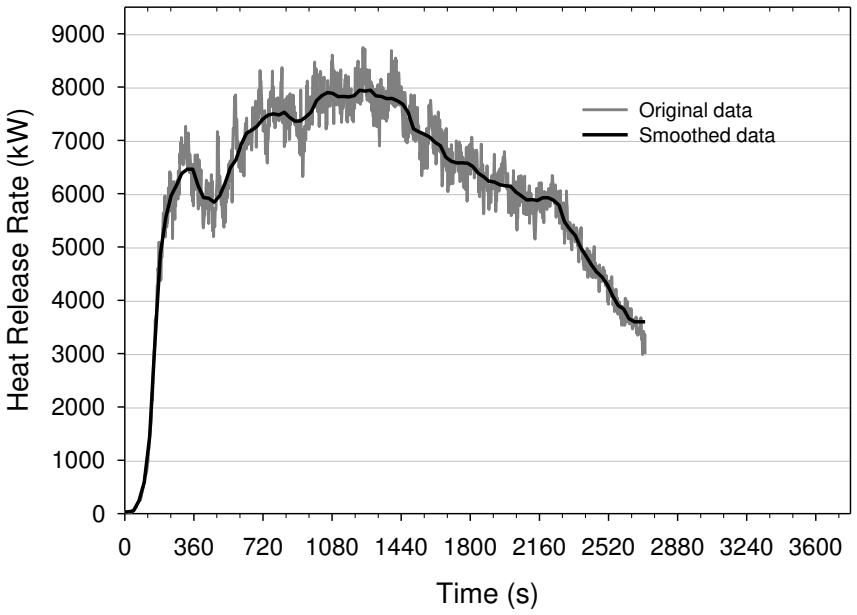

Figure A - 13. HRR vs. time graph for Test PRF-10.

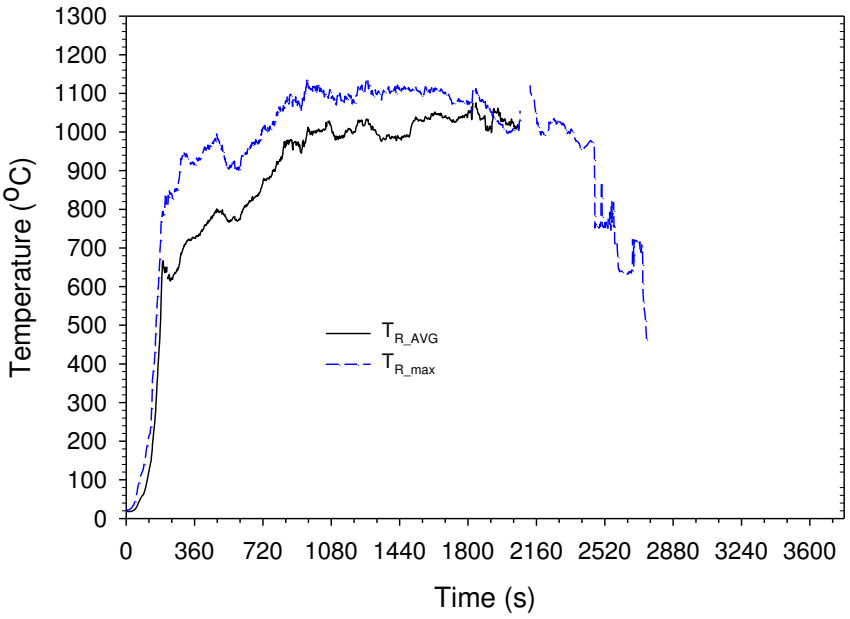

Figure A - 14. Average room temperature (TR_AVG) and maximum (TR_max) temperature profiles for Test PRF-10. (*Note: The T_{R_AVG} curve has a shorter duration than the T_{R_max} curve due to corruption of thermocouple data towards the end of the test*).

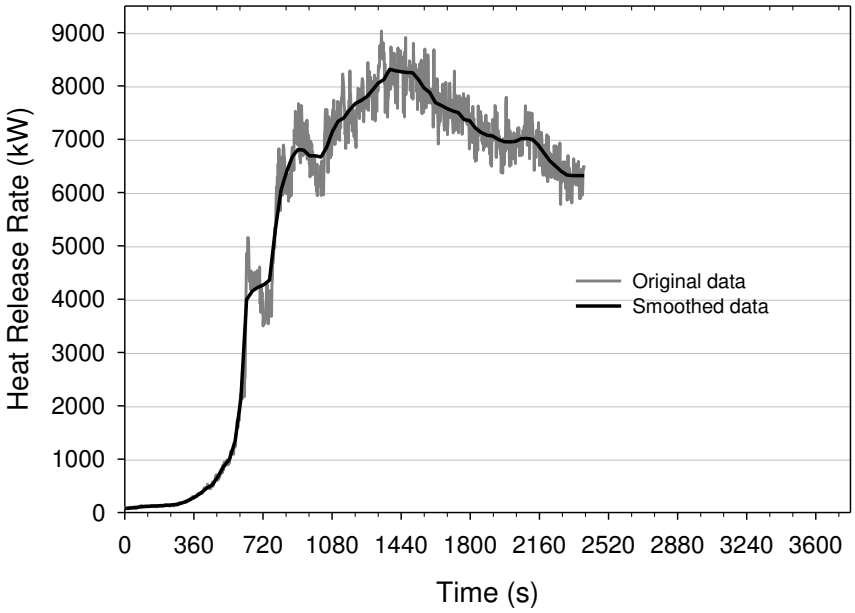

Figure A - 15. HRR vs. time graph for Test PRF-14.

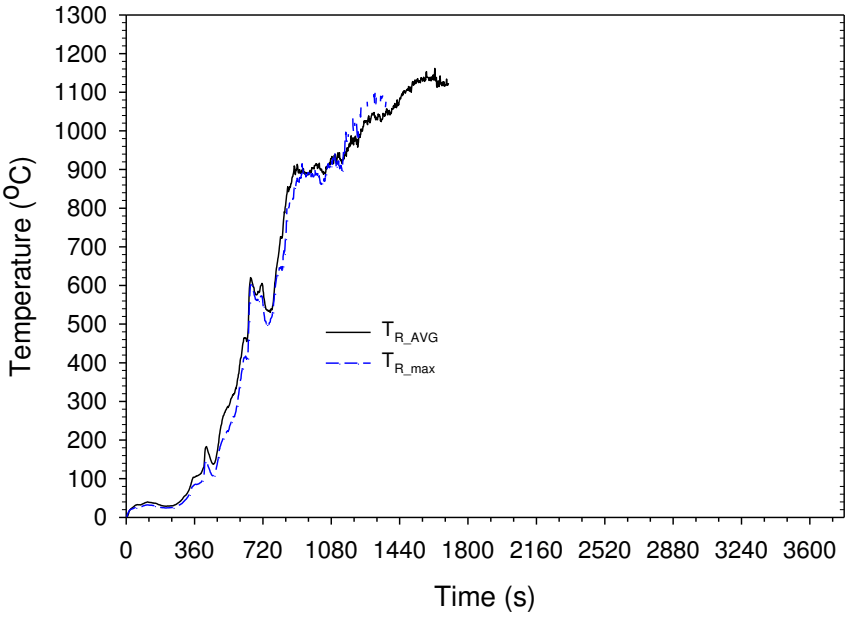

Figure A - 16. Average room temperature (TR_AVG) and maximum (TR_max) temperature profiles for Test PRF-14.